NOVA SCHOOL OF SCIENCE & TECHNOLOGY

DEPARTAMENT OF MATERIALS SCIENCE

BÁRBARA BEATRIZ CALDAS DIAS

BSc in Micro and Nanotechnology Engineering

Functional Materials for Intelligent Food Packaging

MASTER OF SCIENCE IN MICRO AND NANOTECHNOLOGY ENGINEERING

NOVA University Lisbon

October, 2022

Functional Materials for Intelligent Food Packaging

BÁRBARA BEATRIZ CALDAS DIAS

BSc in Micro and Nanotechnology Engineering

Adviser: Dr. Miguel Ângelo Parente Ribeiro Cerqueira
Staff Researcher, International Iberian Nanotechnology Laboratory

Co-adviser: Dr. Luís Miguel Nunes Pereira
Associate Professor, NOVA University Lisbon

Examination Committee:

Chair: Maria Helena Figueiredo Godinho,
PhD, Associate Professor, NOVA University Lisbon

Rapporteurs: Luís Miguel Neves Ferreira Serra Cruz,
Researcher, LAQV-REQUIMTE
Miguel Ângelo Parente Ribeiro Cerqueira,
Staff Researcher, International Iberian Nanotechnology Laboratory

MASTER OF SCIENCE IN MICRO AND NANOTECHNOLOGY ENGINEERING

NOVA University Lisbon
October, 2022

Functional Materials for Intelligent Food Packaging

Para os meus avós.

ACKNOWLEDGMENTS

Este documento representa o término de uma das etapas mais marcantes da minha vida, a conclusão do Mestrado Integrado em Engenharia de Micro e Nanotecnologias. Como tal, esta secção dedica-se a agradecer a todos aqueles que, direta ou indiretamente, nas diferentes esferas da minha vida, contribuíram, de alguma forma para que eu aqui chegasse.

Assim sendo, começo por agradecer à Faculdade de Ciências e Tecnologias, da Universidade Nova de Lisboa, por me ter proporcionado condições de excelência, tanto a nível de formação, enquanto estudante, tanto como pessoa e, ao Departamento de Ciências dos Materiais, pela qualidade de ensino que me foi fornecido.

Por outro lado, é essencial demonstrar a minha gratidão à Professora Elvira Fortunato e ao Professor Rodrigo Martins, por terem criado este curso e ao meu Coordenador de curso, o Professor Hugo Águas. Um especial agradecimento a todos os professores que tive ao longo destes cinco anos, que me inspiraram com as suas conquistas, nacionais e internacionais e, por conseguinte, que consolidaram a minha paixão pelo mundo científico.

Ao meu co-orientador, Professor Luís Pereira, pois foi graças às suas aulas da cadeira de "Materiais Celulósicos e Papel", que me fizeram despertar um enorme interesse relativamente à aplicabilidade da celulose e os seus derivados. Obrigada por ter aceitado este projeto, pela sua disponibilidade e partilha de conhecimentos.

Quero expressar a minha mais profunda e sincera gratidão ao meu orientador, Miguel Cerqueira, pelo seu conhecimento, disponibilidade constante e apoio incansável ao longo destes meses. Ser integrada num grupo de trabalho como o de *Food Processing and Nutrition Group*, onde o profissionalismo, organização, rigor, conhecimento e entreajuda são princípios bem enraizados, foi determinante para a minha evolução como "investigadora". Quero por isso agradecer a todos os membros do grupo e enaltecer a integração, disponibilidade e ajuda demonstradas.

Aos meus colegas de casa em Braga e, claro, amigos que pertencerão para sempre no meu coração, André, Luís e Henrique, agradeço por me terem proporcionado um ambiente único, pela vossa alegria infinita e contagiante, com vocês tudo se tornou mais fácil. Ao Vasco pelas conversas e desabafos, acompanhados sempre por café.

Obrigada às minhas amigas, companheiras desta jornada, Bibs e Miana, pelos almoços emotivos e desabafos, no nosso banco de faculdade, pelas múltiplas sessões de estudo, acompanhadas por risadas, mas acima de tudo, pelo apoio infinito e por estarem sempre ao meu lado. Às Carolinas, Catarina, Inês e Francisco, amizades que levo comigo.

Obrigada à minha Cata, amiga de longa data, que está comigo desde pequenina, e, que sei que vai durar por muitos mais anos. Que desejosa eu estou por ver o futuro que nos espera. À Maria, Sara, Nuno, Grilo, Natas, Catarina, amigos que prevalecem e que me acompanham.

Por fim, agradeço à minha família. Obrigada aos meus tios, Né e Fina, que mesmo de longe se fazem sentir, através da saudade. Obrigada aos meus primos, Raquel, Tânia, Lúcia, Inês, Mário. Obrigada, à tia Manela.

Muito obrigada às minhas três pessoas, pai, mãe e maninho. Esta caminhada não seria possível sem vocês, muito do que sou, devo-o a vocês. Obrigada ao meu pai, pelo seu apoio e pelos seus ensinamentos, nomeadamente por me demonstrar constantemente que tudo é alcançável. Obrigada à minha super-mãe, que

por mais difícil que a vida se encontrasse, e por mais cansativos que os dias fossem, nunca baixou a cabeça. Quem me dera algum dia ser metade da mulher que és. Ao meu maninho, ao meu melhor amigo para a vida, que está sempre lá para mim, nos momentos mais felizes e mais tristes, e que me demonstra todos os dias o seu afeto, mesmo quando estou rabugenta. És o meu orgulho!

Um destaque muito especial para os meus avós. O tempo passa, mas a saudade fica, e aumenta a cada dia. Sou o que sou graças aos valores que me transmitiram. Esta tese é para vocês. Espero que estejam orgulhosos de mim!

Por último, agradeço ao meu Migs, o meu Nando, por todo o amor, carinho, companheirismo e paciência interminável. Que todos os nossos planos e sonhos, a curto e a longo prazo se realizem, pois nós estamos cá para trabalhar e lutar por eles, juntos. Que a nossa relação seja sempre como Mecânica Quântica. Para sempre agradecida, por te ter na minha vida.

Obrigada!

“Failing doesn’t give you a reason to give up,
as long as you believe.” (Uzumaki Naruto).

ABSTRACT

Nowadays, plastic has been used as a common packaging material owing to its transparency, durability, and softness. Nevertheless, in the food packaging field, the increased plastic consumption has caused, not only severe environmental problems, due to their non-biodegradability, but also health threats, as a consequence of the plastic's toxic additives migration.

Generally, cellulose derivatives, namely carboxymethylcellulose (CMC), cellulose acetate (CA) and ethyl cellulose (EC), can be used to develop food packaging films as an alternative to plastics, because of their compatibility, non-toxicity, and higher stability. Additionally, the latest research, for the development of colorimetric pH films to monitor the food freshness, has focused on adding safe and natural pigments, such as, anthocyanins (ANT), curcumin (CUR) and betalains (BE), owing to their pH sensing capabilities.

The main focus of this thesis relies on the development of functional inks that can act as an indicator for food packaging applications. Therefore, ANT, CUR and BE were explored, as well as, CMC, CA and EC were tested for the development and stabilization of indicators. After their development, the films were characterized in terms of their pH sensing characteristics, morphology, chemical interactions, colour and its opacity, mechanical properties, moisture content, and lastly, a food model (salmon) was used for the evaluation of the indicators' capacity.

Initially, a brown colour was observed in CMC, CA and EC-based films, which was associated with the presence of ANT, an orange colour was corelated with the presence of CUR and a pink colour to the addition of BE. When immersed in different pH buffer solutions, it was demonstrated different colour ranges, accordingly to the natural dye used in the CMC and CA-based films. However, for the EC-based films with the incorporation of different pigments, it was verified the maintenance on their colour.

Morphological characteristics suggested a good compatibility between lower concentrations of pigments and the polymers matrix. For higher concentrations, the observation of small aggregates distributed in the films resulted in a low compatibility between the natural dyes and the polymers matrix. These observations were corelated with the films mechanical properties and the Fourier transform infrared spectroscopy analysis.

The results suggest that the intelligent films reported here (CMC and AC-based films) show good capability to be used as indicators and, thus, act as a way to alert food spoilage.

Keywords: Food packaging, carboxymethylcellulose, cellulose acetate, ethyl cellulose, anthocyanins, curcumin, betalains

RESUMO

Atualmente, o plástico tem sido amplamente usado como embalagem, devido à sua transparência e durabilidade. No entanto, na área de embalagens de alimentos, o aumento do consumo de plástico tem provocado graves problemas ambientais, devido à sua não-biodegradabilidade, como também ameaças à saúde, como consequência da migração de aditivos tóxicos.

Usualmente, os derivados de celulose, nomeadamente, carboximetilcelulose (CMC), acetato de celulose (CA) e etilcelulose (EC), são as escolhas preferidas para o desenvolvimento de filmes para embalagens de alimentos, como alternativa aos plásticos, devido à sua compatibilidade, não-toxicidade e estabilidade. Além disso, em investigações recentes, para o desenvolvimento de filmes colorimétricos, através da mudança de pH, de forma a monitorizar a frescura dos alimentos, a adição de pigmentos naturais, tais como, antocianinas (ANT), curcumina (CUR) e betalainas (BE), tem sido o principal foco devido à sua capacidade sensorial com pH.

O principal objetivo desta tese é o desenvolvimento de filmes inteligentes, que possam atuar como indicadores em embalagens de alimentos. Desse modo, foi realizado o estudo dos pigmentos, ANT, CUR e BE, bem como, de vários polímeros, tais como, CMC, CA e EC, para o desenvolvimento e estabilização dos indicadores. Após o seu desenvolvimento, os filmes foram caracterizados, quanto às suas características sensoriais através do pH, a sua morfologia, interações químicas, a cor e a sua opacidade, as propriedades mecânicas, o teor de humidade e, por último, foi utilizado um modelo alimentar (salmão), para a avaliação da capacidade dos indicadores.

Inicialmente, foi observada uma coloração castanha nos filmes à base de CMC, CA e EC, associada à presença de ANT, uma coloração laranja correlacionada com a presença de CUR e uma coloração rosada devido à adição de BE. Quando imersos em diferentes soluções-tampão, foram verificadas diferentes variações de cores, de acordo com o pigmento utilizado nos filmes à base de CMC e CA. No entanto, para os filmes à base de EC, com a incorporação de diferentes pigmentos, não foi verificada a alteração da sua cor.

As características morfológicas sugeriram uma boa compatibilidade entre menores concentrações de pigmentos e a matriz polimérica. Para maiores concentrações, foi observado pequenos agregados distribuídos pelos filmes, o que resultou numa baixa compatibilidade entre os pigmentos e a matriz polimérica. Estas observações foram correlacionadas com as propriedades mecânicas dos filmes e com a análise de espectroscopia no infravermelho por Transformada de Fourier.

Os resultados sugerem que os filmes inteligentes relatados (filmes baseados em CMC e AC) apresentam uma boa capacidade para serem usados como indicadores, e, assim, para alertar a deterioração de alimentos.

Palavras-chave: Embalagens, carboximetilcelulose, acetato de celulose, etilcelulose, antocianinas, curcumina, betalaínas

CONTENTS

LIST OF FIGURES

LIST OF TABLES

ACRONYMS

IIoT	Industrial internet of things
DS	Degrees of substitution
CMC	Carboxymethylcellulose
CA	Cellulose Acetate.
EC	Ethyl Cellulose
ANT	Anthocyanins
CUR	Curcumin
BE	Betalains
PVA	Polyvinyl alcohol
GPC	Gel Permeation Chromatography
SEM	Scanning electron microscopy
FTIR	Fourier-transform infrared
MC	Moisture content
TS	Tensile strength
EB	Elongation at break

SYMBOLS

Symbol	Name
M_n	Number average molecular weight
L*	Lightness
a*	Redness-greenness
b*	Yellowness-blueness
ΔE	Total colour difference
W_i	Initial weight
W_f	Final weight
p	p-value

1

INTRODUCTION

In this Chapter, the motivation for the present work is depicted, followed by a brief explanation of theoretical background concepts related to the goal of this project.

1.1 Context and motivation

Since the beginning of mankind, food spoilage has been a major concern for human beings. From a sensory perspective, it is defined as a process in which a food product is considered unacceptable to the consumers, due to physical damages and chemical transformations, including colour changes, oxidation, or even, off-flavours, resulted from microbial contamination, affecting its quality and safety. Another food spoilage case is related to the nutrients' deterioration, which means that the food product no longer encounters the declared nutritional value [1], [2]. For instance, many microorganisms produce acids which can greatly lower the foods' pH. In the worst circumstances, a serious issue in food safety may occur when it leads to catastrophic consequences for human survival caused by food poisoning. The term product's shelf-life is defined when a food product reaches one of the spoilage conditions mentioned above [3], [4].

The open shelf-life dating marked on the food products' containers includes a 'best-if-used by-date', a 'sell-by date', or a 'better-if-used-by-date' which helps not only with the decision of how long the product may be stored, but also with stock rotation in grocery stores. Additionally, the given date usually assumes appropriate product storage conditions prior to consumption. Understanding what type of product's spoilage may occur, how to reduce the product's deterioration rate, and how to properly measure and detect its occurrence is critical. Table A.1.1, presented in the appendix, lists the critical storage variables and the type of spoilage for different food product categories in which are influenced by various main factors, namely, temperature, pH, and exposure to oxygen and light [4], [5].

It is possible to conclude the meaningful challenges of the dynamic and complex chain of food supply owing to the processing complexity, safety-related matters, consumer needs and behaviour changes, and new laws and regulations enforcement. As part of the 2030 Agenda, the United Nations implemented 17 Sustainable Development Goals in order to address the global challenges and achieve a better and greener future. Zero Hunger is one of these goals which aims to improve and promote a future with food security and sustainable food systems. These challenges may be managed by the development of a smart food supply chain mainly in food packaging [6], [7].

Nowadays, most of the packaging materials are produced from fossil fuels, due to their low cost, good resistance against different environmental factors, and their flexibility for moulding. Nevertheless, these packaging materials not only take a great deal of time to degrade, but also pose danger of releasing chemicals which may reduce the food's quality. Hence, changes in the consumer's desire and interest, regarding health concerns and the need to reduce fossil fuels dependence have led to new approaches in food packaging technologies. Particularly, numerous derived biopolymers, such as, lipids, proteins, and, polysaccharides, have been used as

an alternative to plastics. Among them, polysaccharides are the desired choice due to their abundance, biodegradability, biocompatibility, and non-toxicity [8], [9].

Nevertheless, the development of convenient, rapid and real-time detection methods to evaluate the food's quality is in great demand, introducing the concept of smart packaging, which can be subdivided in two main categories, active and intelligent packaging [7], [10]. Active packaging refers to those that improves the safety and its sensory properties, in order to maintain or extend shelf life. Whereas intelligent packaging has been defined as the one which monitors the packaged food and, consequently, attempts to sense its environmental changes, to inform about their microbiological food quality or its real-time freshness, to manufacturers and consumers [10].

Currently, chemical indicators, particularly, colorimetric indicators, as pH-sensitive dyes, have been used to monitor food quality freshness, providing visual information, detected directly by the naked eyes to consumers. As a result of products' microbial deterioration, with microorganisms' growth and metabolism, during food storage, not only the concentrations of organic acids, namely D-lactate, L-lactic acid, acetic acid, and n-butyrate, are changed, but also, volatile components, specifically, dimethylamine, trimethylamine, and histamine, among others, are produced and released. The media pH of the packaging headspace is changed and, subsequently, it is exhibited colour changes of the pH-sensitive dye in the polymer film. These systems turn into real-time visual indicators which monitor the food spoilage [10], [11].

Previous studies showed that various synthetic pigments and dyes, such as, xylenol [12], bromocresol green [13], methyl red, cresol and chlorophenol [14], have been used for the smart packaging systems development, which are considered toxic and mutagenic. The alternative can be the use of natural dyes, namely, anthocyanins [15], betalains [16], curcumin [17], carotenoids, chlorophyll, tannins, and others, which are advantageous not only due to their biodegradability and eco-friendly feature, but also to guarantee the safety of food products, even if they are in contact with [18].

The presented work aims develop functional inks that can act as an indicator for smart packaging on food applications. Thus, natural dyes, including, anthocyanins (ANT), betalains (BE) and curcumin (CUR), will be explored, as well as cellulose-based materials, such as, carboxymethylcellulose (CMC), cellulose acetate (CA), and ethyl cellulose (EC) will be tested for the development and stabilization of the indicators.

1.2 State of the art

1.2.1 Intelligent Food Packaging

The main functions of packaging are the separation and protection of the products from external environment as well as the prevention from leakage and breakage in order to slow quality decay. As a matter of fact, it has the ability to communicate and to provide convenience to the consumer about important features such as the nutritional content and cooking guidelines. As a result, it offers different types of shape and size containers to simplify the customer's lifestyle.

Conventionally, there were limited food packaging technologies which could accelerate and develop threatening circumstances to the consumer's health as well as to the safety of the product, depending on the storage and external distribution conditions such as light, temperature, microbes, and moisture.

Therefore, up-to-date developments in food packaging technologies are focused on ensuring the challenges stemming the food safety with the reduction of product waste, the consumer demands, the globalization of markets and the increased regulatory requirements with fewer preservatives towards a circular economy and the minimization of the carbon footprint. Particularly, intelligent food packaging systems which enhance packaging functionality with their capability to detect, sense, record the changes in the packed food environment and communicate this information to the consumer. It is important to take into account that these systems do not interact with the product itself [8], [19].

Nevertheless, it is quite challenging the design and production of suitable smart packaging technology, mainly, the improvement of antimicrobial packaging focused on natural derived antimicrobial agents,

biodegradable and bio-preservatives solutions; the optimization of active materials with the ability to preserve the barrier and original mechanical properties, which can increase the extend shelf life and safety of foods; the development of thin film electronics to be incorporated into packaging technologies, as a result of performance issues and, lastly, the difficulty to treat and recycle some types of packaging, leading to the generation of waste from smart packaging which is unsustainable [20].

Henceforth, nanotechnology has a great role in food packaging, restoring food damage as well as overcoming food allergies by eliminating pesticide use, keeping in mind the concerns about the safety associated with packaging. For instance, packaging embedded with nanomaterials is a key opportunity to develop appropriate and safe advanced packaging materials, since it responds to environmental conditions, alerting the consumer of contamination or, even, repairing itself [20], [21].

Even with all the present limitations and challenges associated with food packaging, such as the development of functional materials based on natural and bio-based compounds, due to the compounds' instability and the combination with other materials, the advantages of researching for new types of sustainable intelligent food packaging systems is widespread.

Accordingly, intelligent packaging systems incorporate two main technologies, indicators and sensors devices to communicate relevant information about product quality and safety, as shown in Figure 1 [22].

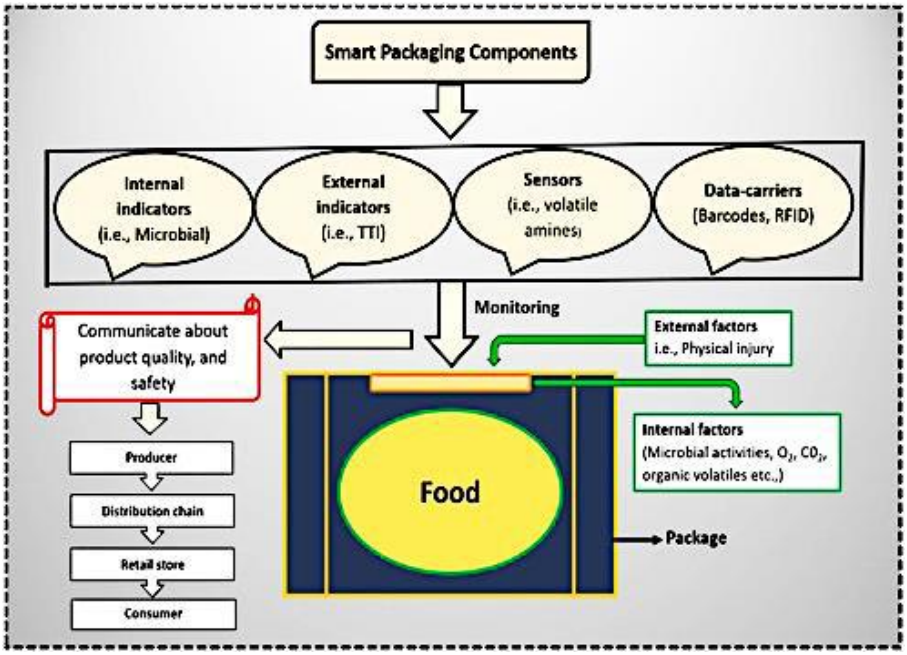

Figure 1 – Smart packaging concept in food [22].

For instance, sensors are defined as devices which not only detect, locate, quantify, and provide information about the packaged product's impairment but also attempt to undo undesirable modifications that have arisen in the food product [22]. Mainly, sensors involve two components, a receptor, which detect a certain chemical or physical analytes' presence, composition, concentration, or activity, and convert that information into an energy form that can be measured and transformed into an electrical signal by a transducer, which is the second component. In food packaging, sensors can help to detect toxins and pathogens, as well as allergen from various food sources such as seafood and tree nuts, that might be harmful to human health [23]. Whereas indicators, which exhibit good reliability and stability, monitor, and inform about detected changes not only in a product, such as, the concentration of a certain substance, but also in its environment [22].

1.2.2 Bio-based materials for the development of smart packaging films

Cellulose is a natural biopolymer, composed of glucose monomers, joined by β–1,4 linkages. Generally, it is synthetized by plants, such as, cotton and woods, but it is also produced by certain bacteria. The chemical structure of cellulose remains the same, regardless of its source.

Cellulose derivatives have gained research interest, due to their respect for the environment, availability, processing simplicity, biodegradability, flexibility, and significant physico-mechanical properties. Nowadays, they are used in numerous commercial products, specifically from textiles and paper to foods and pharmaceuticals [24], [25].

1.2.2.1 Carboxymethylcellulose

Among the various biopolymers, carboxymethylcellulose (CMC) is the major cellulose ether, composed of a linear polysaccharide of anhydro-glucose, represented in Figure A.2.1.1. The repeating units are connected by 1,4–β–D–glucan monomers in which the hydroxyl groups are partially replaced by anionic carboxymethyl groups (–CH_2COOH).

CMC is widely used in the food processing, food packaging, and pharmaceutical industry owing to its high hydrophilic capacity, absorbing more than 50% in weight of water, biocompatibility, and formability. However, it is importance to notice that CMC presents low water resistance and so, weak water vapor barrier properties [26], [27].

1.2.2.2 Cellulose acetate

Cellulose acetate (CA) is an important organic cellulose ester, produced from cellulosic raw materials, including wood and cotton, in which the hydroxyl groups from the native cellulose are substituted by acetyl groups, as shown in Figure A.2.1.2. Despite the fact that CA can be processed with a range of degrees of substitution (DS), the most usual form of CA has an acetate group on approximately 2–2.5 of every three hydroxyls. Among other things, the CA solubility depends on the DS, in which it is possible to verify that CA with DS of 2 – 2.5 is soluble acetone, methyl acetate, and dioxane [28], [29].

CA has gained a greater interest due its biodegradability, non-toxicity, with excellent optical properties, and high toughness but with some flexibility, that supports high tension at room temperature [30], [31].

1.2.2.3 Ethyl cellulose

Ethyl cellulose (EC) is another important cellulose derivative, extracted from wood pulp or cotton, and then is chemically modified. Thus, EC is a linear polysaccharide, constituted of glucose unit with β–1,4–glycosidic linkages, which involve the replacement of some of the hydroxyl (–OH) functional groups with ethoxy group (–O–CH_2–CH_3), as observed in Figure A.2.1.3 [32], [33].

Essentially, EC is considered a hydrophobic polymer, odourless and colourless, with an amorphous nature containing low amounts of the crystalline domain. Considering its properties, it is mainly used as a thin-film coating material and as an emulsifier in food supplements and flavourings in capsules [33], [34].

1.2.3 Bioactive compounds and their utility

The latest research is focused on non-toxic, non-invasive, non-destructive and safe naturally derived pigments extracted from fruits and plants, including, anthocyanins, betalains, and curcumin. Table A.2.2.1, presented in the appendix, summarizes the bio-based intelligent packaging films' applications, including these natural derived pigments, for monitoring the quality of seafood and meat products.

1.2.3.1 Anthocyanins

Anthocyanins are non-toxic, water-soluble, and natural pigments, part of the flavonoid family, which contribute to the red, pink, blue, and purple colours of various fruits, vegetables and flowers. These pigments, not only, exhibit significant antioxidant and antimicrobial properties, but also, colour changes under pH

conditions. Consequently, anthocyanin films can be used as intelligent pH indicators to monitor the food spoilage process accompanied by pH changes [35], [36].

As observed in Figure A.2.2.1, at highly acidic conditions, anthocyanins are in the form of the most stable and water-soluble species, the flavylium cation, resulting in the red colour. Upon an increase in the pH, acidic up to neutral, it is induced the flavylium cation deprotonation, forming the neutral quinoidal base and, subsequently, inducing the purple colour. Then, at highly alkaline conditions, the deprotonation of neutral quinoidal base species generates the anionic quinoidal base, changing to an intense blue [37], [38].

It is important to consider that the anthocyanins source influence significantly its functional and physical properties. Silva-Pereira et al. studied the use of the red cabbage anthocyanin (RCA) as a pH sensitive dye to prepare colorimetric films, in which it was verified an optimal performance, due to its highly sensitive to acidity and alkalinity [39]. Besides, Vo et al. verified that RCA in chitin-polyvinyl alcohol (PVA) based films demonstrate colour variations with pH changes, and good mechanical properties, in which it was effective in monitoring the pork slices spoilage [40].

Zhang et al. combined anthocyanins, obtained from roselle, with a mixture of starch-chitosan, in order to create an indicator film. It was confirmed that anthocyanins-based visual indicator films are an outstanding choice for gas sensors to monitor the pork freshness, since it was found, when basic volatile nitrogen compounds were presented in pork, visual colour change, from red to yellow [15].

Particularly, when compared to red cabbage and roselle, purple sweet potato is much richer in anthocyanins, which are mainly in acylated forms, resulting in their good stability and antioxidant activity. Choi et al. explained that films based on agar and potato starch with purple sweet potato anthocyanins are reliable to detect meat products' quality variations, since they showed colour variations from red (pH 2) to dark green (pH 10) [41].

1.2.3.2 Betalains

Betalains are a water-soluble nitrogenous pigments produced by plants, such as, red pitaya, red beetroot, amaranth and prickly pear. Structurally speaking, these pigments can be subdivided into betacyanins, which corresponds to a red-purple colour, with a maximum wavelength around 540 nm, and yellow/orange betaxanthins, with a maximum wavelength around 480 nm. As shown in Figure A.2.2.2, betacyanins are the result of the condensation of betalamic acid (the chromophore) and cyclo-3,4-dihydroxyphenylalanine (cyclo-Dopa), whereas betaxanthins are formed by the condensation of betalamic acid and different amino compounds. Notably, at alkaline conditions, betalains can undergo structural and colour changes, from red to yellow, since it is structurally stable in the pH range of 3–7 [16].

Apriliyanti et al. reported that betalains, extracted from red pitaya, and incorporated into glucomannan and PVA-based films, effectively, monitored, the fish freshness along with sensitivity to ammonia [42]. After eight days, the films' colour altered from pink to yellow, due to an increase in the total volatile basic nitrogen, when used for fish packaging. Similarly, Qin et al. developed starch-based films with red pitaya extracts which displayed enhanced sensitivity to ammonia, along with mechanical and antioxidant properties, appropriate for monitoring shrimp spoilage [16]. Additionally, Yao et al. reported that chitosan/PVA-based films with cactus pear peel extracts depicted colour variations, as the volatile compounds released from shrimp, while monitoring its freshness [43].

1.2.3.3 Curcumin

Curcumin, [1,7-bis(4-hydroxy-3-methoxyphenyl)-1,6-heptadiene-3,5-dione], is a polyphenolic compound extracted from turmeric (the root of *Curcuma longa* L.).

Its chemical structure is shown in Figure A.2.2.3. In the past few years, curcumin has been incorporated into the packaging systems due to its functional properties improvement, such as antioxidant properties, antimicrobial activity, UV protection and enhanced mechanical strength of the film [44], [45]. Besides, c2urcumin exhibits a pH-responsive colour-changing property when incorporated into natural polymers, such as,

starch, chitosan and cellulose derivatives films which enables the production of intelligent packaging films [17], [46].

It is important to consider that curcumin solubilizes in oils, ethanol, chloroform, and dimethyl sulfoxide. In aqueous solutions, curcumin stability is pH-dependent, with an optimum cut-off point ranging from pH 1–7, in which the solutions are yellow, due to the neutral form of the majority of diferuloyl methane species. However, under highly alkaline conditions, the colour changes to orangish-red, as a consequence of the reaction of phenolic hydroxyl groups with hydroxyl ions which forms the phenoxide anion [47], [10].

Liu et al. stated that the addition of curcumin to k-carrageenan films produced indicative pH films with thermal stability and good barrier properties, for shrimp and pork freshness evaluation. Besides, as the pH became more alkaline, film's yellow colour turned to a red colour palette [48]. In the case of curcumin incorporated in tara gum/PVA films, it was reported by Wang et al. that it exhibited an instantaneous response on exposure to pH variations, in which the yellow films transitioned to orangish-red, when exposed to highly alkaline conditions [49]. Ezati et al., demonstrated that curcumin incorporated in composite films based on pectin containing sulfur nanoparticles can also be used to identify pH changes, in food packaging, since a pronounced colour change was shown, from yellow, under acidic conditions, to reddish-brown when the pH increased [50].

2

MATERIALS AND METHODS

The content in this chapter presents the materials and methods for the production and characterization of the CMC, CA and EC films with and without ANT, CUR and BE.

2.1 Films Preparation

2.1.1 Buffer solutions preparation

Buffer solutions of 13 different pH were prepared in accordance with Suppadit et al., presented in Table B.1.1, located in appendix. The pH was measured with a SevenCompact pH meter combined with a pH Electrode, from Mettler Toledo, USA, and a Microstirrer magnetic stirrer, from Velp Scientifica, Italy.

For the preparations of the buffer solutions, all the chemicals and solvents used were of analytical grade. Sodium phosphate dibasic (Na_2HPO_4), Potassium hydrogen phthalate (KHP) and sodium tetraborate decahydrate ($Na_2B_4O_7{\cdot}10H_2O$) were purchased by VWR Chemicals, USA; potassium dihydrogen phosphate (KH_2PO_4) and potassium chloride (KHP) from Sigma-Aldrich, USA; Sodium hydroxide (NaOH) from Fisher Chemical, USA and Hydrochloric acid (HCl) from José Manuel Gomes dos Santos, LDA, Portugal.

2.1.2 Extraction of Anthocyanins from red roses

The crude extract, which is a mixture of pigments, namely carotenoids, anthocyanins and flavonoids, was extracted from red roses according to Sampaio et al. [51] Red roses were purchased from the local market. Approximately, 50 g of petals roses were triturated with a mortar and pestle and then, mixed with 250 mL of Acetone (Carlo Erba Reagents, France) and 20 mL of HCl (Fisher Chemical, USA). Afterwards, the solution was covered with an aluminum foil, in order to be protected from light and heat, and was let to macerate over 20 min. Subsequently, the solution was filtered twice through a standard filter paper (Fisher Scientific, USA).

After this period, the solvent was removed from the supernatant using a rotary evaporator (RV 10 digital V, IKA, Germany) at 38 °C and stored in an ultra-low freezer for 24h at –80 °C (TSX Series Ultra-Low Freezer, ThermoFisher Scientific Co., Ltd., MA, USA). Finally, the solution was freeze-dried (LyoQuest, Telstar, Japan), under vacuum, protected from light using a tinfoil, over one week. The crude extract obtained is presented in Figure B.2.1.

2.1.3 pH-sensitive property

The pH-sensitive property of anthocyanins, curcumin and betalains was determined by dissolving 0.5% (w/w) of each dried extract in 5 mL of different buffer solutions, from pH 1 –13. The colour changes were captured by a digital camera (EOS M5 combined with EF-22 mm f/2 STM, Canon, Japan), after 1 minute.

2.1.4 Preparation of carboxymethylcellulose films

Natural dyes, namely, ANT and CUR [0.5%, 1% and 2% (w/v)] were dispersed in ethanol (99.8%) (Honeywell, USA), under stirring at 300 rpm, during 6 h, at room temperature. CMC (EMD Milipore Corp., USA) aqueous solution was prepared by dissolving 2% (w/v) CMC in ethanol/distilled water [1:1, (v/v)], under stirring at 300 rpm, during 18 h, at room temperature. Besides, it was added a concentration of 0.5% (v/v) of glycerol (≥ 99%) (Fisher Chemical, USA), according to Michelin et al. [52]. Afterwards, the final film-forming solutions were obtained by mixing these solutions (CMC and each indicator, ANT and CUR, 1:1, (v/v)) at 300 rpm, during 12 h.

For the production of CMC/BE film-forming solution, BE was dispersed in ethanol-water, under stirring at 300 rpm, during 6 h, at room temperature. CMC aqueous solution was prepared by dissolving 2% (w/v) CMC in 100% distilled water, under stirring at 300 rpm, during 18 h, at room temperature. Glycerol was also added in the solution, as a plasticizer, with a concentration of 0.5% (v/v). Afterwards, the final film-forming solutions were produced by mixing these two solutions [CMC and BE, 1:1, (v/v)], at 300 rpm, during 12 h.

The ANT, CUR and BE solubilization procedures for the development of CMC-based films are shown, respectively, Table B.3.1, Table B.4.1 and Table B.5.1, presented in appendix.

The CMC solutions (without natural dyes) were prepared as the control films. To produce the films, 28 mL of the film-forming solutions, specifically, neat CMC, CMC/ANT, CMC/CUR and CMC/BE were cast onto a Petri dish, with 9.5 cm diameter, and dried in an oven (UF160TS, Memmert, Germany) at 35 °C for 24 h.

It is important to consider that curcumin, was purchased from Gold Coast ingredients (USA), and its source is turmeric. While betalains corresponded to the Vegetable Juice Colour 45067, which its source was red beet, obtained from Food Ingredient Solutions, LLC, (USA).

2.1.5 Preparation of cellulose acetate films

The film-forming solution was prepared by dissolving 10% (w/v) of Cellulose Acetate (Sigma-Aldrich, USA), in which it has a number average molecular weight (M_n) of 50,000 by GPC (Gel Permeation Chromatography) in acetone (Carlo Erba Reagents, France). The solution was heated to 40 °C on a hot plate stirrer for about 18 h and then, cooled to room temperature. The control cellulose acetate films were produced by K-Hand Coater (RK Print Coat Instruments, United Kingdom). The optimization of cellulose acetate is presented in Table B.6.1, Table B.6.2, Table B.6.3, Table B.6.4 and Table B.6.5, in appendix.

From Table B.6.1 to Table B.6.4 it is used cellulose acetate (Sigma-Aldrich, USA), in which it has a number average molecular weight (M_n) of 30,000 by GPC.

The ANT, CUR and BE indicators were added to acetone in quantities of 0.5, 1 and 2% (w/v) and were magnetically stirred, during 6 h. The solutions were then decanted, in order to separate the insoluble solids from the liquid. Afterwards, the final film-forming solutions were produced by mixing these solutions [CA and each indicator, 2:1, (v/v)], at 300 rpm, during 12 h. The EC/ANT, EC/CUR and EC/BE films were produced by K-Hand Coater (RK Print Coat Instruments, United Kingdom).

2.1.6 Preparation of ethyl cellulose films

Film-forming solutions of ethyl cellulose (Sigma-Aldrich, USA) were prepared by dissolving 10% (w/v) ethyl cellulose in ethanol. Then, it was added to the film-forming solution, distilled diacetylated monoglyceride, known as MyVacet 9–45K (Kerry Ingredients & Flavours, *EMEA* Region, Ireland), as a plasticizer, at a constant concentration of 20% (w/w) of ethyl cellulose, under agitation (350 rpm) at room temperature, for 18 h. The ethyl cellulose and MyVacet 9–45K concentrations were chosen based on preliminary studies, shown in Table B.7.1, Table B.7.2, Table B.7.3, and Table B.7.4, in appendix. The control ethyl cellulose film was produced by K-Hand Coater.

Meanwhile, natural dyes were prepared as follows. ANT, CUR and BE solutions were produced by dispersing 0.5%, 1% and 2% (w/v) in ethanol, at room temperature, under stirring at 300 rpm, during 6 h. Lastly, the film-forming solutions were produced by mixing these solutions (EC and each indicator, 2:1, v/v) at 300 rpm, during 12 h. The EC/ANT, EC/CUR and EC/BE films were produced by K-Hand Coater.

2.2 Films characterization

As this work was developed, different films characterizations were handled, allowing for an accurate stage evaluation and proceed through the next steps.

2.2.1 Films pH sensing characteristics

The CMC, CA and EC films with and without ANT, CUR and BE were cut into 1×1 cm^2, after which the films colouration was demonstrated, when were exposed to 20 μL of the prepared buffer solutions, in the pH region 1 to 13. After 1 minute of the colour changes occurrence, the films images were recorded by a digital camera (EOS M5 combined with EF-22 mm f/2 STM, Canon, Japan).

2.2.2 Colour and opacity of the films

The films colour was determined by using a portable colorimeter (CR 400, Minolta, Japan). As standards for calibration, it was used white and black plates. To evaluate the films colour, L* (lightness), a* (redness-greenness), b* (yellowness-blueness) values were examined, in which three film replicates were carried out with five reflectance measurements each. In order to determine the films opacity, it was used the Hunterlab method, through the relationship between film opacity on a black standard and a white standard. The total colour difference (ΔE) was calculated as follows in equation 1:

$$\Delta E = \sqrt{(L^* - L)^2 + (a^* - a)^2 + (b^* - b)^2} \quad (1)$$

where L* = 95.83, a* = −0.02 and b* = 2.32; L* = 95.77, a* = −0.10 and b* = 2.70 and L* = 96.05, a* = 0.25 and b* = 2.12 represented colour values of neat CMC 5050, CMC 100 and CA.

2.2.3 Scanning electron microscopy (SEM)

Micrographs of the CMC and CA films with and without the indicators were examined by SEM under (Quanta FEG 650, FEI, USA) with an accelerating voltage of 5 kV, at different magnifications. Prior to observation, the films were fixed on aluminium stubs, by using carbon adhesive tape, and the surface was coated with a thin gold layer.

2.2.4 Fourier-transform infrared (FTIR) spectroscopy

The FTIR spectra of the samples were obtained with a Bruker FT-IR VERTEX 80/80v (Boston, USA) at a resolution of 4 cm^{-1}, with 64 scans and in the wavenumber range of $4000 - 400$ cm^{-1}, by Attenuated Total Reflectance mode (ATR) technique with a platinum crystal accessory. The FTIR analysis was performed in triplicate and aimed to determine the surface differences at the molecular scale of the prepared films induced by the addition of ANT, CUR and BE.

2.2.5 Mechanical Properties

The films thickness was measured using a micrometer (Schut Geometrical Metrology, Netherlands), and reported as the average from five random points. The average values were used to calculate the films mechanical properties.

The films tensile strength (TS, MPa) and elongation at break (EB, %) were measured by an auto tensile tester (Autograph AGS-X Series, USA) with the software TRAPEZIUM LITE X, equipped with a 500 N load cell. The films thickness was also used for determining the tensile strength (TS). Before the mechanical properties' measurements, rectangular thin specimen strips were prepared (2 mm × 5 mm), which were clamped between grips with an initial distance of 50 mm. The force and deformation were recorded during extension at 12.5 mm/min. Five replicates per experimental sample were conducted and all testing occurred at room temperature.

2.2.6 Moisture content

The films moisture content (MC) was measured by drying the film samples (2 cm × 2 cm) in an oven, at 105 °C for 24 h, until the equilibrium weight was achieved. The MC values were calculated, in triplicate for each film, as the weight loss percentage relative to the original weight, using the following Equation (2):

$$\text{Moisture content } (\%) = \frac{(W_i - W_f)}{W_i} \times 100 \quad (2)$$

Where W_i and W_f were the original and final weights of film samples, respectively (measured using a ENTRIS224 – 1S Analytical Balance, Sartorius, Germany).

2.2.7 Visual analysis of the films

To conduct the visual analysis, the film samples (2 cm × 2 cm) were used as labels for monitoring the quality of a food product. Atlantic salmon, purchased from a local market, was placed at the bottom of each container, and the films were applied near its headspace. The prepared samples were stored at room temperature, and the films colour was observed without taking out of the container. The films images were recorded by a digital camera over 5 days.

2.2.8 Statistical analysis

Statistical analysis was performed using VassarStats website. One-way analysis of variance and Turkey's test were applied to detect difference of means, in which $p < 0.05$ was defined to be statistically significant. It is important to consider that different letters (a – d) in the same columns indicated a significantly difference ($p < 0.05$).

3

EXPERIMENTAL RESULTS

In this chapter, the results of the current work are exposed and discussed, according to the main goal of this project.

3.1 Colour changes of buffer solutions with indicators

Anthocyanin (ANT) was successfully extracted from roses. The colour change in buffer solutions with an ANT concentration of 0.5% from pH 1 to 13 is shown in Figure 2. Visually, at pH 1 and 2, the extract solution displayed a red colour, and then, at pH 3, it revealed a crimson colour. However, when the pH solution was increased to pH 4–6, the crimson colour became paler. At pH 7, the colour of the extract solution became purple, which intensified as the pH increase to 10. Then, at pH 11, it showed an intense blue colour. Lastly, at pH 12 and 13, the indicator turned to a khaki colour. The change in colour upon contact with different pH values, showed clearly the advantage associated with the use of anthocyanin as a pH indicator. It is worth mentioning that anthocyanins extracted from red roses are sensitive and, so, undergo full-colour changes within 5 seconds. Besides, since it is a crude extract, the obtained colour changes are different from the purified extract of roses. [51]

The visual colour changes of betalains solutions, at various pH, from 1 to 13, is shown in Figure 3. At pH 1, the solution exhibited a purplish red colour. When the pH was between 2 and 8, the colour did not change significantly, confirming that this indicator is colour stable in the pH range 3 to 7. Additionally, the solution's colour was changed from red to purple, as the pH increased to 10. As the pH reaches to alkaline conditions (pH 13), the solution's colour was turned into yellow due to the conversion of betalains to betaxanthins.

Curcumin solutions' visual colour change, from 1 to 13, is shown in Figure 4. As observed in this image, below pH 8, curcumin was yellow, which is possible to conclude that the optimum pH range is from pH 1 to 7. At pH 8, it was enhanced in colour into yellow-orange. As the pH increased further, in alkaline conditions, the yellow-orange colour transitioned to red which became more intense, into a dark red/reddish brown colour. Curcumin is an ideal natural dye for the development of intelligent packaging to monitor the food's quality due to its reversible structural transformations, visible at naked eye, with its colour changes at different pH.

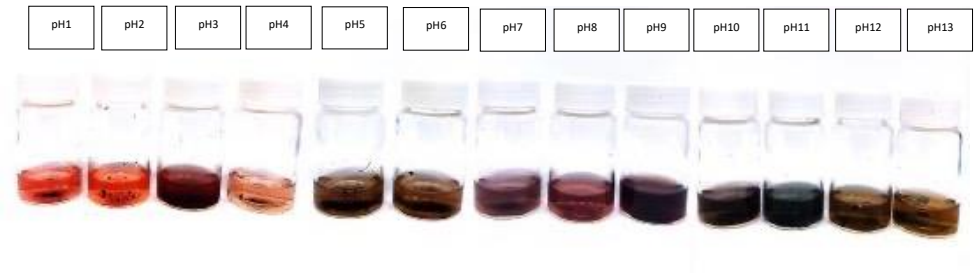

Figure 2 – Colour changes in buffer solutions with anthocyanin from pH 1 to 13.

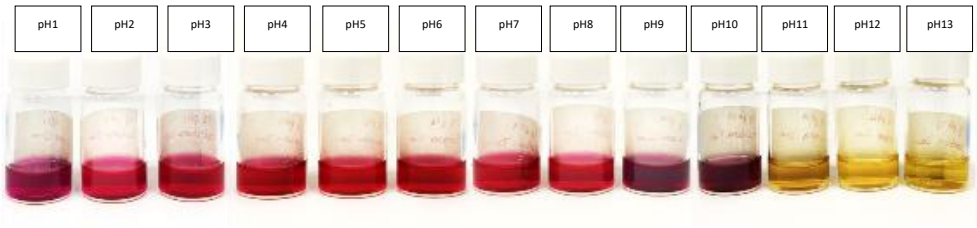

Figure 3 – Colour changes in buffer solutions with betalains from pH 1 to 13.

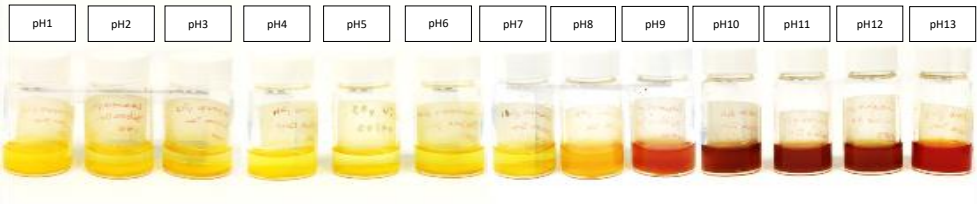

Figure 4 – Colour changes in buffer solutions with curcumin from pH 1 to 13.

3.2 Films' characterization

3.2.1 CMC-based films

After analysing the natural dyes solubilization, for the development of CMC-based films, it was verified that anthocyanins (ANT) and curcumin (CUR), when dissolved in ethanol/distilled water mixture, as solvent, solubilized better (Table B.3.1 and Table B.4.1, respectively).

The visual appearance of CMC-based films in ethanol/distilled water solution [1:1, (v/v)], is represented in Figure C.1.1.1. As expected, the control films exhibited an uniform, transparent and smooth surface, as observed in Figure C.1.1.1 (a). Whereas Figure C.1.1.1 (b) to C.1.1.1 (d), demonstrated the incorporation of the indicator ANT into the CMC-based films. The films remained visually homogeneous, thin and flexible, in the presence of the natural dye with an intense brown colour which was significantly influenced due to the increase of ANT concentration. Also, CMC-based films with the incorporation of curcumin showed not only a visually homogeneous curcumin distribution into the film, but also an intense orange colour as the indicator concentration increased. Thus, the concentration of curcumin had a significant influence on the colour of CMC-based films, as observed in Figure C.1.1.1 (e) to C.1.1.1 (g).

When betalains was dissolved in the three different solvents, it was verified that this indicator solubilized better in water, as solvent (Table B.5.1). Taking that into consideration, it was prepared CMC-based films (in an 100% of distilled water solution), which showed an uniform and transparent surface, as observed in Figure C.1.1.2 (a). Figure C.1.1.2 (b) to C.1.1.2 (d) reveals not only that the films became darker as the indicator's concentration increased, but also a visually homogeneous betalains distribution into the films.

3.2.2 CA-based films

In order to prepare the optimized cellulose acetate films, different concentrations, from 1 to 10% (w/v) of CA, with the number average molecular weight of 30,000 by GPC, were solubilized in acetone, and dried at ambient temperature, during overnight. However, as shown in Table B.6.1, presented in annexes, the CA films were relatively strong and stiff, with low flexibility.

Then, the same procedure was carried out, but with the addition of two different plasticizers, glycerol, and MyVacet 9-45K, in a ratio of 0.5% (w/w) of CA. Nevertheless, the same results were observed, as shown in Table B.6.2 and Table B.6.3, respectively. Then, based on the results obtained in the article [53], it was used MyVacet 9-45K, in a ratio of 20% (w/w) of CA. In Table B.6.4, it was verified that the CA films presented higher flexibility, for higher concentrations of CA (7-10%).

Lastly, it was tested different concentrations, from 1 to 10% (w/v), of cellulose acetate, with the number average molecular weight of 50,000 by GPC, in which they were solubilized in acetone, without any plasticizer. Moreover, it was tried another production process with the use of a K-Hand Coater, which provides a simple, but effective means of applying surface coatings onto a glass plate. For lower concentrations of CA (1-6%), the solutions were not viscous enough to create a film. For higher CA concentrations (7-9%), the solutions were viscous enough to create a film, but with low flexibility. Lastly, for a concentration of 10% of CA, the solution was not only viscous enough to create a film, but also, had higher flexibility. Consequently, it was observed that this was the optimized film, as shown in Table B.6.5.

As observed in Figure C.1.2.1 (a), the neat CA films without natural dyes, produced by K-Hand Coater had become transparent, deprived of aggregates. Figure C.1.2.1 (b) to C.1.2.1 (d) demonstrated CA-based films with the incorporation of ANT, which showed not only a visually homogeneous ANT distribution into the film, but also an intense brown colour as the indicator concentration increased. It is possible to conclude that the concentration of ANT had a significant influence on the colour of CA-based films. Additionally, Figure C.1.2.1 (f) to C.1.2.1 (h) presented the incorporation of the indicator CUR into the CA-based films. The films remained visually flexible, in the presence of the natural dye with an intense orange colour which was significantly influenced due to the increase of CUR concentration. Figure C.1.2.1 (h) to C.1.2.1 (j) presented the incorporation BE into the CA film. In the presence of betalains, an intense homogeneous pink colour was observed which was significantly influenced due its concentration increasing. Also, the films remained visually thin and flexible.

3.2.3 EC-based films

The neat EC films were developed and optimized based on the results presented elsewhere [53]. Additionally, a concentration of 10% of Ethyl Cellulose (w/v) in ethanol was used. Also, the plasticizer MyVacet 9–45K was tested in different concentrations (0, 10 and 20%).

As it was verified in the article [53], the use of MyVacet 9–45K in a ratio of 20% (w/w) of ethyl cellulose was the most efficient plasticizer grade. However, the films dried at 60 °C (Table B.7.1) and 35 °C (Table B.7.2) did not correspond to the obtained films elsewhere [53], that can be justified by the presence of air bubbles inside the EC films.

Afterwards, it was tried another production process with the use of a K-Hand Coater. It was possible to observe that for lower concentrations of MyVacet, the solutions were not viscous enough to form a film, but when the concentrations increased to 20%, the solutions were viscous enough to create a film with flexibility (Table B.7.3). The results are in agreement with the published work [53].

Then, two coating machines were tested, the K-Hand Coater and the K-Control Coater (RK Print Coat Instruments, United Kingdom), which is an automatic machine in which it was exerted with a constant pressure (2) and speed (from 1 to 10). It is important to verify that the close wound bars used, produce coating thicknesses from 40 to 150 µm, depending on the bar colour (Table B.7.5). It was possible to verify that the films produced by the K-Control coater have lower thicknesses when compared to the films produced manually

(Table B.7.4). Additionally, it was decided to produce the ethyl cellulose and acetate cellulose films manually with the Black Bar.

As observed in Figure C.1.3.1 (a), the control EC films produced by K-Hand Coater had become colourless and uniform without forming aggregates. Figure C.1.3.1 (b) to C.1.3.1 (d) shows the incorporation of the indicator ANT into the EC-based films. The increase of ANT concentration influenced the films colour to an intense brown colour. Nevertheless, the EC-based films remained visually homogeneous, thin and flexible. Similarly, EC-based films with the incorporation of CUR showed an intense and homogeneous orange colour, as the indicator concentration increased. Thus, the concentration of curcumin had a significant influence on the colour of CMC-based films, as observed in Figure C.1.3.1 (e) to C.1.3.1 (g). Lastly, Figure C.1.3.1 (h) to C.1.3.1 (j) revealled a visually homogeneous betalains distribution into the films, which not became darker as the indicator's concentration increased, as well.

3.3 Films pH sensing characteristics

For the evaluation of the pH sensing capacity of the films, CMC, CA and EC films without and with the incorporation of anthocyanins, curcumin and betalains [0.5, 1 and 2% (w/w)] were immersed in buffer solutions with pH ranged from 1 to 13. Commonly, the colour change on these pH indicative films occurred very quickly, usually in less than 1 minute.

Figure C.2.1, Figure C.2.2 and Figure C.2.3, illustrates the CMC/ANT [0.5, 1 and 2% (w/w)] colour variations in function of the pH values, which could be attributed to the ANT chemical structure transformations. For instance, Figure 5, represents the CMC film incorporated with 0.5% (w/w) ANT, in which at pH 1, this film shown a reddish colour [Figure 5 (b)], and markedly changed its colour from reddish to brown as the pH increased to 10 [Figure 5 (c)]. With an increase of pH to 13, the film's colour became a dark green [Figure 5 (d)].

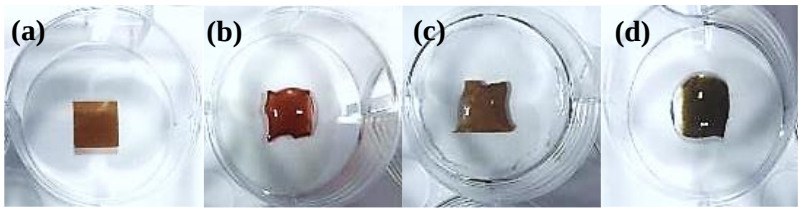

Figure 5 – Carboxymethylcellulose-based films with the incorporation of 0.5% (w/w) of anthocyanins. (a) control film without the immersion in buffer solutions, (b) resulted film at pH 1, (c) at pH 10 and (d) at pH 13, respectively.

At the same pH levels, the colour of CMC/ANT films gradually intensified when ANT content increased. Additionally, it was possible to verify that ANT is sensitive to pH change, which causes its structural changes. Also, the vivid colour changes of CMC/ANT films against the pH values have enabled their application as pH indicator in food packaging. Yoshida et al. evaluated the colour indicator response of chitosan/anthocyanins films by the immersion in buffer solutions (pH 2 to 13). It was demonstrated that the films became pink when submitted to acid pH, it became bluish/green in a neutral pH, and, it was a yellow colour basic pH [54]. Perhaps, the pH colour variation differences between chitosan/ANT films, presented in the article [54], and CMC/ANT films, prepared during this project, were due to the impurity of the ANT crude extract.

The resulting visual colour changes of CMC/CUR films are shown in Figure C.2.4, Figure C.2.5 and Figure C.2.6. The CMC/CUR [0.5, 1 and 2% (w/w)] films presented yellow in colour in a pH range between 1 and 10. When the pH increased from 11 to 13, a sudden change in colour was detected, indicating a strong orange colour under alkaline conditions. Figure 6 demonstrates the colour variations of CMC/CUR (0.5 (w/w)).

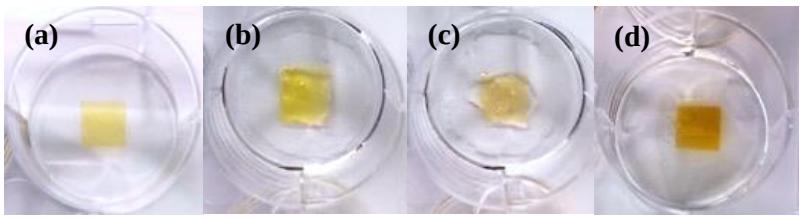

Figure 6 – Carboxymethylcellulose-based films with the incorporation of 0.5% (w/w) of curcumin. (a) control film without the immersion in buffer solutions, (b) resulted film at pH 1, (c) at pH 10 and (d) at pH 13, respectively.

Furthermore, not only the orange colour was enhanced with the increase of alkalinity, but also, as the amount of the indicator increased, from 0.5% to 2%, the film's colour intensified as well, under the same pH (verified in Figure 7). This phenomenon can be explained by the changes of the predominant CUR structure under different pH conditions, in which the phenolic hydroxyl group could readily react with OH to form phenoxide anion. The CMC/CUR [0.5, 1 and 2% (w/w)] composite films can be used to detect pH changes in packaged foods, since the colour changed from yellow to orange with increasing pH. Similar pH-reactive colour changes were observed in different pH values by Wu et al. (2019) and Liu et al. (2018) [45], [48].

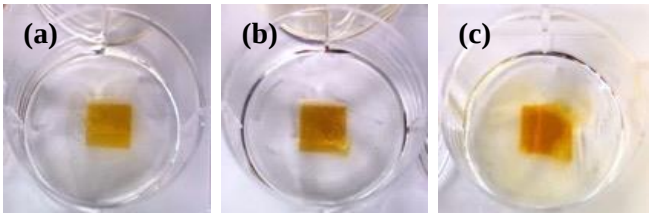

Figure 7 – At pH 13, (a) carboxymethylcellulose-based films with the incorporation of 0.5% (w/w) of curcumin. (b) carboxymethylcellulose-based films with the incorporation of 1% (w/w) of curcumin, (c) carboxymethylcellulose-based films with the incorporation of 2% (w/w) of curcumin.

The photographs of CMC/BE [0.5, 1 and 2% (w/w)] films in different pH solutions are shown in Figure C.2.7, Figure C.2.8 and Figure C.2.9. The CMC/BE [0.5, 1 and 2% (w/w)] composite films gradually changed their colour from pink to yellow, when the pH increased from 10 to 13 (proved in Figure 8). The films colour change was attributed to the betalains pH-sensitive property under alkaline conditions, due to the degradation of red betacyanins into yellow betalamic acid. Qin et al. also reported that starch/polyvinyl alcohol films containing betalains from red pitaya present colour changes, from pink to yellow, in alkaline medium [55].

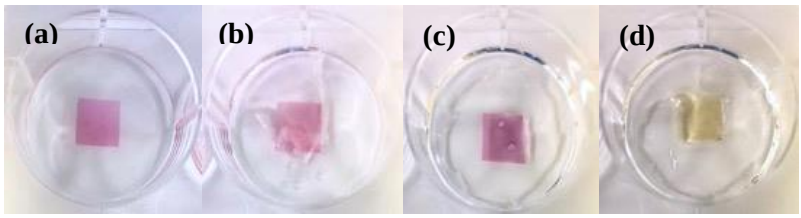

Figure 8 – Carboxymethylcellulose-based films with the incorporation of 2% (w/w) of betalains. (a) control film without the immersion in buffer solutions, (b) resulted film at pH 1, (c) at pH 10 and (d) at pH 13, respectively.

As observed in Figure C.2.10, the neat CMC film continue to be transparent and colourless, under acidic and basic conditions, since no indicator was added (demonstrated in Figure 9). This result further confirmed the pH-sensitive property of CMC/ANT, CMC/CUR and CMC/BE films was attributed to the indicators, which was consistent with the pH-sensitive property of them. It is important to verify that all CMC films presented pH-dependent swelling characteristics, in which it was observed the solvents' diffusion into the polymer network that caused an abrupt visual change in the CMC films [56].

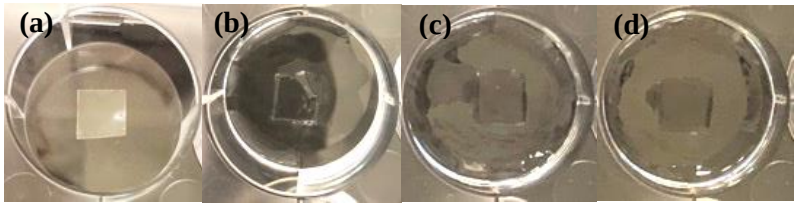

Figure 9 – Neat carboxymethylcellulose-based films. (a) control film without the immersion in buffer solutions, (b) resulted film at pH 1, (c) at pH 10 and (d) at pH 13, respectively.

Figure C.2.11 exhibited the CA/ANT [0.5% (w/w)] composite film, under different pH conditions, from 1 to 13, in which it was preserved its pink colour. Also, the CA/ANT [1% (w/w)], Figure C.2.12, composite film maintained its pink colour, from pH 1 to 9. However, when the pH increased from 10 to 13, its colour turned to a light and bright colour. Lastly, the CA/ANT [2% (w/w)] film, Figure C.2.13, did not change its brown colour under acidic conditions. When it was immersed in alkaline solutions, the film changed its colour to green. Figure 10 sums up the colour variations of CA/ANT films.

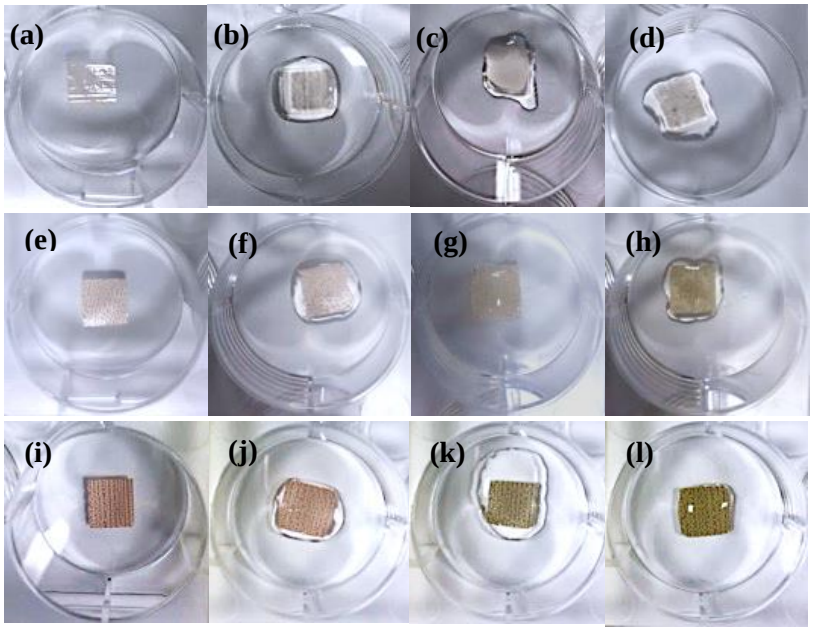

Figure 10 – Cellulose acetate-based films with the incorporation of 0.5% (w/w) of anthocyanins: (a) control film without the immersion in buffer solutions, (b) resulted film at pH 1, (c) at pH 10 and (d) at pH 13, respectively. Cellulose acetate-based films with the incorporation of 1% (w/w) of anthocyanins: (e) control film without the immersion in buffer solutions (f) resulted film at pH 1, (g) at pH 10 and (h) at pH 13, respectively. Cellulose acetate-based films with the incorporation of 2% (w/w) of anthocyanins: (i) control film without the immersion in buffer solutions, (j) resulted film at pH 1, (k) at pH 10 and (l) at pH 13, respectively.

As presented in Figure C.2.14, Figure C.2.15 and Figure C.2.16 the CA/CUR [0.5, 1 and 2% (w/w)] composite films also showed a pronounced colour change from yellow to orange when immersed in different buffer solutions (pH 1 – 13). Nevertheless, the CA/CUR [0.5, 1 and 2% (w/w)] composite films only changed their colour from yellow to orange only at pH 13. Hence, these films presented pH resistance, from pH 1 to 12. The colour variations of CA/CUR are summarized in Figure 11.

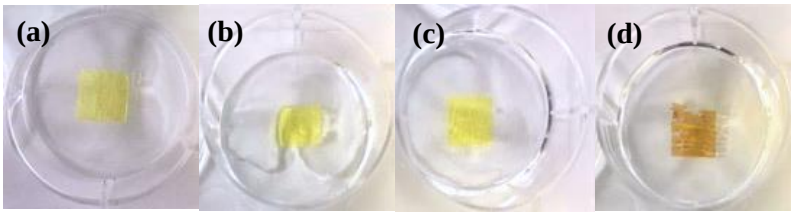

Figure 11 – Cellulose acetate-based films with the incorporation of 2% (w/w) of curcumin: (a) control film without the immersion in buffer solutions, (b) resulted film at pH 1, (c) at pH 10 and (d) at pH 13, respectively.

The CA/BE [0.5, 1 and 2% (w/w)] composite films also showed a pronounced colour change from pink to transparent when immersed in a buffer solution in the pH range of 1 – 13. The corresponding visual images are shown in Figure C.2.17, Figure C.2.18 and Figure C.2.19. The betalains pH-sensitive property under alkaline conditions was due to the degradation of red betacyanins into colourless *cyclo-Dopa* 5-O-(malonyl)-*β*-glucoside. [57] This phenomenon is observed in Figure 12.

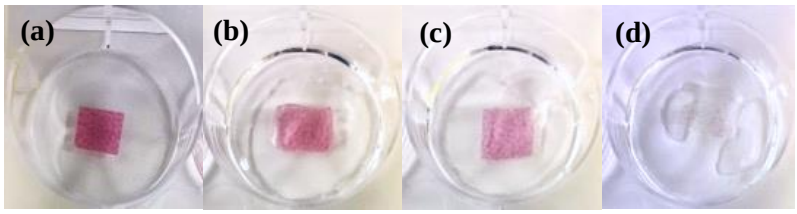

Figure 12 – Cellulose acetate-based films with the incorporation of 2 %(w/w) of betalains: (a) control film without the immersion in buffer solutions, (b) resulted film at pH 1, (c) at pH 10 and (d) at pH 13, respectively.

The control CA films demonstrated to be colourless and showed no significant colour change in different buffer solutions (Figure 13). Also, Figure C.2.20 presents the neat CA films immersed in buffer solutions with pH ranged from 1 to 13. It is important to notice that the pH-sensitive property of the CA films incorporated with the different indicators was attributed to the ANT, CUR and BE.

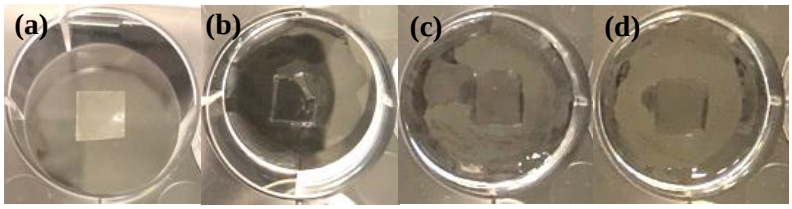

Figure 13 – Neat cellulose acetate-based films: (a) control film without the immersion in buffer solutions, (b) resulted film at pH 1, (c) at pH 10 and (d) at pH 13, respectively

As shown in Figure C.2.21 to Figure C.2.30, the EC composite films without and with the incorporation of anthocyanins, curcumin and betalains, did not present a colour response after being immersed to different buffer solutions, from pH 1 to 13. This occurrence is verified in Figure 14.

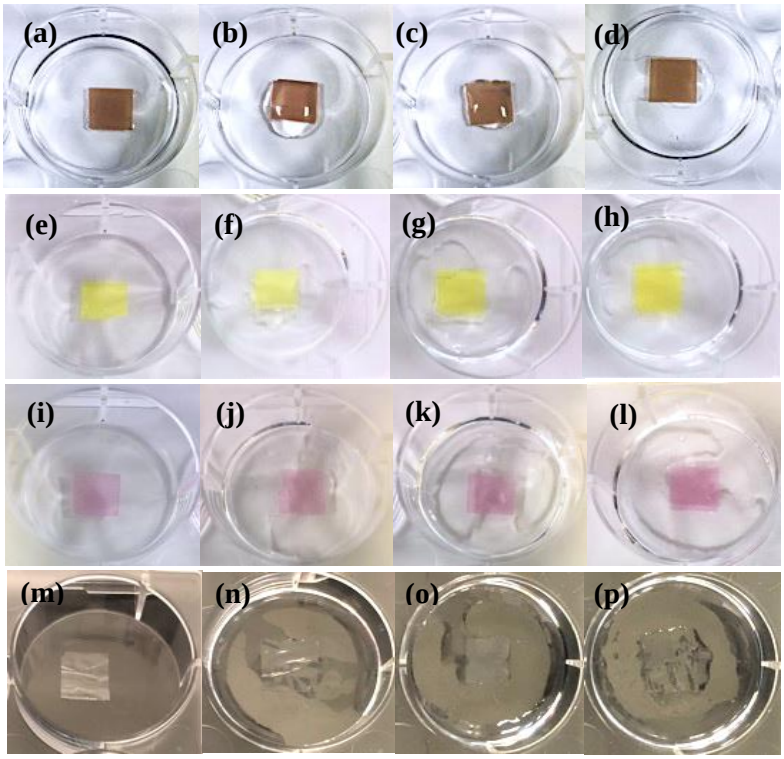

Figure 14 – Ethyl cellulose-based films with the incorporation of 2% (w/w) of anthocyanins: (a) control film without the immersion in buffer solutions, (b) resulted film at pH 1, (c) at pH 10 and (d) at pH 13, respectively. Ethyl cellulose-based films with the incorporation of 2% (w/w) of curcumin: (e) control film without the immersion in buffer solutions, (f) resulted film at pH 1, (g) at pH 10 and (h) at pH 13, respectively. Ethyl cellulose-based films with the incorporation of 2% (w/w) of betalains: (i) control film without the immersion in buffer solutions, (j) resulted film at pH 1, (k) at pH 10 and (l) at pH 13, respectively. Neat ethyl cellulose-based films: (a) control film (b) resulted film at pH 1, (c) at pH 10 and (d) at pH 13, respectively.

It was concluded that the EC composite films and CA/ANT [0.5% (w/w)] could not be used to detect pH changes in packaged foods, due to its pH resistance: Therefore, it was decided not to characterize these films.

3.4 Colour and Opacity of the films

The colour and the opacity values of the CMC and CA-based films are listed in below. Generally, the L* (lightness) value ranges from 0 (black) to 100 (white); the a* value ranges from –80 (greenness) to 100 (redness); and the b* value ranges from –80 (blueness) to 70 (yellowness). Table 1 represents the colour parameters and opacity values of CMC-based films with the incorporation of ANT [0.5, 1 and 2% (w/w)]. As it was concluded in Figure C.1.1.1 (a), CMC 5050 film was transparent and colourless. Consequently, the CMC 5050 film demonstrated to have the highest L* value, but the lowest opacity and total colour difference (ΔE) values, when compared to CMC/ANT films.

The CMC-based films with the incorporation of ANT showed an intense brown colour as the indicator concentration increased [Figure C.1.1.1 (b) to C.1.1 1 (d)]. Moreover, when ANT contents increased from 0.5 to 2%, the films showed a significant decrease ($p < 0.05$) of L* value (lightness) from 44.06 to 15.44 (darkness-shift). By contrast, a significant increase of opacity ($p < 0.05$) from 27.47 ± 3.90 to 92.34 ± 9.99% was observed. The total colour difference (ΔE) also increased, which indicated a good colour variation of the indicator. It is important to mention that for ANT/CMC (0.5 and 1%) films, the a* and b* parameters were higher when compared to ANT/CMC (2%) film, which indicated that for lower ANT concentrations, the films were more reddish and yellow. The colorimetric parameters of the indicator are similar to the colour variation of PVA/CMC incorporated with red cabbage anthocyanin, in which the increase of content resulted in the

decrease of L* and the increase of ΔE value, suggesting the appearance of the films' colour could be influenced by the natural dye content [36].

Table 1 – Colour parameters and opacity values of carboxymethylcellulose-based films with the incorporation of anthocyanins.

Films	L*	a*	b*	Opacity (%)	ΔE
CMC 5050	95.77 ± 1.19^{a}	-0.10 ± 0.07^{a}	2.70 ± 0.57^{ab}	7.42 ± 0.94^{a}	0
CMC/ANT (0.5%)	44.06 ± 3.52^{b}	27.28 ± 2.41^{b}	15.00 ± 4.05^{b}	27.47 ± 3.90^{b}	60.29 ± 2.88
CMC/ANT (1%)	33.26 ± 12.88^{bc}	27.62 ± 2.51^{b}	8.23 ± 9.93^{ab}	43.91 ± 17.77^{c}	76.04 ± 1.32
CMC/ANT (2%)	15.44 ± 11.71^{c}	7.71 ± 5.13^{a}	-6.56 ± 6.90^{a}	92.34 ± 9.99^{d}	76.09 ± 1.12

Values reported are the mean ± sd. Different letters (a – d), in the same column, indicate a statically difference ($p < 0.05$).

Figure C.1.1.1 (e) to C.1.1.1 (g) demonstrated the incorporation of the indicator CUR into the CMC-based films, in which an intense orange colour was observed, with the increase of the natural dye concentration. Additionally, as shown in Table 2, with the addition of curcumin, in concentration ranged from 0.5 to 2%, the L* value gradually decreased from 79.03 to 65.31 (darkness-shift), while the opacity, a* (redness-shift), b* (yellowness-shift), and ΔE parameters presented higher values in relation to ones obtained for the neat CMC-based films. These results were consistent with the results of Liu et al. in which films-based on k-carrageenan incorporated with curcumin were produced. It was concluded that the film colour is CUR content dependent, since the films showed a decrease of L* (from 96.16 to 61.88), an increase of the b* parameter (from 4.82 to 65.29), and an increase the ΔE value (2.99 to 75.84), when compared to the control film [48].

Table 2 – Colour parameters and opacity values of carboxymethylcellulose-based films with the incorporation of curcumin.

Films	L*	a*	b*	Opacity (%)	ΔE
CMC 5050	95.77 ± 1.19^{a}	-0.10 ± 0.07^{a}	2.70 ± 0.57^{a}	7.42 ± 0.94^{a}	0
CMC/CUR (0.5%)	79.03 ± 1.86^{b}	12.20 ± 2.72^{b}	46.28 ± 0.61^{b}	16.59 ± 0.62^{b}	49.43 ± 0.76
CMC/CUR (1%)	71.85 ± 0.78^{c}	22.84 ± 0.71^{c}	41.48 ± 0.58^{c}	23.07 ± 1.90^{c}	52.04 ± 0.24
CMC/CUR (2%)	65.31 ± 1.64^{d}	29.20 ± 1.51^{d}	35.17 ± 1.29^{d}	32.13 ± 2.11^{d}	54.30 ± 1.01

Values reported are the mean ± sd. Different letters (a – d), in the same column, indicate a statically difference ($p < 0.05$).

Table 3 represents the colour parameters and opacity values of CMC-based films with the incorporation of BE [0.5, 1 and 2% (w/w)]. As it was concluded in Figure C.1.1.2 (a), CMC 100 films were transparent and colourless with the highest L* value, but the lowest opacity and total colour difference (ΔE) value. The CMC/BE films showed an intense pink colour as the indicator concentration increased [Figure C.1.1.2 (b) to C.1.1.2 (d)]. Furthermore, it was verified lower L*, ranging from 46.62 to 33.49 values, but higher opacity values (from 19.01 to 31.95%) when compared to the neat CMC film ($p < 0.05$). Also, the total colour difference (ΔE) was significantly affected by the addition of BE, which increased to 89.90 with the addition of BE. Lastly, a higher value of the parameter a* above zero indicated the colour tendency to red, confirming that once applied in the film matrix, the natural colour changing pigment keeps its property of becoming pinker.

Similar observation has been reported previously for PVA/gelatin food packaging film incorporated with betalains. It was verified that the incorporation of BE affected significantly the films opacity, since it was higher (0.149) when compared to the neat film opacity (0.031). Also, the L* value of neat film (40.98) was higher than the active film (32.87), indicating that films incorporated with betalains were darker. It was also concluded that BE presence in the films were responsible for giving its pink colour, due the significant increase of the a* parameter, compared to control film [58].

Table 3 – Colour parameters and opacity values of carboxymethylcellulose-based films with the incorporation of betalains.

Films	L*	a*	b*	Opacity (%)	ΔE
CMC 100	95.83 ± 0.26^{a}	-0.02 ± 0.08^{a}	2.32 ± 0.31^{a}	7.77 ± 0.83^{a}	0
CMC/BE (0.5%)	46.62 ± 1.98^{b}	74.98 ± 1.45^{b}	-24.44 ± 4.02^{b}	19.01 ± 0.76^{b}	94.05 ± 1.26
CMC/BE (1%)	34.45 ± 3.52^{c}	66.85 ± 7.14^{bc}	-2.55 ± 5.85^{a}	31.38 ± 5.25^{c}	91.79 ± 2.84
CMC/BE (2%)	33.49 ± 1.46^{c}	63.78 ± 3.46^{c}	4.81 ± 1.68^{a}	31.95 ± 2.31^{c}	89.90 ± 1.34

Values reported are the mean ± sd. Different letters (a – d), in the same column, indicate a statically difference ($p < 0.05$).

As indicated from the data, the CMC films colour is dependent on the indicator's contents, whereas the reduction of lightness and the increase in opacity, as a consequence of the incorporation of natural extracts into the CMC polymer and other materials have also been observed by other researchers [52]. The colour results of the produced CA films with the incorporation of ANT are presented in Table 4. As expected from Figure C.1.2.1 (a), the CA films were transparent and colourless with the lowest opacity and total colour difference (ΔE) values. Figure C.1.2.1 (b) to C.1.2.1 (d) demonstrated that the CA-based films with the incorporation of ANT showed an intense brown colour, as the indicator concentration increased, which was possible that it had a significant influence on the CA-based films colour.

Compared to those values of neat CA film, the values of a* and b* of CA/ANT increased considerably ($p < 0.05$), indicating that the colour of the colorimetric films changed to red and yellow as increasing anthocyanin content. Additionally, the ΔE of the CA/ANT films were much higher than the neat CA films, indicating the CA/ANT films were more coloured. However, the increase of anthocyanins content resulted in the decrease of L* and opacity parameters, suggesting that the colour appearance could be influenced by the content of anthocyanins. Freitas et al. also found that the addition of anthocyanins, extracted from red cabbage, in CA films increases the a* parameter [59].

Table 4 – Colour parameters and opacity values of cellulose acetate-based films with the incorporation of anthocyanins.

Films	L*	a*	b*	Opacity (%)	ΔE
CA	96.05 ± 0.14^{a}	0.25 ± 0.02^{a}	2.12 ± 0.13^{a}	8.10 ± 0.21^{a}	0
CA/ANT (0.5%)	87.23 ± 1.49^{b}	3.90 ± 0.72^{b}	11.12 ± 1.54^{bc}	12.35 ± 1.98^{a}	13.81 ± 2.26
CA/ANT (1%)	85.23 ± 1.60^{b}	6.57 ± 1.23^{c}	10.32 ± 0.44^{b}	91.68 ± 3.61^{b}	15.70 ± 1.88
CA/ANT (2%)	68.64 ± 1.84^{c}	11.21 ± 0.63^{d}	12.97 ± 0.18^{c}	97.32 ± 0.80^{c}	32.22 ± 1.81

Values reported are the mean ± sd. Different letters (a – d), in the same column, indicate a statically difference ($p < 0.05$).

Figure C.1.2.1 (f) to C.1.2.1 (h) presented the incorporation of the indicator CUR into the CA-based films in which the presence of the natural dye with an intense orange colour was significantly influenced due to the increase of CUR concentration. As displayed in Table 5, considering the lightness parameter, no significant difference was observed with the addition of curcumin in the CA films. Nevertheless, when compared to the opacity values, the CA/CUR (2%) film had a significant difference ($p < 0.05$) in relation to CA/CUR [0.5 and 1% (w/w)]. The increase of CUR concentration, markedly decreased the a* value, while the b* (yellowness-shift) value increased from 2.05 to 31.88. Bitencourt et al. reported that the L * values decreased and b * parameter increased for gelatin-based films with Curcuma ethanol extract when compared to the control films [46].

Table 5 – Colour parameters and opacity values of cellulose acetate-based films with the incorporation of curcumin.

Films	L*	a*	b*	Opacity (%)	ΔE
CA	96.05 ± 0.14^{a}	0.25 ± 0.02^{a}	2.12 ± 0.13^{a}	8.10 ± 0.21^{a}	0
CA/CUR (0.5%)	96.58 ± 0.36^{ab}	0.16 ± 2.54^{a}	2.05 ± 4.38^{a}	11.40 ± 2.61^{a}	3.58 ± 1.99
CA/CUR (1%)	97.02 ± 0.31^{b}	-4.84 ± 2.11^{b}	13.12 ± 3.95^{b}	10.56 ± 0.25^{a}	12.31 ± 4.45
CA/CUR (2%)	96.57 ± 0.20^{ab}	-13.10 ± 0.72^{c}	31.88 ± 1.78^{c}	15.88 ± 1.82^{b}	32.79 ± 1.91

Values reported are the mean ± sd. Different letters (a – d), in the same column, indicate a statically difference ($p < 0.05$).

As observed in Figure C.1.2.1 (h) to C.1.2.1 (j), an intense pink colour was verified with the betalains incorporation into the CA film, which was significantly influenced due its concentration increasing. Lastly for the CA/BE films, Table 6, it was verified a significant decrease in the L* and b* parameters ($p < 0.05$), whereas the a* value significantly increased ($p < 0.05$), as a function of increasing betalains extract quantities. These results were caused by an increase in BE pigments characterized by a pink-reddish colour in the films. Qin et al. (2020) found a pink colour for starch/PVA film containing betacyanins-rich red pitaya peel extract. The films' pink colour deepened when BE content increased, which was in agreement with the gradually increased luminance and ΔE value [43].

Table 6 – Colour parameters and opacity values of cellulose acetate-based films with the incorporation of betalains.

Films	L*	a*	b*	Opacity (%)	ΔE
CA	96.05 ± 0.14^{a}	0.25 ± 0.02^{a}	2.12 ± 0.13^{a}	8.10 ± 0.21^{a}	0
CA/BE (0.5%)	84.20 ± 0.93^{b}	14.94 ± 1.03^{b}	-0.38 ± 0.23^{b}	15.65 ± 0.86^{ab}	19.56 ± 1.40
CA/BE (1%)	82.27 ± 5.07^{b}	17.18 ± 5.53^{b}	-0.78 ± 0.23^{bc}	15.00 ± 5.54^{a}	22.56 ± 7.46
CA/BE (2%)	70.89 ± 4.44^{c}	30.36 ± 4.55^{c}	-0.89 ± 0.17^{c}	24.74 ± 4.61^{b}	39.90 ± 6.33

Values reported are the mean ± sd. Different letters (a – d), in the same column, indicate a statically difference ($p < 0.05$).

3.5 SEM analysis

SEM micrographs of the neat CMC 5050 and CMC/ANT films surface are shown in Figure 15. The morphology of neat CMC film [Figure 15 (a)] exhibited a smooth surface, but with the presence of some irregularities, that can be related with the incomplete dispersion of the polymer. Whereas, with the incorporation of anthocyanins [Figure 15 (b) to 15 (d)] the intelligent films showed heterogeneous and irregular surface patterns, with aggregated spherical structures. Moreover, as the ANT concentration increased, the number of small particulates grown as well. These spheres could be related to the low interaction between the polymer matrix and anthocyanins. It was concluded that the films surfaces were greatly influenced by the presence of ANT. Rajeswari et al. (2020) reported similar observations in which starch and chitosan-based films with the incorporation of roselle anthocyanins showed a heterogeneous structure. The small aggregate structures were explained by the destruction of the orderly arrangement between the chitosan and starch with the incorporation of ANT [60].

The surface morphology of the neat CMC 5050 and CMC/CU films is shown in

Figure 16. The curcumin incorporation did not significantly alter the film's surface, suggesting that this indicator was well dispersed on the films surfaces and strongly connected to CMC matrix. Nevertheless, the films' surfaces were not as compact as the one without curcumin. From

Figure 16 (b) to 16 (d), some curcumin crystal particles, characteristic of the co-existence of crystalline and amorphous phases, were observed, indicating that, during the production of these films, CUR crystals would precipitate, and randomly stack in the CMC 5050 matrix with the solvents' evaporation, which agrees with the reported by Qianyuan et al (2017) [44].

SEM images on the surface of CMC 100 films with and without betalains are shown in Figure 17. The surface of the neat CMC 100 film exhibited a smooth, continuous, and well-connected network, indicating that all the CMC and water were evenly mixed and had good compatibility. After the addition of 0.5% (w/w) of betalains into the CMC matrix, the film's surface remained smooth and uniform, indicating that the BE lower content was well compatible with the polymer. However, when the betalains content increased, some particles on the surface of the CMC/BE films were observed, reflecting a heterogeneous morphology. This was due to the excessive BE aggregated in the film and reduced the compatibility of film's components. Yao et al. also reported that the surface of quaternary ammonium chitosan/polyvinyl alcohol film became uneven after the addition of betalains-rich cactus pears [43].

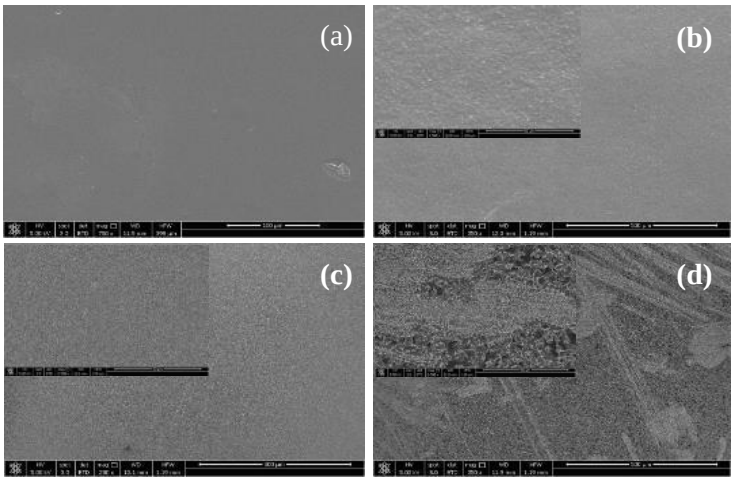

Figure 15 – SEM micrographs of carboxymethylcellulose-based films with (a) 0% (w/w) anthocyanins, (b) 0.5% (w/w) anthocyanins, (c) 1% (w/w) anthocyanins, and (d) 2% (w/w) anthocyanins. The neat CMC 5050 film was taken at 750x magnification. The carboxymethylcellulose/anthocyanins films were taken at 250x magnification, and the insert images at 2500x magnification.

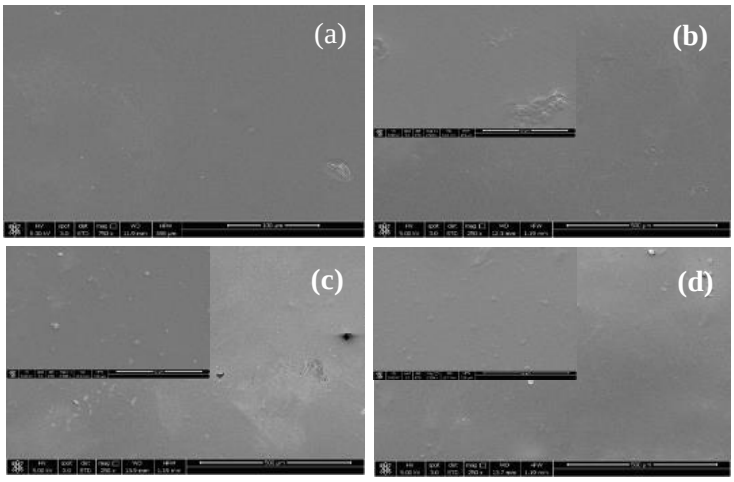

Figure 16 – SEM micrographs of carboxymethylcellulose-based films with (a) 0% (w/w) curcumin, (b) 0.5% (w/w) curcumin, (c) 1% (w/w) curcumin, and (d) 2% (w/w) curcumin. The neat carboxymethylcellulose 5050 film was taken at 750x magnification. The carboxymethylcellulose/curcumin films were taken at 250x magnification, and the insert images at 2500x magnification.

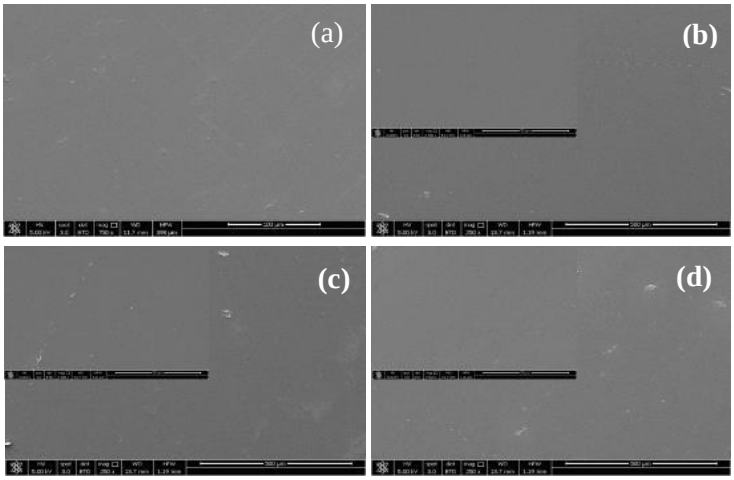

Figure 17 – SEM micrographs of carboxymethylcellulose-based films with (a) 0% (w/w) betalains, (b) 0.5% (w/w) betalains, (c) 1% (w/w) betalains, and (d) 2% (w/w) betalains. The neat carboxymethylcellulose 5050 film was taken at 750x magnification. The carboxymethylcellulose/betalains films were taken at 250x magnification, and the insert images at 2500x magnification.

The surface morphology of the CA films with and without anthocyanins was probed by SEM. (Figure 18). As observed in Figure 18 (a), the CA surface film was smooth, with a continuous structure. Also, no crystal grains were detected, suggesting that the membrane components were uniformly blend. The images showed clear differences between films with and without anthocyanins, where the neat CA-based film presented a smooth and homogeneous surface, compared to CA/ANT-based films (Figure 18 (b) – 14(c)) which have become increasingly heterogeneous and rougher, when ANT concentration has increased. Besides, the higher ANT content [2% (w/w)] had a significant effect on the matrix microstructure, with the occurrence of some cracks, that can be caused by the effect of ANT on the CA microstructure. Freitas et al. developed and characterized intelligent cellulose acetate-based films using red cabbage and reported similar finding on the film's microstructure [59].

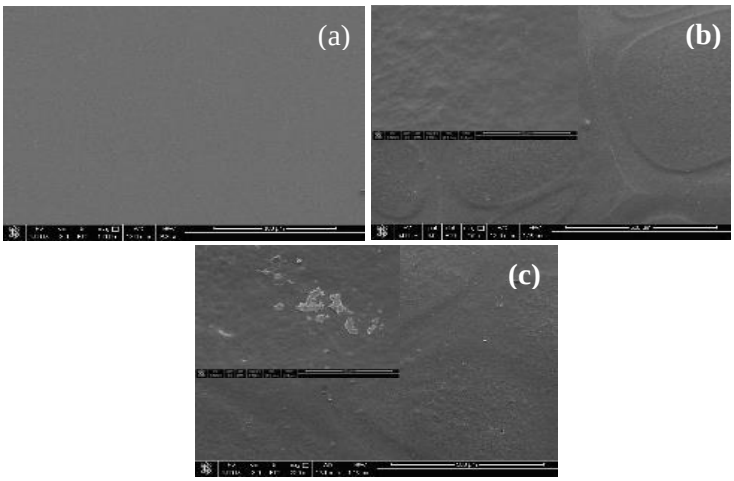

Figure 18 – SEM micrographs of cellulose acetate-based films with (a) 0% (w/w) anthocyanins, (b) 1% (w/w) anthocyanins, and (c) 2% (w/w) anthocyanins. The neat cellulose acetate film was taken at 750x magnification. The cellulose acetate/anthocyanins films were taken at 250x magnification, and the insert images at 2500x magnification.

When low concentrations (0.5 – 1% (w/w)) of curcumin were added, it was verified a well distribution of CUR in the CA matrix, forming a smooth surface composite film (Figure 19). However, when a high concentration of CUR (2% (w/w)) was incorporated, the composite film surface homogeneity got worse and evident CUR agglomerations were observed, due to its precipitation in the polymer matrix. It was concluded that

only for lower CUR contents, there was a good compatibility with CA, which agrees with the reported by Liu et al. (2018) [5].

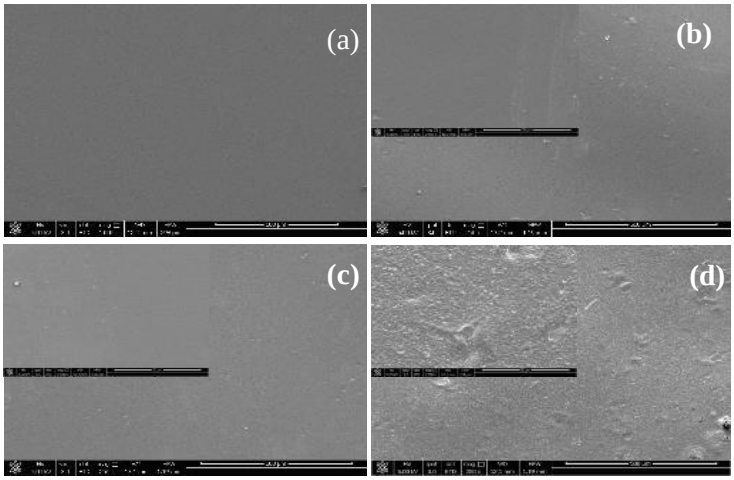

Figure 19 – SEM micrographs of cellulose acetate-based films with (a) 0% (w/w) curcumin, (b) 0.5% (w/w) curcumin, (c) 1% (w/w) curcumin, and (d) 2% (w/w) curcumin. The neat cellulose acetate film was taken at 750x magnification. The cellulose acetate/curcumin films were taken at 250x magnification, and the insert images at 2500x magnification.

The surface morphology of the CA films with and without betalains was also evaluated by SEM. As shown in Figure 20 (a), the CA film was smooth and uniform without any cracks or pores, indicating that cellulose acetate and acetone had good compatibility. The CA/BE (0.5%) film surface remained smooth, but locally wrinkled. Additionally, when BE content increased to 1 – 2% (w/w), the films surface became gradually rough, with visible BE agglomerations, due to a compatibility reduction between BE and CA. Yao et al. also reported that the films cross-sectional microstructures were greatly influenced by the betalains content [43].

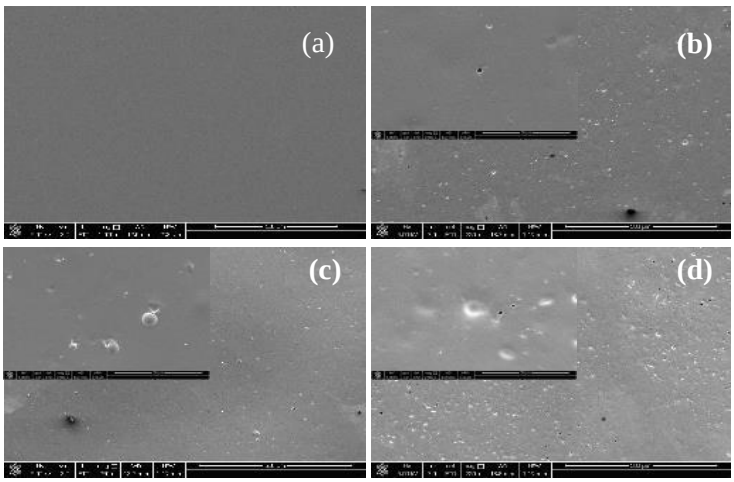

Figure 20 – SEM micrographs of cellulose acetate-based films with (a) 0% (w/w) betalains, (b) 0.5% (w/w) betalains, (c) 1% (w/w) betalains, and (d) 2% (w/w) betalains. The neat cellulose acetate film was taken at 750x magnification. The cellulose acetate/betalains films were taken at 250x magnification, and the insert images at 2500x magnification.

3.6 FTIR analysis

FTIR can be used for the evaluation of biopolymers and nanofillers miscibility and compatibility testing, because of its rapid and non-destructive nature [61]. Figure 21 (a) shows the FTIR spectra of the CMC-based film (CMC 5050) with increasing concentrations of ANT. The aim was to detect the characteristic peaks and, possible chemical bonding between materials.

In the spectra of CMC-based films, it was observed a broad peak, between 3500 and 3000 cm^{-1}, which corresponded to O–H stretching and intermolecular or intramolecular H-bonding. In the spectra of the pure CMC film, a small band at 2926 cm^{-1} was presented, which was related to the C–H stretching vibration of the alkane group of the biopolymer chain. The peak at 1589 cm^{-1} was attributed to the asymmetric stretching vibration of the carboxyl group. Additionally, the peaks found at 1412 and 1321 cm^{-1} were due to –OH stretching in-plane and C–H stretching in symmetric of CMC, respectively. Lastly, the C–O stretching and C–C stretching groups, in the polysaccharide structure, corresponded to the peaks at 1103 and 1024 cm^{-1}, respectively [9], [35], [62].

The incorporation of ANT in the CMC-based films leaded to a slight change in their structural characteristics. The appearance of a new peak at 1718 cm^{-1} is related to the incorporation of ANT in the films, which corresponds to C=O stretching of rose anthocyanins extract. Besides, it was concluded that the ANT incorporation did not significantly change in the functional groups of the composite films [63].

Figure 21 (b) represents the FTIR spectra with the typical peaks and bands of CMC-based films with and without the incorporation of CUR. When compared to the pure CMC spectra of Figure 21 (a), it was confirmed the same peaks in the CMC 5050 film used for the incorporation of CUR.

It was also verified in the composite films, similar peak patterns, when compared to the pure CMC film. Furthermore, it was concluded that the CMC chemical structure was not altered after the curcumin incorporation due to no significant change in the functional groups of the composite films [48]. It can also be corelated to SEM analysis, in which the curcumin incorporation did not significantly alter the film's surface, concluding that this indicator was well dispersed on the polymer matrix [

Figure 16 (b) to 16 (d)].

The FTIR spectra of the control CMC film, dissolved in 100% of distilled water, and those containing BE is represented in Figure 21 (c). In the spectra of the pure CMC 100 film, it was observed the same peaks, between 2000 and 1000 cm^{-1}, when compared to the control CMC 5050 film. However, it was also verified a wider peak at 3253 cm^{-1}, shifted to the right.

The incorporation of different concentrations of BE in the CMC-based films showed similar peaks regarding the entire FTIR spectra. Nevertheless, when BE was added to the film, the intensity peaks at 3261, 2928 and 2881 cm^{-1} increased, which represent the hydroxyl vibrations, NH2 stretching, and symmetric and asymmetric CH_2 and CH stretching vibrations, respectively. The polar BE presence in the red beet extract, which contain several aromatic groups and, −OH and −NH bonds, may be the cause to the increase of these intensity peaks [64].

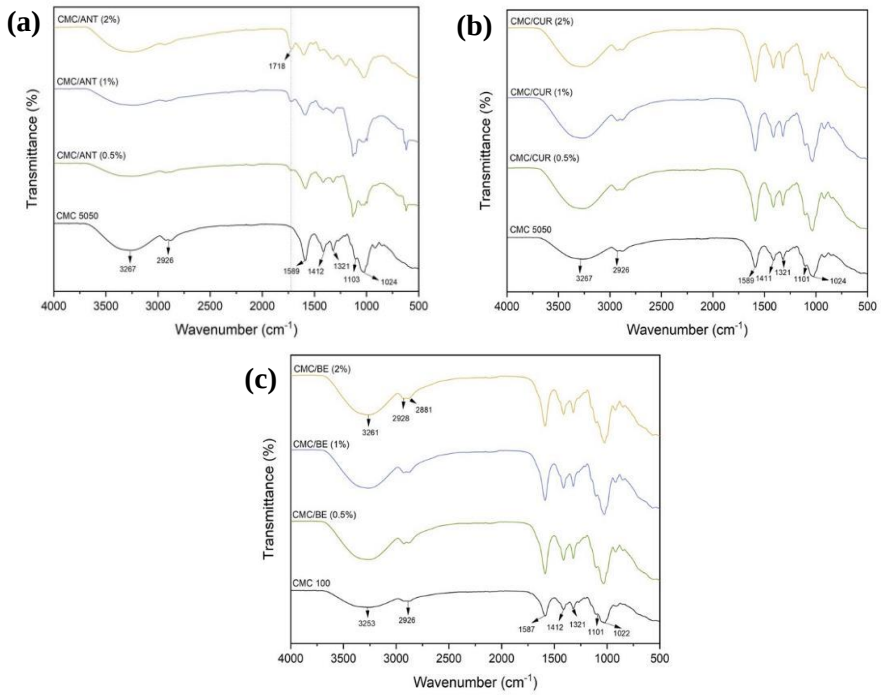

Figure 21 – (a) FT-IR spectra of carboxymethylcellulose-based films with 0% (w/w) anthocyanins (black line), 0.5% (w/w) anthocyanins (green line), 1% (w/w) anthocyanins (blue line), and 2% (w/w) anthocyanins (orange line), (b) FT-IR spectra of carboxymethylcellulose-based films with 0% (w/w) curcumin (black line), 0.5% (w/w) curcumin (green line), 1% (w/w) curcumin (blue line), and 2% (w/w) curcumin (orange line), (c) FT-IR spectra of carboxymethylcellulose-based films with 0% (w/w) betalains (black line), 0.5% (w/w) betalains (green line), 1% (w/w) betalains (blue line), and 2% (w/w) betalains (orange line).

The below spectra in Figure 22 (a), was evaluated by FTIR, from 4000 to 500 cm^{-1} which represented the different ANT concentrations in CA films. In the spectra of the control CA film, a small band at 3481 cm^{-1} was presented, which was related to the OH functional groups. The peak at 1736 cm^{-1} was attributed to the C=O functional groups. Additionally, the peaks found at 1367 and 1215 cm^{-1} were due to CH3, respectively. Lastly, the ether C–O–C functional groups corresponded to the peak 1032 cm^{-1}. The incorporation of different concentrations of ANT in the CA-based films showed a slight change in the peaks intensity which was attributed to the chemical and physical interaction changes between the aromatic rings of anthocyanins and CA. Also, the peak appeared at 1651 cm^{-1} is assigned to the stretching vibration of the C=C aromatic ring, which confirmed that ANT was successfully incorporated into the surface structure of cellulose acetate [63].

Figure 22 (b) represents the FTIR spectra with the typical peaks and bands of CA-based films with and without the incorporation of CUR. When compared to the pure CA spectra of Figure 22 (a), it was confirmed the same peaks in the CA film used for the incorporation of CUR. The FTIR spectra of the CA/CUR films were not significantly different compared with the control CA film since no change in the peak positions were observed. However, as the concentration of curcumin increased, the peaks intensity decreased [48]. Lastly, Figure 22 (c) represents the FTIR spectra with the typical peaks and bands of CA-based films with and without the incorporation of BE. When compared to the pure CA spectra of Figure 22 (b) and Figure 22 (c), it was confirmed the same peaks in the CA film used for the incorporation of CUR. In comparison with the spectra of the control CA film, the intensity of the peaks 3481, 2926 and 2856 cm^{-1} increased when a concentration of 0.5% of betalains was added to the film, which corresponded to hydroxyl vibrations, NH_2 stretching, symmetric and asymmetric CH_2 and CH stretching vibrations, respectively [64].

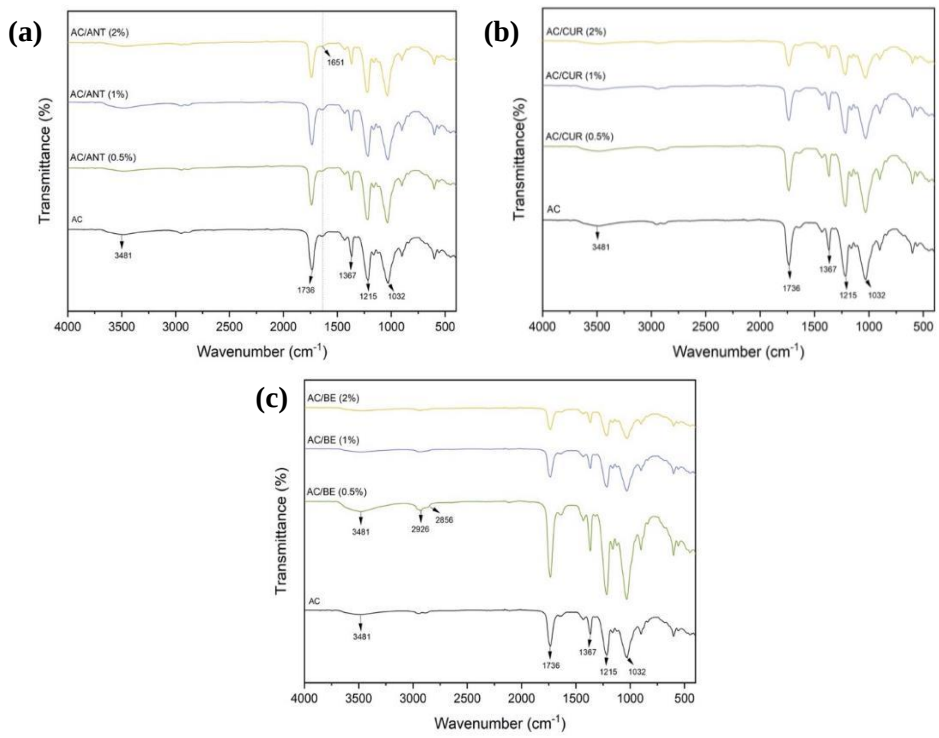

Figure 22 – (a) FT-IR spectra of cellulose acetate-based films with 0% (w/w) anthocyanins (black line), 0.5% (w/w) anthocyanins (green line), 1% (w/w) anthocyanins (blue line), and 2% (w/w) anthocyanins (orange line), (b) FT-IR spectra of cellulose acetate-based films with 0% (w/w) curcumin (black line), 0.5% (w/w) curcumin (green line), 1% (w/w) curcumin (blue line), and 2% (w/w) curcumin (orange line), (c) FT-IR spectra of cellulose acetate-based films with 0% (w/w) betalains (black line), 0.5% (w/w) betalains (green line), 1% (w/w) betalains (blue line), and 2% (w/w) betalains (orange line).

3.7 Mechanical Properties

The mechanical properties of the CMC 5050-based composite films are presented in Table 7 and Table 8. The thickness of the neat CMC 5050 film was 59.20 ± 4.15 μm and it decreased significantly ($p < 0.05$) by the addition of anthocyanins and curcumin. The same results were observed in Table 9 with CMC 100 film (86.43 ± 1.42 μm) and the addition of betalains ($p < 0.05$). Considering that the film thickness depends on the film's nature and composition, it may affect the alignment, sorting and compacting of the molecules not only from CMC, but also from the indicators' addition and their interactions [65]. However, due to the increase in the indicator solid content, from 0.5 to 2%, the films thickness increased.

Generally, within the polymer matrix, the intramolecular interactions and component distributions density determines the mechanical properties, including the composite film strength, flexibility and stiffness [50]. It is important to take into consideration that films applied for food packaging need to possess superior ability to withstand the stress in order to maintain their integrity during shipping, handling and storage [65].

As it was verified in Table 7 and Table 8, the tensile strength (TS) and elongation at break (EB) of the neat CMC 5050 film were 16.50 ± 3.18 MPa and 16.84 ± 4.53%, respectively, indicating that the CMC film is relatively strong with low flexibility. Similar results were observed according to Roy et al. [9].

In Table 7, it was observed that the CMC/ANT (0.5%) film had relatively higher TS ($p < 0.05$) than the neat CMC 5050 film, possible due to the hydrogen bonds between anthocyanins molecules and CMC molecules, resulting in stronger interfacial adhesion between CMC and ANT [35]. However, the TS of the CMC incorporated films decreased with the concentration high contents of ANT [1 and 2% (w/w)], owing to the reduction of interfacial interaction in the polymer matrix by the addition of ANT [38]. This was also verified in the SEM analysis (Figure 15) in which it was concluded that the films surface' were greatly influenced by the presence of ANT, since, as the ANT concentration increased, the number of small particulates grown as well. These spheres could be related to the low interaction between the polymer matrix and anthocyanins.

The decrease of EB ($p < 0.05$) of the CMC-based films incorporated with ANT was probably caused by the natural plant anthocyanin high rigidity, which restrains the polymer chains motion, reducing its flexibility. This observation is consistent with the previous reports [37].

Table 7 – Tensile strength (TS) and elongation at break (EB) of carboxymethylcellulose-based films with the incorporation of anthocyanins.

Films	Thickness (μm)	TS (MPa)	EB (%)
CMC 5050	59.20 ± 4.15^{a}	16.50 ± 3.18^{a}	16.84 ± 4.53^{a}
CMC/ANT (0.5%)	21.25 ± 0.64^{b}	50.55 ± 2.51^{b}	2.73 ± 0.65^{b}
CMC/ANT (1%)	29.95 ± 1.92^{b}	28.74 ± 2.35^{c}	1.60 ± 0.41^{b}
CMC/ANT (2%)	46.30 ± 5.80^{c}	7.47 ± 5.02^{d}	1.97 ± 0.20^{b}

Values reported are the mean ± sd. Different letters (a – d), in the same column, indicate a statically difference ($p < 0.05$).

As observed in Table 8, the strength (TS) and flexibility (EB) did not change significantly ($p < 0.05$) with the addition of CUR, which indirectly indicates good mixing and compatibility between the filler and the polymer matrix. In the SEM and FTIR analysis,

Figure 16 and Figure 21 (b), respectively, was also concluded that the CUR incorporation did not significantly alter the film's surface, suggesting that this indicator was well dispersed on the films surfaces and strongly connected to CMC matrix. Ezati et al. (2020) reported that the addition of curcumin did not affect the mechanical properties of pectin films. However, it is important to highlight that the curcumin concentration used (0.4% (w/w) curcumin) was lower than the current work [2]. Also, according to Roy et al. (2020), the addition of curcumin had no significant effect on the mechanical properties of the CMC films [9].

Table 8 – Tensile strength (TS) and elongation at break (EB) of carboxymethylcellulose -based films with the incorporation of curcumin.

Films	Thickness (μm)	TS (MPa)	EB (%)
CMC 5050	59.20 ± 4.15^{a}	16.50 ± 3.18^{a}	16.84 ± 4.53^{a}
CMC/CUR (0.5%)	31.67 ± 2.20^{b}	18.95 ± 2.08^{a}	12.07 ± 2.06^{a}
CMC/CUR (1%)	36.70 ± 2.81^{b}	18.06 ± 1.05^{a}	16.16 ± 2.00^{a}
CMC/CUR (2%)	37.72 ± 2.99^{b}	16.04 ± 1.75^{a}	16.27 ± 1.92^{a}

Values reported are the mean ± sd. Different letters (a – d), in the same column, indicate a statically difference ($p < 0.05$).

In Table 9, it was verified that the pure CMC 100 film showed a tensile strength of 13.41 ± 3.98 MPa and an elongation of break of 13.03 ± 2.18%. The inclusion of betalains in the CMC films had an effect on the TS, in which was significantly higher as compared to the neat film, probably due to the presence of hydroxyl groups in the phenolic compounds of BE which interact with CMC, obtaining a stronger interfacial adhesion [58]. This was also verified in the SEM analysis (Figure 17), after the addition of BE (0.5%), indicating that the natural dye was well compatible with the polymer. These results are in agreement with previous study where the incorporation of betalains into PVA/gelatin films increased the TS significantly [58]. Normally, the TS and EB are inversely related as films with higher tensile strength, have lower EB values. Besides, the EB in CMC/BE films decreased nearly twice as much as CMC 100 film, which was probably caused by the intermolecular forces strengthen between adjacent macromolecules, restraining the movements of polymeric chains [16].

Table 9 – Tensile strength (TS) and elongation at break (EB) of carboxymethylcellulose-based films with the incorporation of betalains.

Films	Thickness (μm)	TS (MPa)	EB (%)
CMC 100	86.43 ± 1.42^{a}	13.41 ± 3.98^{a}	13.03 ± 2.18^{a}

CMC/BE (0.5%)	39.60 ± 2.73^{b}	21.95 ± 1.53^{b}	6.05 ± 1.38^{b}
CMC/BE (1%)	54.45 ± 1.80^{c}	20.08 ± 1.45^{b}	4.84 ± 1.62^{b}
CMC/BE (2%)	56.80 ± 4.36^{c}	23.61 ± 4.29^{b}	4.80 ± 0.20^{b}

Values reported are the mean ± sd. Different letters (a – d), in the same column, indicate a statically difference ($p < 0.05$).

The mechanical properties of the different CA films were also studied, and the results are summarized in Table 10, Table 11 and Table 12. The thickness of the neat CA film was 20.67 ± 1.48 μm and it increased by the addition of the different indicators. This suggests that higher contents of indicators can produce more complex matrices between them and CA, thereby causing the films thickness to be relatively higher.

The CA film showed a tensile strength of 86.14 ± 2.02 MPa and an elongation of break of 3.69 ± 0.72 %. The inclusion of anthocyanins in the CA, the TS decreased significantly ($p < 0.05$), and EB did not alter significantly ($p > 0.05$). The results indicated that the TS of the CA/ANT films decreased from 79.10 ± 1.18 MPa to 9.49 ± 2.14 MPa, which might be due to the fact that ANT molecules interrupted the interaction with CA molecules. This observation is consisted to the SEM analysis (Figure 18), in which the films have become increasingly heterogeneous and rougher, when ANT concentration has increased. Nevertheless, the EB parameter was not affected by the addition of anthocyanins. Freitas et al. (2020) found that by adding anthocyanins extracted from red cabbage to cellulose acetate film, the intermolecular interactions between the polymer and the natural dye weakened. Consequently, the TS decrease was also verified [59].

Table 10 – Tensile strength (TS) and elongation at break (EB) of cellulose acetate-based films with the incorporation of anthocyanins.

Films	**Thickness (μm)**	**TS (MPa)**	**EB (%)**
CA	20.67 ± 1.48^{a}	86.14 ± 2.02^{a}	3.69 ± 0.72^{a}
CA/ANT (0.5%)	11.27 ± 1.55^{a}	79.10 ± 1.18^{b}	4.05 ± 1.11^{a}
CA/ANT (1%)	31.40 ± 3.93^{b}	9.73 ± 2.22^{c}	3.00 ± 0.20^{a}
CA/ANT (2%)	38.20 ± 4.57^{b}	9.49 ± 2.14^{c}	2.41 ± 0.54^{a}

Values reported are the mean ± sd. Different letters (a – d), in the same column, indicate a statically difference ($p < 0.05$).

In assessing the mechanical properties of CA/CUR films (Table 11), it was evident that the TS of composite film decreased significantly with increasing CUR content, owing to the reduction of interfacial interaction in the polymer matrix by the addition of CUR. It was also verified in the SEM analysis (Figure 19), a well distribution of CUR in the CA matrix, forming a smooth surface composite film for a lower concentration [0.5% (w/w)] of curcumin. When a high concentration of CUR [1 – 2% (w/w)] was incorporated, evident CUR agglomerations were observed, indicating that only for lower CUR contents, there was a good compatibility, between the polymer and the natural dye. Qianyun Ma et al. observed that the incorporation of a small molecule compound, namely CUR, can decrease the composite films TS, similar to a plasticizer [44]. On the other hand, the films TS was still higher, which can be explained by the uniform CUR dispersion in the CA matrix and the good interfacial interaction between them.

Table 11 – Tensile strength (TS) and elongation at break (EB) of cellulose acetate-based films with the incorporation of curcumin.

Films	**Thickness (μm)**	**TS (MPa)**	**EB (%)**
CA	20.67 ± 1.48^{a}	86.14 ± 2.02^{a}	3.69 ± 0.72^{a}
CA/CUR (0.5%)	21.60 ± 2.28^{a}	90.35 ± 5.40^{a}	3.41 ± 1.20^{a}
CA/CUR (1%)	21.80 ± 4.23^{a}	46.50 ± 1.72^{b}	2.69 ± 0.19^{a}
CA/CUR (2%)	32.57 ± 3.27^{b}	41.57 ± 2.79^{b}	3.45 ± 0.56^{a}

Values reported are the mean ± sd. Different letters (a – d), in the same column, indicate a statically difference ($p < 0.05$).

As observed in Table 12, the TS value obtained for CA-based film incorporated with 1 and 2 % BE were significantly reduced ($p < 0.05$), probably due to the reduction of interfacial interaction between the polymer matrix and the natural dye. However, for films with lower betalains concentration [0.5% (w/w)], no significant difference was observed compared with the neat CA-based film. These observations were accurate to the SEM analysis (Figure 20), in which the films surface of CA/BE [1 and 2% (w/w)] became gradually rough, with visible agglomerations, due to a compatibility reduction between BE and CA. Similarly, Akhtar et al. (2013) found that the HPMC films tensile strength was reduced by the addition of beetroot, due to the film matrix density reduction caused by betalains extract [66].

Table 12 – Tensile strength (TS) and elongation at break (EB) of cellulose acetate-based films with the incorporation of betalains.

Films	Thickness (μm)	TS (MPa)	EB (%)
CA	20.67 ± 1.48^{a}	86.14 ± 2.02^{a}	3.69 ± 0.72^{a}
CA/BE (0.5%)	21.57 ± 2.38^{a}	73.53 ± 4.38^{b}	2.93 ± 0.35^{a}
CA/BE (1%)	23.97 ± 4.69^{a}	44.62 ± 3.75^{c}	3.17 ± 0.46^{a}
CA/BE (2%)	17.83 ± 6.44^{b}	41.03 ± 4.85^{c}	3.18 ± 0.99^{a}

Values reported are the mean ± sd. Different letters (a – d), in the same column, indicate a statically difference ($p < 0.05$).

3.8 Moisture Content

Moisture content (MC) values of CMC-based films are presented in Table 13, Table 14 and Table 15. It is important to notice that, in the film's network, the water molecules occupancy in the total void volume determine the moisture content of the film. Therefore, higher moisture content will indicate a looser micro-structure of the film.

As it is verified in Table 13 and Table 14, the neat CMC 5050 present a high moisture content percentage, which can be related to their hydrophilic nature. The moisture content of CMC/ANT films significantly reduced ($p < 0.05$) from 26.19% to 22.11% (Table 13). Since anthocyanins contain an abundance of hydroxyl groups, it can form intermolecular hydrogen bonds with hydrophilic groups in CMC, which could reduce their interactions. As a consequence, it would cut the water interactions, and so, the MC reduction. Zhang et al. prepared an intelligent pH film based on PVA hydrogel incorporated with ANT, in which its moisture content was reduced significantly, as well [15].

Table 13 – Moisture content of carboxymethylcellulose-based films with the incorporation of anthocyanins.

Films	MC (%)
CMC 5050	28.52 ± 0.60^{a}
CMC/ANT (0.5%)	26.19 ± 0.60^{b}
CMC/ANT (1%)	25.00 ± 0.76^{b}
CMC/ANT (2%)	22.11 ± 0.61^{c}

Values reported are the mean ± sd. Different letters (a – d), in the same column, indicate a statically difference ($p < 0.05$).

In Table 14, it is shown that the CMC/CUR films present higher moisture content values (29.45% – 31.04%). With the incorporation of curcumin into CMC-based films, the curcumin molecules can interact with ethanol, increasing the hydrophobic character. Musso et al. (2017) also documented that the addition of curcumin into gelatin films, prepared by casting using ethanol-water mixture, caused an increase in the MC [10].

Table 14 – Moisture content of carboxymethylcellulose-based films with the incorporation of curcumin.

Films	MC (%)
CMC 5050	28.52 ± 0.60^{a}

CMC/CUR (0.5%)	29.45 ± 0.27^{a}
CMC/CUR (1%)	30.66 ± 0.19^{b}
CMC/CUR (2%)	31.04 ± 0.61^{b}

Values reported are the mean ± sd. Different letters (a – d), in the same column, indicate a statically difference ($p < 0.05$).

As verified in Table 15, CMC 100 films present a high moisture content percentage, which can be related to their hydrophilic nature. For the CMC/BE, the addition of betalains reduced the moisture content of CMC film and the lowest moisture content (25.50%) was observed in CMC/BE (2%) film. The reduction in the moisture content of CMC/BE films was due to the hydrogen bonds formed between CMC and betalains which reduced their interactions, and thereby limiting the water molecules occupancy in the total void volume. Recently, Qin et al. also documented the addition of betalains significantly reduced the moisture content in starch/PVA films [16].

Table 15 – Moisture content of carboxymethylcellulose-based films with the incorporation of betalains.

Films	**MC (%)**
CMC 100	32.59 ± 0.46^{a}
CMC/BE (0.5%)	29.65 ± 0.56^{b}
CMC/BE (1%)	27.92 ± 0.65^{c}
CMC/BE (2%)	25.50 ± 0.36^{d}

Values reported are the mean ± sd. Different letters (a – d), in the same column, indicate a statically difference ($p < 0.05$).

In Table 16, it is shown the moisture content of CA films with and without the indicators. The neat CA films present a high moisture content ($22.49 \pm 0.46\%$). The addition of ANT reduced the moisture content of CA films from 22.05% to 17.85%. This was possibly due to formation of hydrogen bonds and so, the reduction of the availability of hydroxyl groups, limiting the water interactions [15].

Table 16 – Moisture content of cellulose acetate-based films with the incorporation of anthocyanins.

Films	**MC (%)**
CA	22.49 ± 0.46^{a}
CA/ANT (0.5%)	22.05 ± 0.77^{a}
CA/ANT (1%)	21.94 ± 0.76^{a}
CA/ANT (2%)	17.85 ± 0.57^{b}

Values reported are the mean ± sd. Different letters (a – d), in the same column, indicate a statically difference ($p < 0.05$).

As verified in Table 17, the addition of different quantities of curcumin extract to CA-based films led to a significant decrease of moisture content values (22.53% – 16.37%). Considering the hydrophobic nature of curcumin, the increase in curcumin extract concentrations used with CA resulted in a major variation in the total void volume. Rachtanapun et al. studied the CUR effects on the properties of chitosan films, in which the moisture content reduced, as well [46].

Table 17 – Moisture content of cellulose acetate-based films with the incorporation of curcumin.

Films	**MC (%)**
CA	22.49 ± 0.46^{a}
CA/CUR (0.5%)	22.53 ± 0.97^{a}
CA/CUR (1%)	18.61 ± 0.91^{b}
CA/CUR (2%)	16.37 ± 0.27^{c}

Values reported are the mean ± sd. Different letters (a – d), in the same column, indicate a statically difference ($p < 0.05$).

The incorporation of betalains into CA-based films had moisture content values around 21.02 – 22.53%, which indicates that the films had a tight microstructure (Table 18). Consequently, the BE addition did not affect the MC ($p < 0.05$). Kanatt et al. developed BE incorporated into PVA/gelatin to monitor the fish and chicken meat freshness. It was also observed that addition of betalains did not change the MC when compared to the neat film [58].

Table 18 – Moisture content of cellulose acetate-based films with the incorporation of betalains.

Films	MC (%)
CA	22.49 ± 0.46^{a}
CA/BE (0.5%)	22.53 ± 0.97^{a}
CA/BE (1%)	21.67 ± 0.26^{a}
CA/BE (2%)	21.02 ± 0.81^{a}

Values reported are the mean ± sd. Different letters (a – d), in the same column, indicate a statically difference ($p < 0.05$).

3.9 Visual analysis of the films

The CMC, CA and EC films with the incorporation of 2% (w/w) of curcumin and betalains were used to monitor the freshness of salmon, which are shown in the appendix. The desirable and visible films' colour changes were evident only after 3 days, which alerted the consumer about the spoiled product.

The change in colour was detectable and more evident in CMC films containing curcumin and betalains, Figure C.3.1 and Figure C.3.2, respectively, in which it was possible to observe an increase of colour's intensity and the swelling phenomenon.

As observed in Figure C.3.3, after 3 days, a colour change from pink to white in the CA/BE (2%) film, which is corelated with the films' colour change under alkaline conditions. Nevertheless, the CA/CUR 2% film did not present any colour change, detectable by the naked eye (Figure C.3.4).

Figure C.3.5 and Figure C.3.6 depict the EC films with the addition of 2% (w/w) of curcumin and betalains, respectively. Any visible colour change was observed which is corelated with the films' colour maintenance for different pH.

4

CONCLUSION AND FUTURE PERSPECTIVES

The field of intelligent food packaging systems has been evolving due to the advantages it offers. The more researchers are able to develop new functional materials for intelligent food packaging, the more we will ensure their capability to detect and record the packed food environment changes, as well as, to communicate this information to the consumer. A way to obtain new functional materials is by using various synthetic pigments and dyes. However, they are considered toxic and mutagenic. Therefore, the use of natural dyes is a promising way to obtain new functional inks, overcoming the challenges stemming the food safety with the reduction of product waste, towards a circular economy and the minimization of the carbon footprint.

The purpose of this project was development of new functional inks that can act as indicators for food packaging applications, with the incorporation of natural dyes, namely, anthocyanins, curcumin, and betalains, into cellulose-based materials, such as, carboxymethylcellulose, cellulose acetate, and ethyl cellulose.

Initially, it was analysed the colour changes of buffer solutions with ANT, CUR and BE, from pH 1 to 13. It was verified colour variations of ANT, CUR, and BE, upon contact with different pH values, which showed clearly the advantage associated with the use of these natural dyes as a pH indicators. Thus, we conducted the study with ANT, CUR and BE. Afterwards, the incorporation of the natural dyes (with the following concentrations: 0.5, 1 and 2% (w/w)) into CMC-based films, CA-based films and EC-based films were prepared, in which their visual appearance exhibited to be uniform, with a smooth surface. It also was observed visually homogeneous natural dyes distribution into the films, as well as an intense colour as the indicator concentration increased. Also, a brown colour was observed in CMC, CA and EC-based films, which was associated with the presence of ANT, an orange colour was corelated with the presence of CUR and a pink colour to the addition of BE.

For the evaluation of the films' pH sensing characteristics, CMC, CA and EC films with and without the incorporation of ANT, CUR and BE were immersed in buffer solutions from pH at 1 to 13. It was observed colour variations in function of the pH values in the CMC-based films with ANT, CUR and BE [0.5, 1 and 2% (w/w)], which could be attributed to the natural dyes chemical structure transformations.

For CMC/ANT [0.5, 1 and 2% (w/w)] films, a reddish colour was observed in acidic conditions, a brown colour, in a neutral pH, and, lastly a violet colour, in basic pH. The CMC/CUR [0.5, 1 and 2% (w/w)] films presented yellow in colour in a pH ranged between 1 and 10, which changed to orange as the pH increased from 11 to 13. The CMC/BE [0.5, 1 and 2% (w/w)] composite films gradually changed their colour from pink to yellow, in alkaline conditions. Additionally, it was verified that all CMC films presented pH-dependent swelling characteristics, in which it was observed the solvents' penetration into the polymer network that caused an abrupt visual change in the CMC films.

For CA/ANT [0.5% (w/w)] film, it was observed the preservation of its colour, under different pH conditions, from 1 to 13. Also, for the CA/ANT [1% (w/w)] film maintained its pink colour, from pH 1 to 9. When the pH increased from 10 to 13, its colour turned to a light and bright colour. Lastly, for the CA/ANT [2% (w/w)] film, it was observed a colour change to green, under basic conditions. CA/CUR [0.5, 1 and 2% (w/w)] composite films also showed a pronounced color change from yellow to orange, at pH 13. Hence, these films presented pH resistance, from pH 1 to 12. The CA/BE [0.5, 1 and 2% (w/w)] composite films also showed a pronounced color change from pink to transparent when immersed in basic conditions.

Lastly, for the EC composite films with the incorporation of anthocyanins, curcumin and betalains, did not present a color response after being immersed to different buffer solutions, from pH 1 to 13. It was

concluded that the EC composite films could not be used to detect pH changes in packaged foods, due to its pH resistance.

Morphological characteristics for CMC/ANT, CMC/BE composite films, and CA-based films with the addition of ANT, CUR and BE, evaluated by SEM, suggested a good compatibility between lower concentrations of pigments and the polymers matrix. Nevertheless, for higher concentrations, the observation of small aggregates distributed in the films, resulted in a low compatibility between the natural dyes and the polymers matrix. These observations were corelated with the mechanical properties analysis, which resulted in the decrease of the TS, with due to the lost compatibility between the polymer and the pigments.

For CMC/CUR films it was verified that the curcumin incorporation did not significantly alter the film's surface, suggesting that this indicator was well dispersed on the films surfaces and strongly connected to CMC matrix. I the FTIR analysis, it was, also, concluded that the CMC chemical structure was not altered after the curcumin incorporation due to no significant change in the functional groups of the composite films. Lastly, the TS did not alter significantly with the addition of CUR, which indicated a good compatibility between CUR and the polymer matrix.

The results suggest that the intelligent films reported here (CMC and AC-based films) can be efficient packaging alternatives for alerting food spoilage, owing to the pH variation information during the transport and storage.

Nevertheless, there is always room for improvement. The films physicochemical and mechanical properties containing ANT, CUR, or BE demonstrated to be affected not only due to the natural dyes' concentration, but also with the polymer used. Therefore, these factors should be considered for the design of this type of intelligent packaging system.

Additionally, new techniques for the production of the films could be conducted, namely, the use of *eletrospinning*, *ultrasonic spray* or *electrohydrodynamic printing* for the development of the indicators.

Further investigations should be conducted to improve the pH-sensitivity films, namely, more evaluations are required to confirm its thermostability, photostability, the water vapor permeability, safety and possible side effects of natural dyes-loaded packaging systems, before their application in the industrial scale.

REFERENCES

[1] Z. Aghaei, B. Emadzadeh, B. Ghorani e R. Kadkhodaee, "Cellulose Acetate Nanofibres Containing Alizarin as a Halochromic Sensor for the Qualitative Assessment of Rainbow Trout Fish Spoilage," *Food and Bioprocess Technology,* 2018.

[2] P. Ezati e J. W. Rhim, "pH-responsive chitosan-based film incorporated with alizarin for intelligent packaging applications," *Food Hydrocolloids,* 2020.

[3] H. Dong, Z. Ling e X. Zhang, "Smart colorimetric sensing films with high mechanical strength and hydrophobic properties for visual monitoring of shrimp and pork freshness," *Sensors and Actuators, B: Chemical,* 2020.

[4] D. Kilcast e P. Subramaniam, The stability and shelf life of food, 2000.

[5] Y. Liu, Y. Ma e Y. Liu, "Fabrication and characterization of pH-responsive intelligent films based on carboxymethyl cellulose and gelatin/curcumin/chitosan hybrid microcapsules for pork quality monitoring," *Food Hydrocolloids,* 2022.

[6] T. V. Vo, T. H. Dang e B. H. Chen, "Synthesis of intelligent pH indicative films from chitosan/poly(vinyl alcohol)/anthocyanin extracted from red cabbage," *Polymers,* 2019.

[7] V. Gomes, A. S. Pires e N. Mateus, "Pyranoflavylium-cellulose acetate films and the glycerol effect towards the development of pH-freshness smart label for food packaging," *Food Hydrocolloids,* 2022.

[8] P. Müller e M. Schmid, "Intelligent packaging in the food sector: A brief overview," *Foods,* 2019.

[9] S. Roy, H. J. Kim e J. W. Rhim, "Synthesis of Carboxymethyl Cellulose and Agar-Based Multifunctional Films Reinforced with Cellulose Nanocrystals and Shikonin," *ACS Applied Polymer Materials,* 2021.

[10] Y. S. Musso, P. R. Salgado e A. N. Mauri, "Smart edible films based on gelatin and curcumin," *Food Hydrocolloids,* 2017.

[11] H. z. Chen, M. Zhang e B. Bhandari, "Novel pH-sensitive films containing curcumin and anthocyanins to monitor fish freshness," *Food Hydrocolloids,* 2020.

[12] Y. S. Soliman, W. B. Beshir e A. A. Abdel-Fattah, "Radiation-induced coloration of xylenol blue/film containing hexachloroethane for food irradiation applications," *Journal of Radioanalytical and Nuclear Chemistry,* 2016.

[13] A. Pacquit, J. Frisby e D. Diamond, "Development of a smart packaging for the monitoring of fish spoilage," *Food Chemistry,* 2007.

[14] S. Dong, M. Luo e G. Peng, "Broad range pH sensor based on sol-gel entrapped indicators on fibre optic," *Sensors and Actuators, B: Chemical,* 2008.

[15] Y. Zhang, E. Butelli e C. Martin, "Engineering anthocyanin biosynthesis in plants," *Current Opinion in Plant Biology,* 2014.

[16] Y. Qin, Y. Liu e X. Zhang, "Development of active and intelligent packaging by incorporating betalains from red pitaya (Hylocereus polyrhizus) peel into starch/polyvinyl alcohol films," *Food Hydrocolloids,* 2020.

[17] N. Aliabbasi, M. Fathi e Z. Emam-Djomeh, "Curcumin: A promising bioactive agent for application in food packaging systems," *Journal of Environmental Chemical Engineering,* 2021.

[18] N. Bhargava, V. S. Sharanagat e R. S. Mor, "Active and intelligent biodegradable packaging films using food and food waste-derived bioactive compounds: A review," *Trends in Food Science and Technology,* 2020.

[19] C. M. Noronha, S. M. De Carvalho e R. C. Lino, "Characterization of antioxidant methylcellulose film incorporated with α-tocopherol nanocapsules," *Food Chemistry,* 2014.

[20] D. Schaefer e W. M. Cheung, "Smart Packaging: Opportunities and Challenges," *Procedia CIRP,* 2018.

[21] G. Asadi e S. Mousavi, "Application of Nanotechnology in Food Packaging," 2006.

[22] I. Ahmed, H. Lin e L. Zou, "An overview of smart packaging technologies for monitoring safety and quality of meat and meat products," *Packaging Technology and Science,* 2018.

[23] S. M. Borisov e I. Klimant, "Optical nanosensors - Smart tools in bioanalytics," *Analyst,* 2008.

[24] J. E. McDonald, D. J. Rooks e A. J. McCarthy, "Methods for the isolation of cellulose-degrading," *Methods in Enzymology,* 2012.

[25] R. G. J. H.-K. B. Ergun, "Cellulose," *Encyclopedia of Food and Health,* 2015.

[26] J. S. Yaradoddi, N. R. Banapurmath e S. V. Ganachari, "Biodegradable carboxymethyl cellulose based material for sustainable packaging application," *Scientific Reports,* 2020.

[27] S. Roy e J. W. Rhim, "Carboxymethyl cellulose-based antioxidant and antimicrobial active packaging film incorporated with curcumin and zinc oxide," *International Journal of Biological Macromolecules,* 2020.

[28] S. Fischer, K. Thümmler e B. Volkert, "Properties and applications of cellulose acetate," *Macromolecular Symposia,* 2008.

[29] P. A. Freitas, R. R. Silva e T. V. de Oliveira, "Development and characterization of intelligent cellulose acetate-based films using red cabbage extract for visual detection of volatile bases," *LWT,* 2020.

[30] S. Zepnik, S. Kabasci e R. Kopitzky, "Extensional flow properties of externally plasticized cellulose acetate: Influence of plasticizer content," *Polymers,* 2013.

[31] S. Wan, Y. Sun e X. Qi, "Improved bioavailability of poorly water-soluble drug curcumin in cellulose acetate solid dispersion," *AAPS PharmSciTech,* 2012.

[32] M. Davidovich-Pinhas, "Oleogels," *Polymeric Gels,* 2018.

[33] P. Ahmadi, A. Jahanban-Esfahlan e A. Ahmadi, "Development of Ethyl Cellulose-based Formulations: A Perspective on the Novel Technical Methods," *Food Reviews International,* 2022.

[34] S. Ebnesajjad, "Characteristics of Adhesive Materials," *Handbook of Adhesives and Surface Preparation: Technology, Applications and Manufacturin,* 2010.

[35] H. M. d. Silva, A. B. Mageste e S. J. B. e. Silva, "Anthocyanin immobilization in carboxymethylcellulose/starch films: A sustainable sensor for the detection of Al(III) ions in aqueous matrices," *Carbohydrate Polymers,* 2020.

[36] D. Liu, Z. Cui e M. Shang, "A colorimetric film based on polyvinyl alcohol/sodium carboxymethyl cellulose incorporated with red cabbage anthocyanin for monitoring pork freshness," *Food Packaging and Shelf Life,* 2021.

[37] Y. Qin, Y. Liu e H. Yong, "Preparation and characterization of active and intelligent packaging films based on cassava starch and anthocyanins from Lycium ruthenicum Murr," *International Journal of Biological Macromolecules,* 2019.

[38] G. Jiang, X. Hou e X. Zeng, “Preparation and characterization of indicator films from carboxymethyl-cellulose/starch and purple sweet potato (Ipomoea batatas (L.) lam) anthocyanins for monitoring fish freshness,” *International Journal of Biological Macromolecules,* 2020.

[39] M. C. Silva-Pereira, J. A. Teixeira e V. A. Pereira-Júnior, “Chitosan/corn starch blend films with extract from Brassica oleraceae (red cabbage) as a visual indicator of fish deterioration,” *LWT,* 2015.

[40] T. V. Vo, T. H. Dang e B. H. Chen, “Synthesis of intelligent pH indicative films from chitosan/poly(vinyl alcohol)/anthocyanin extracted from red cabbage,” *Polymers,* 2019.

[41] I. Choi, J. Y. Lee e M. Lacroix, “Intelligent pH indicator film composed of agar/potato starch and anthocyanin extracts from purple sweet potato,” *Food Chemistry,* 2017.

[42] M. W. Apriliyanti, A. Wahyono e M. Fatoni, “The Potency of betacyanins extract from a peel of dragon fruits as a source of colourimetric indicator to develop intelligent packaging for fish freshness monitoring,” *IOP Conference Series: Earth and Environmental Science,* 2018.

[43] X. Yao, H. Hu e Y. Qin, “Development of antioxidant, antimicrobial and ammonia-sensitive films based on quaternary ammonium chitosan, polyvinyl alcohol and betalains-rich cactus pears (Opuntia ficus-indica) extract,” *Food Hydrocolloids,* 2020.

[44] Q. Ma, L. Du e L. Wang, “Tara gum/polyvinyl alcohol-based colorimetric NH3 indicator films incorporating curcumin for intelligent packaging,” *Sensors and Actuators, B: Chemical,* 2017.

[45] C. Wu, J. Sun e M. Chen, “Effect of oxidized chitin nanocrystals and curcumin into chitosan films for seafood freshness monitoring,” *Food Hydrocolloids,* 2019.

[46] P. Rachtanapun, W. Klunklin e P. Jantrawut, “Characterization of chitosan film incorporated with curcumin extract,” *Polymers,* 2021.

[47] N. Aliabbasi, M. Fathi e Z. Emam-Djomeh, “Curcumin: A promising bioactive agent for application in food packaging systems,” *Journal of Environmental Chemical Engineering,* 2021.

[48] J. Liu, H. Wang e P. Wang, “Films based on κ-carrageenan incorporated with curcumin for freshness monitoring,” *Food Hydrocolloids,* 2018.

[49] L. Wang, J. Xue e Y. Zhang, “Preparation and characterization of curcumin loaded caseinate/zein nanocomposite film using pH-driven method,” *Industrial Crops and Products,* 2019.

[50] P. Ezati e J. W. Rhim, “pH-responsive pectin-based multifunctional films incorporated with curcumin and sulfur nanoparticles,” *Carbohydrate Polymers,* 2020.

[51] C. Sampaio, L. Sousa e A. Dias, “Separation of Anthocyaninic and Nonanthocyaninic Flavonoids by Liquid-Liquid Extraction Based on Their Acid-Base Properties: A Green Chemistry Approach,” *Journal of Chemical Education,* 2020.

[52] M. Michelin, A. M. Marques, L. M. Pastrana, J. A. Teixeira e M. A. Cerqueira, “Carboxymethyl cellulose-based films: Effect of organosolv lignin incorporation on physicochemical and antioxidant properties,” *Journal of Food Engineering,* 2020.

[53] R. Hypola, I. Husson e F. Sundholm, “Evaluation of physical properties of plasticized ethyl cellulose films cast from ethanol solution”.

[54] C. M. Yoshida, V. B. V. Maciel e M. E. D. Mendonça, “Chitosan biobased and intelligent films: Monitoring pH variations,” *LWT,* 2014.

[55] Y. Qin, Y. Liu e X. Zhang, “Development of active and intelligent packaging by incorporating betalains from red pitaya (Hylocereus polyrhizus) peel into starch/polyvinyl alcohol films,” *Food Hydrocolloids,* 2020.

[56] A. Aravamudhan, D. M. Ramos e A. A. Nada, "Natural Polymers: Polysaccharides and Their Derivatives for Biomedical Applications," *Natural and Synthetic Biomedical Polymers,* 2014.

[57] H. M. Azeredo, "Betalains: Properties, sources, applications, and stability - A review," 2009.

[58] S. R. Kanatt, "Development of active/intelligent food packaging film containing Amaranthus leaf extract for shelf life extension of chicken/fish during chilled storage," *Food Packaging and Shelf Life,* 2020.

[59] P. A. Freitas e R. R. Silva, "Development and characterization of intelligent cellulose acetate-based films using red cabbage extract for visual detection of volatile bases," 2020.

[60] A. Rajeswari, E. J. S. Christy e E. Swathi, "Fabrication of improved cellulose acetate-based biodegradable films for food packaging applications," *Environmental Chemistry and Ecotoxicology,* 2020.

[61] Ł. Łopusiewicz, P. Kwiatkowski e E. Drozłowska, "Preparation and characterization of carboxymethyl cellulose-based bioactive composite films modified with fungal melanin and carvacrol," *Polymers,* 2021.

[62] T. Liang, G. Sun e L. Cao, "A pH and NH3 sensing intelligent film based on Artemisia sphaerocephala Krasch. gum and red cabbage anthocyanins anchored by carboxymethyl cellulose sodium added as a host complex," *Food Hydrocolloids,* 2019.

[63] V. A. Pereira, I. N. Q. Arruda e R. Stefani, "Active chitosan/PVA films with anthocyanins from Brassica oleraceae (Red Cabbage) as Time-Temperature Indicators for application in intelligent food packaging," *Food Hydrocolloids,* 2015.

[64] M. J. Cejudo-Bastante, C. Cejudo-Bastante e M. J. Cran, "Optical, structural, mechanical and thermal characterization of antioxidant ethylene vinyl alcohol copolymer films containing betalain-rich beetroot," *Food Packaging and Shelf Life,* 2020.

[65] Y. Liu, Y. Cai e X. Jiang, "Molecular interactions, characterization and antimicrobial activity of curcumin-chitosan blend films," *Food Hydrocolloids,* 2016.

[66] M. J. Akhtar, M. Jacquot e M. Jamshidian, "Fabrication and physicochemical characterization of HPMC films with commercial plant extract: Influence of light and film composition," *Food Hydrocolloids,* 2013.

[67] T. Suppadit, N. Sunthorn e P. Poungsuk, "Use of anthocyanin extracted from natural plant materials to develop a pH test kit for measuring effluent from animal farms," 2011.

A

APPENDIX – INTRODUCTION

A.1 Context and motivation

Table A.1.1 – Major mechanisms for deterioration of various food categories. Adapted from [4].

Food product category	Critical storage variables	Deterioration mechanics
Dairy products	Oxidation, bacterial growth	Oxygen, temperature, humidity
Fresh fish and seafood	Oxidation, microbial growth	Oxygen, temperature
Frozen meat	Oxidation, freezer burn (drying)	Oxygen, temperature, humidity
Fruit	Microbial growth, moisture loss, enzymatic activity	Oxygen, temperature, humidity, light
Bakery products	Microbial growth, oxidation	Oxygen, temperature, humidity

A.2 State of the art

A.2.1 Bio-based materials for the development of smart packaging films

The cellulose derivatives, namely, carboxymethylcellulose, cellulose acetate and ethyl cellulose, are illustrated below.

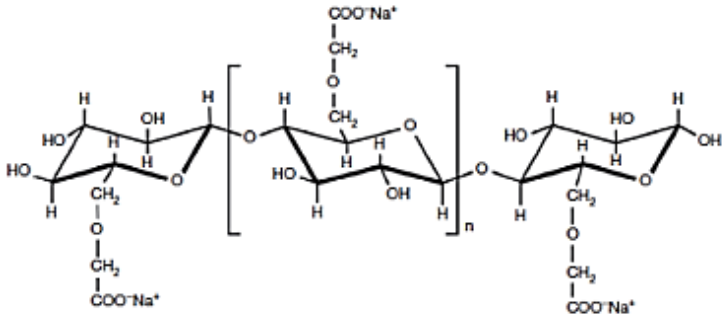

Figure A.2.1.1 – Structure of chemically modified cellulose: Carboxymethylcellulose (CMC) [25].

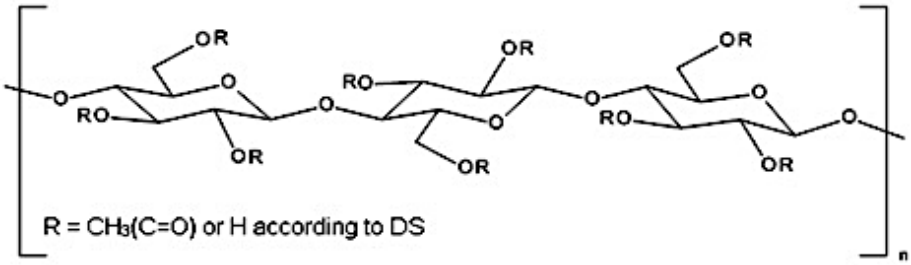

Figure A.2.1.2 – Structure of chemically modified cellulose: cellulose acetate (CA) [30].

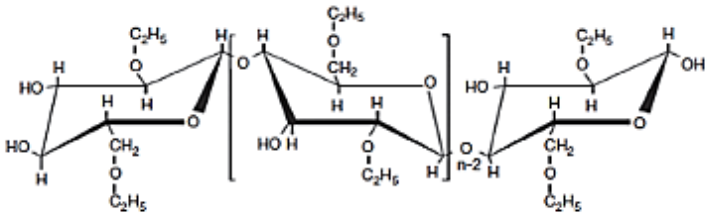

Figure A.2.1.3 – Structure of chemically modified cellulose: Ethyl Cellulose (EC) [25].

A.2.2 Bioactive compounds and their utility

The following table presents a detailed analysis regarding the state-of-the-art related to the development of intelligent films, including the use of natural derived pigments, for monitoring the quality of seafood and meat products.

Table A.2.2.1 – Overview of bio-based films for intelligent food packaging.

Bioactive Compound	Source	Base Film	Activation Mode	Indication (colour change)	Application	Reference
Anthocyanin	Red Cabbage	Chitosan/Corn Starch	Volatile components	Pink-Blue-Yellow	Fish	[39]
		Chitosan/PVA	pH	Pink to Yellowish/Pale-Green	Pork	[40]
	Roselle calyx	Chitosan/Starch/PVA	pH	Red-Green-Yellow	Pork	[15]
	Purple Sweet Potato	Agar/Potato	pH	Red to Green	Pork	[41]
Betalains	Red Pitaya	Glucomannan/PVA	Volatile components	Pink to Yellow	Fish	[42]
		Starch/PVA	Volatile components	Purple to Yellow	Shrimp	[16]
	Cactus Pears	Chitosan/PVA	Volatile components	Purple-Orange-Yellow	Shrimp	[43]
Curcumin	Turmeric	k-carrageenan	pH	Yellow to Red	Shrimp and Pork	[48]
		Tara Gum/PVA	pH	Yellow to Orange-Red	Shrimp	[49]
		Pectin Powder/Glycerol	Volatile components	Yellow to Brown	Shrimp	[2]

The natural derived pigments, namely, anthocyanins, betalains and curcumin, are illustrated below.

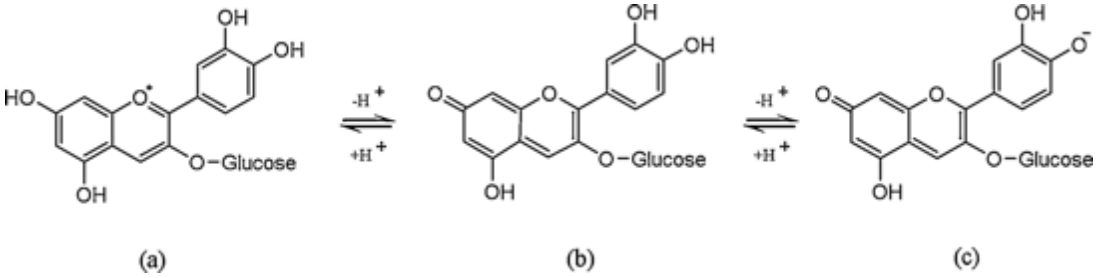

Figure A.2.2.1 – Acid – Base Equilibria of Anthocyanins: (a) flavylium cations; (b) neutral quinoidal base; (c) anionic quinoidal base [35].

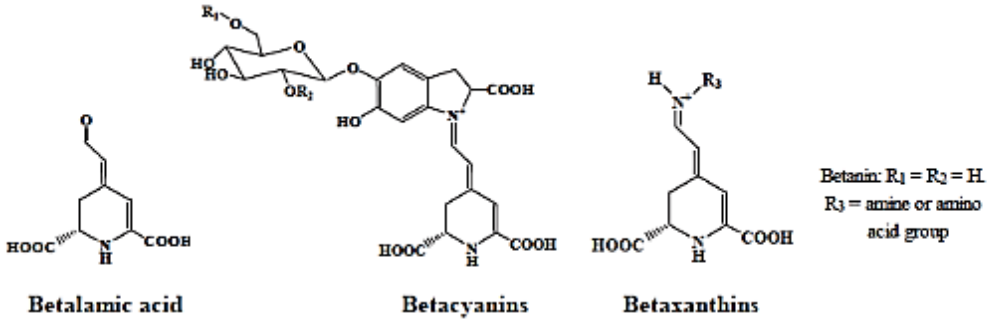

Figure A.2.2.2 – Chemical structure of betalamic acid, betacyanins and betaxanthins [16].

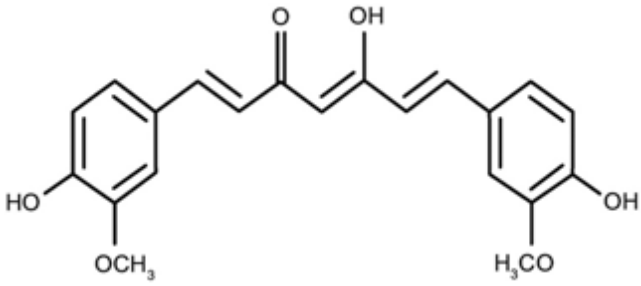

Figure A.2.2.3 – Chemical structure of curcumin [47].

B

APPENDIX – EXPERIMENTAL PROCEDURE

B.1 Buffer Solutions

Table B.1.1 – Ratio (v/v) of the 13 different salt solutions for the preparation of the buffer solutions applied in the pH region 1 – 13 [66].

pH	KCl (0.2 M)	KHP (0.1 M)	KH_2PO_4 (0.1 M)	$Na_2B_4O_7 \cdot 10H_2O$ (0.025 M)	Na_2HPO_4 (0.05 M)	NaOH (0.1 M)	HCl (0.1M)	HCl (0.2M)
1	50	-	-	-	-	-	-	134
2	50	-	-	-	-	-	-	13
3	-	100	-	-	-	-	44.6	-
4	-	100	-	-	-	-	0.2	-
5	-	100	-	-	-	45.2	-	-
6	-	-	100	-	-	11.2	-	--
7	-	-	100	-	-	58.2	-	-
8	-	-	-	100	-	-	41	-
9	-	-	-	100	-	-	9.2	-
10	-	-	-	100	-	36.6	-	-
11	-	-	-	-	100	35.6	-	-
12	-	-	-	-	100	53.8	-	-
13	50	-	-	-	-	132	-	-

B.2 Anthocyanins extracted from red roses

Figure B.2.1 – Crude extract obtained.

B.3 Anthocyanins Solubilization

Table B.3.1 – Anthocyanins solubilization for the development of CMC/ANT films.

	Anthocyanins Concentration (%)	**Ethanol (v/v)**	**Distilled Water (v/v)**	**Results**
Solution A (25 mL)	0.5	100%	-	ANT did not solubilize completely.
	1	100%	-	
	2	100%	-	
Solution B (25 mL)	0.5	-	100%	ANT did not solubilize completely.
	1	-	100%	
	2	-	100%	
Solution C (80 mL)	0.5	50%	50%	ANT was totally solubilized in this solution.
	1	50%	50%	
	2	50%	50%	

B.4 Curcumin Solubilization

Table B.4.1 – Curcumin solubilization for the development of CMC/CUR films.

	Curcumin Concentration (%)	Ethanol (v/v)	Distilled Water (v/v)	Results
Solution A (25 mL)	0.5	100%	-	CUR did not solubilize completely.
	1	100%	-	
	2	100%	-	
Solution B (25 mL)	0.5	-	100%	CUR did not solubilize completely.
	1	-	100%	
	2	-	100%	
Solution C (80 mL)	0.5	50%	50%	CUR was totally solubilized in this solution.
	1	50%	50%	
	2	50%	50%	

B.5 Betalains Solubilization

Table B.5.1 – Betalains solubilization for the development of CMC/BE films.

	Betalains Concentration (%)	Ethanol (v/v)	Distilled Water (v/v)	Results
Solution A (25 mL)	0.5	100%	-	BE did not solubilize completely.
	1	100%	-	
	2	100%	-	
Solution B (25 mL)	0.5	-	100%	BE was totally solubilized in this solution.
	1	-	100%	
	2	-	100%	
Solution C (80 mL)	0.5	50%	50%	BE did not solubilize completely
	1	50%	50%	
	2	50%	50%	

B.6 Optimization of the control cellulose acetate film

Table B.6.1 – Optimization of the neat cellulose acetate film without plasticizer.

CA (%)	M_n	Acetone (%)	Plasticizer	Evaporation Process	Result
1	30,000 by GPC	100	-	Dried at ambient temperature	Relatively strong and stiff with low flexibility
2	30,000 by GPC	100	-	Dried at ambient temperature	Relatively strong and stiff with low flexibility
3	30,000 by GPC	100	-	Dried at ambient temperature	Relatively strong and stiff with low flexibility
4	30,000 by GPC	100	-	Dried at ambient temperature	Relatively strong and stiff with low flexibility
5	30,000 by GPC	100	-	Dried at ambient temperature	Relatively strong and stiff with low flexibility
6	30,000 by GPC	100	-	Dried at ambient temperature	Relatively strong and stiff with low flexibility
7	30,000 by GPC	100	-	Dried at ambient temperature	Relatively strong and stiff with low flexibility
8	30,000 by GPC	100	-	Dried at ambient temperature	Relatively strong and stiff with low flexibility
9	30,000 by GPC	100	-	Dried at ambient temperature	Relatively strong and stiff with low flexibility
10	30,000 by GPC	100	-	Dried at ambient temperature	Relatively strong and stiff with low flexibility

Table B.6.2 – Optimization of the neat cellulose acetate film, with the use of Glycerol as plasticizer.

CA (%)	M_n	Acetone (%)	Plasticizer – Glycerol (%)	Evaporation Process	Result
1	30,000 by GPC	100	0.5	Dried at ambient temperature	Relatively strong and stiff with low flexibility

2	30,000 by GPC	100	0.5	Dried at ambient temperature	Relatively strong and stiff with low flexibility
3	30,000 by GPC	100	0.5	Dried at ambient temperature	Relatively strong and stiff with low flexibility
4	30,000 by GPC	100	0.5	Dried at ambient temperature	Relatively strong and stiff with low flexibility
5	30,000 by GPC	100	0.5	Dried at ambient temperature	Relatively strong and stiff with low flexibility
6	30,000 by GPC	100	0.5	Dried at ambient temperature	Relatively strong and stiff with low flexibility
7	30,000 by GPC	100	0.5	Dried at ambient temperature	Relatively strong and stiff with low flexibility
8	30,000 by GPC	100	0.5	Dried at ambient temperature	Relatively strong and stiff with low flexibility
9	30,000 by GPC	100	0.5	Dried at ambient temperature	Relatively strong and stiff with low flexibility
10	30,000 by GPC	100	0.5	Dried at ambient temperature	Relatively strong and stiff with low flexibility

Table B.6.3 – Optimization of the neat cellulose acetate film, with the use of MyVacet 9–45K, as plasticizer.

CA (%)	**M_n**	**Acetone (%)**	**Plasticizer – MyVacet 9-45K (%)**	**Evaporation Process**	**Result**
1	30,000 by GPC	100	0.5	Dried at ambient temperature	Relatively strong and stiff with low flexibility
2	30,000 by GPC	100	0.5	Dried at ambient temperature	Relatively strong and stiff with low flexibility
3	30,000 by GPC	100	0.5	Dried at ambient temperature	Relatively strong and stiff with low flexibility

4	30,000 by GPC	100	0.5	Dried at ambient temperature	Relatively strong and stiff with low flexibility
5	30,000 by GPC	100	0.5	Dried at ambient temperature	Relatively strong and stiff with low flexibility
6	30,000 by GPC	100	0.5	Dried at ambient temperature	Relatively strong and stiff with low flexibility
7	30,000 by GPC	100	0.5	Dried at ambient temperature	Relatively strong and stiff with low flexibility
8	30,000 by GPC	100	0.5	Dried at ambient temperature	Relatively strong and stiff with low flexibility
9	30,000 by GPC	100	0.5	Dried at ambient temperature	Relatively strong and stiff with low flexibility
10	30,000 by GPC	100	0.5	Dried at ambient temperature	Relatively strong and stiff with low flexibility

Table B.6.4 – Optimization of the neat cellulose acetate film, with the use of MyVacet 9–45K as plasticizer.

CA (%)	**M_n**	**Acetone (%)**	**Plasticizer – MyVacet 9-45K (%)**	**Evaporation Process**	**Result**
1	30,000 by GPC	100	20	Dried at ambient temperature	Relatively strong and stiff with low flexibility
2	30,000 by GPC	100	20	Dried at ambient temperature	Relatively strong and stiff with low flexibility
3	30,000 by GPC	100	20	Dried at ambient temperature	Relatively strong and stiff with low flexibility
4	30,000 by GPC	100	20	Dried at ambient temperature	Relatively strong and stiff with low flexibility
5	30,000 by GPC	100	20	Dried at ambient temperature	Relatively strong and stiff with low flexibility

6	30,000 by GPC	100	20	Dried at ambient temperature	Relatively strong and stiff with low flexibility
7	30,000 by GPC	100	20	Dried at ambient temperature	Relatively strong and stiff with higher flexibility
8	30,000 by GPC	100	20	Dried at ambient temperature	Relatively strong and stiff with higher flexibility
9	30,000 by GPC	100	20	Dried at ambient temperature	Relatively strong and stiff with higher flexibility
10	30,000 by GPC	100	20	Dried at ambient temperature	Relatively strong and stiff with higher flexibility

Table B.6.5 – Optimization of the neat cellulose acetate film. To produce the films, it was used a K-Hand Coater.

CA (%)	**M_n**	**Acetone (%)**	**Plasticizer**	**Evapora-tion Pro-cess**	**Coating Bar Colour**	**Quantity Deposited (mL)**	**Result**
1	50.000 by GPC	100	-	K-Hand Coater (Manual)	Black	10	Not viscous enough to create a film
2	50.000 by GPC	100	-	K-Hand Coater (Manual)	Black	10	Not viscous enough to create a film
3	50.000 by GPC	100	-	K-Hand Coater (Manual)	Black	10	Not viscous enough to create a film
4	50.000 by GPC	100	-	K-Hand Coater (Manual)	Black	10	Not viscous enough to create a film
5	50.000 by GPC	100	-	K-Hand Coater (Manual)	Black	10	Not viscous enough to create a film
6	50.000 by GPC	100	-	K-Hand Coater (Manual)	Black	10	Not viscous enough to

							create a film
7	50.000 by GPC	100	-	K-Hand Coater (Manual)	Black	10	A film with low flexibility was produced
8	50.000 by GPC	100	-	K-Hand Coater (Manual)	Black	10	A film with low flexibility was produced
9	50.000 by GPC	100	-	K-Hand Coater (Manual)	Black	10	A film with low flexibility was produced
10	50.000 by GPC	100	-	K-Hand Coater (Manual)	Black	10	A film with higher flexibility was produced

B.7 Optimization of the control Ethyl Cellulose film

Table B.7.1 – Optimization of the neat ethyl cellulose film, with and without the use MyVacet 9–45K, as plasticizer. The films were dried in an oven, at 60 °C, overnight.

EC (%)	Ethanol (%)	Plasticizer – MyVacet 9-45K (%)	Evaporation Process	Quantity Deposited (mL)
10	100	-	Dried at 60 °C	30
10	100	10	Dried at 60 °C	30
10	100	20	Dried at 60 °C	30

Table B.7.2 – Optimization of the neat ethyl cellulose film, with and without the use MyVacet 9–45K, as plasticizer. The films were dried in an oven, at 35 °C, overnight.

EC (%)	Ethanol (%)	Plasticizer – MyVacet 9-45K (%)	Evaporation Process	Quantity Deposited (mL)
10	100	-	Dried at 35 °C	30
10	100	10	Dried at 35 °C	30
10	100	20	Dried at 35 °C	30

Table B.7.3 – Optimization of the neat ethyl cellulose film, with and without the use MyVacet 9–45K, as plasticizer. To produce the films, it was used a K-Hand Coater.

EC (%)	Ethanol (%)	Plasticizer – MyVacet 9-45K (%)	Evaporation Process	Coating Bar	Quantity Deposited (mL)	Result
10	100	-	K-Hand Coater (Manual)	Black	5	Not viscous enough to create a film
10	100	10	K-Hand Coater (Manual)	Black	5	Not viscous enough to create a film
10	100	20	K-Hand Coater (Manual)	Black	5	A film with higher flexibility was produced

Table B.7.4 – Optimization of the neat ethyl cellulose film, with the use MyVacet 9–45K, as plasticizer. To verify the best evaporation process, it was used a K-Hand Coater and a K-Control Coater to produce the films.

EC (%)	Ethanol (%)	Plasticizer – MyVacet 9-45K (%)	Evaporation Process	Coating Bar Colour	Quantity Deposited (mL)	Measures (µm)
10	100	20	K-Hand Coater (Manual)	Black	5	25,3
10	100	20	K-Control Coater (Automatic)	Black	5	7,1
10	100	20	K-Hand Coater (Manual)	Orange	5	27,5
10	100	20	K-Control Coater (Automatic)	Orange	5	6,4
10	100	20	K-Hand Coater (Manual)	Brown	5	20,7
10	100	20	K-Control Coater (Automatic)	Brown	5	11,1
10	100	20	K-Hand Coater (Manual)	Blue	5	17,6
10	100	20	K-Control Coater (Automatic)	Blue	5	11,1
10	100	20	K-Hand Coater (Manual)	Grey	5	16,8

10	100	20	K-Control Coater (Auto-matic)	Grey	5	12,5

Table B.7.5 – Coating thicknesses with the use of a K-Control Coater equipped with different coating bars.

Colour Bar	**Wet Film Deposit (µm)**
Black	40
Orange	60
Brown	80
Blue	100
Grey	150

C

APPENDIX – EXPERIMENTAL RESULTS

C.1 Films' characterization

C.1.1 CMC-based films

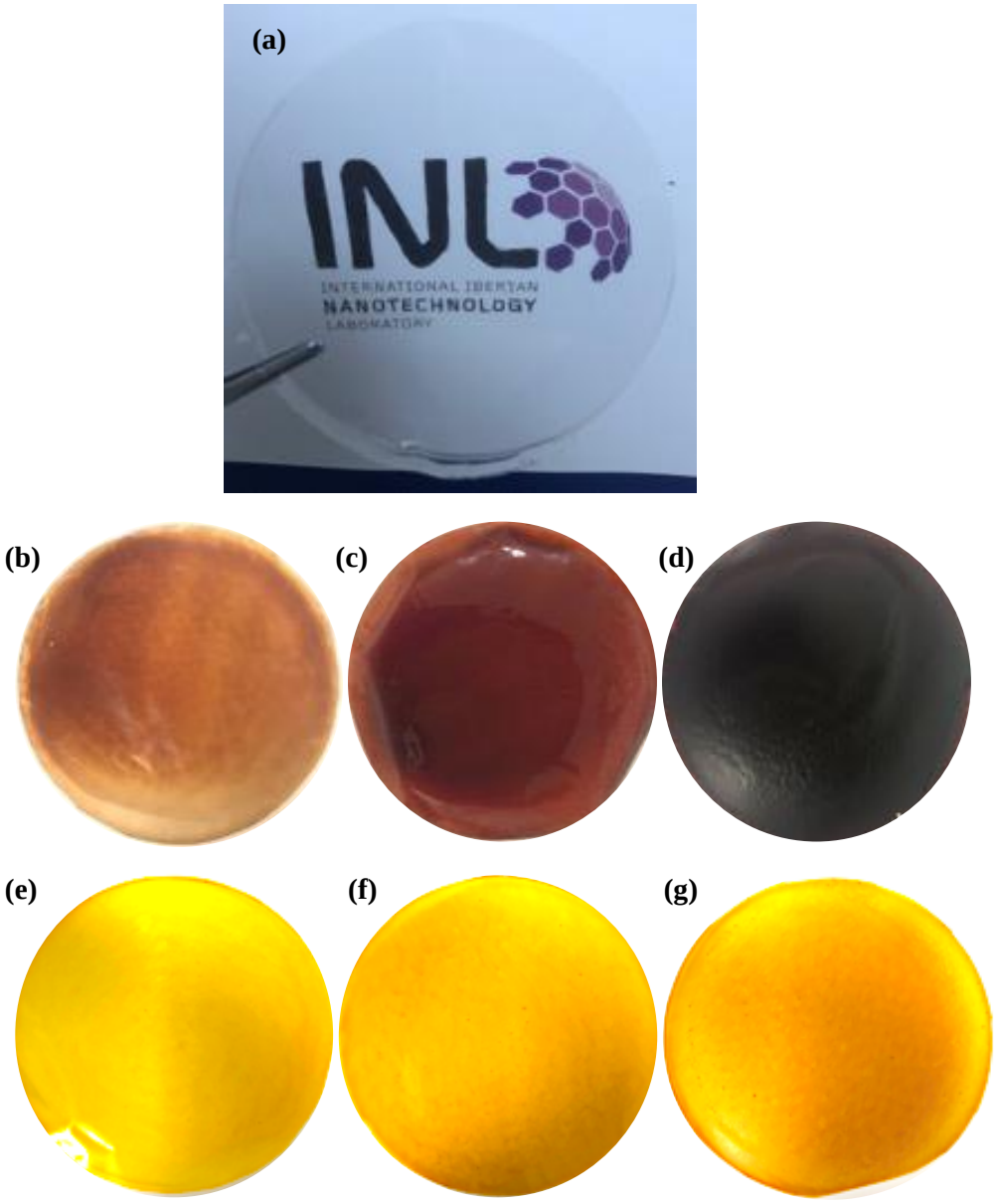

Figure C.1.1.1 – CMC-based films with (a) 0% (w/w) natural dye, (b) 0.5% (w/w) anthocyanins, (c) 1% (w/w) anthocyanins, (d) 2% (w/w) anthocyanins, (e) 0.5% (w/w) curcumin, (f) 1% (w/w) curcumin and (g) 2% (w/w) curcumin.

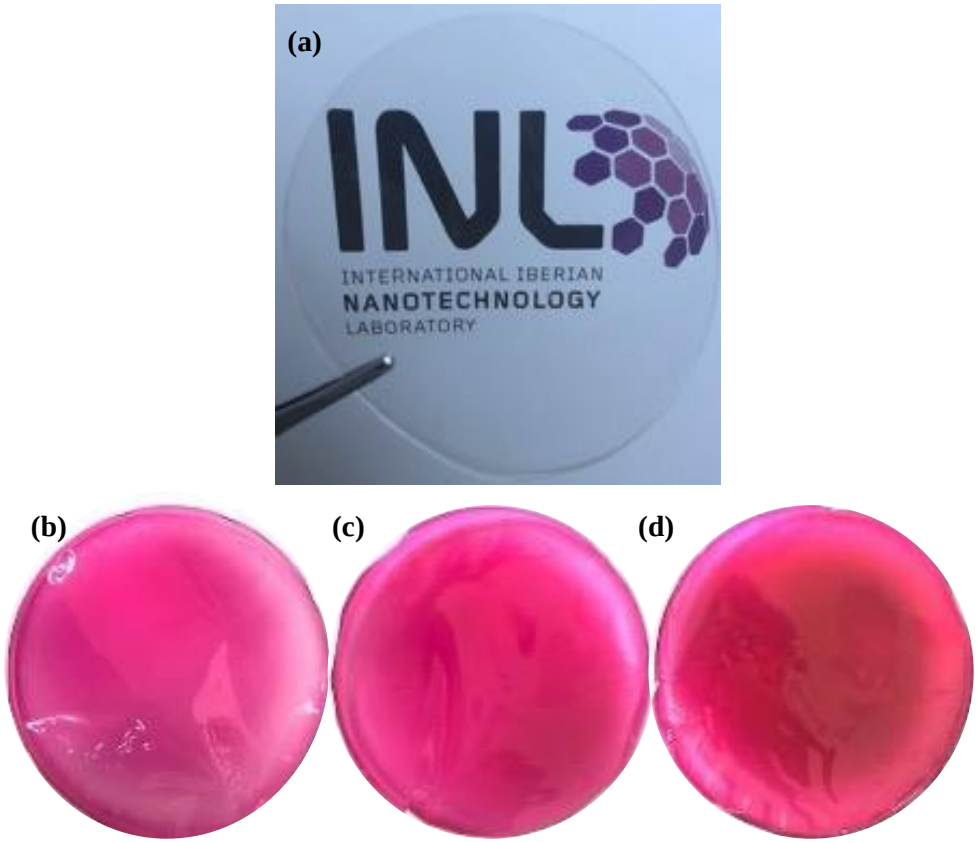

Figure C.1.1.2 – CMC-based films with (a) 0% (w/w) natural dye, (b) 0.5% (w/w) betalains, (c) 1% (w/w) betalains, (d) 2% (w/w) betalains.

C.1.2 CA-based films

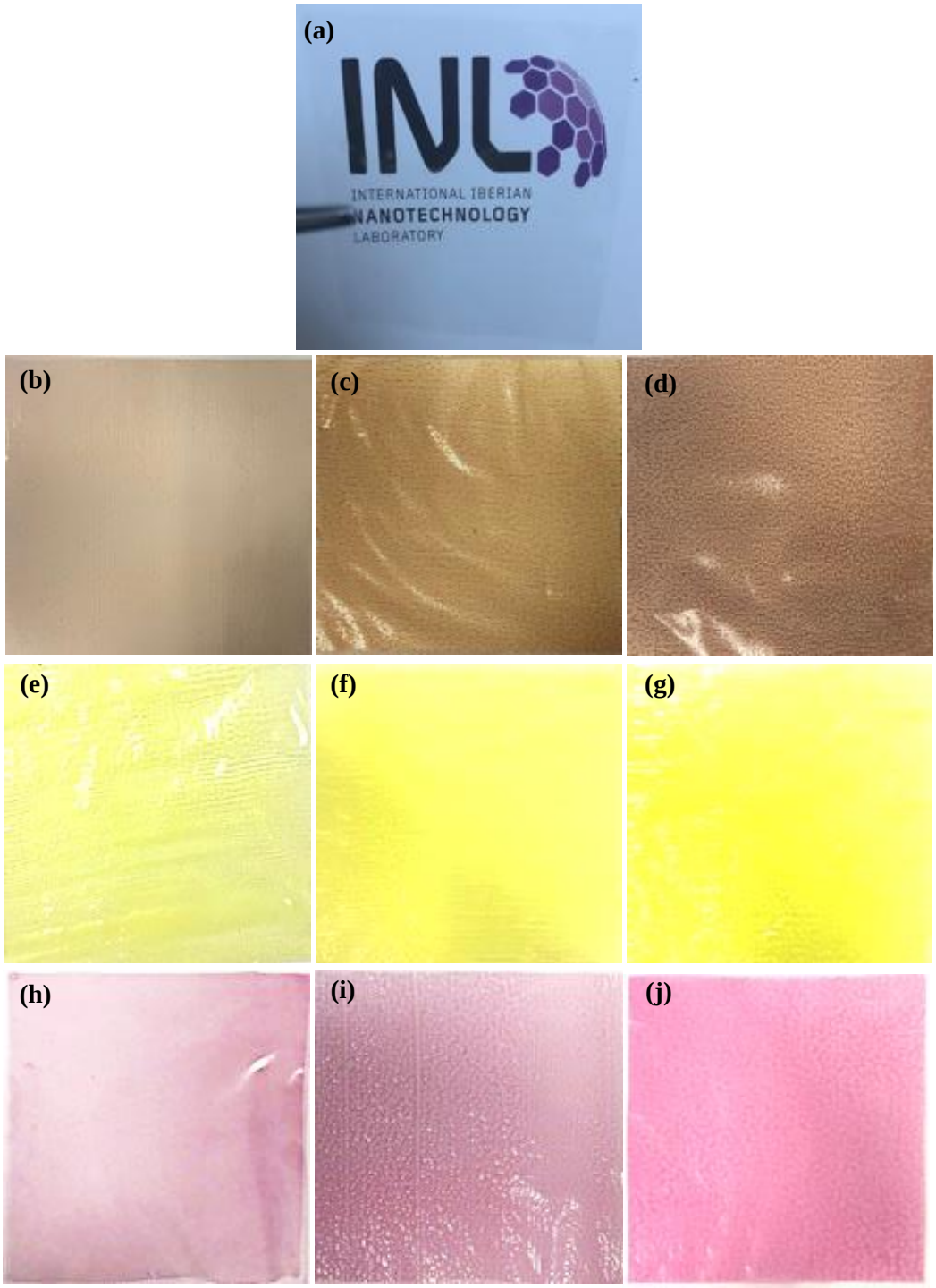

Figure C.1.2.1 – AC-based films with (a) 0% (w/w) natural dye, (b) 0.5% (w/w) anthocyanins, (c) 1% (w/w) anthocyanins, (d) 2% (w/w) anthocyanins, (e) 0.5% (w/w) curcumin, (f) 1% (w/w) curcumin, (g) 2% (w/w) curcumin, (h) 0.5% (w/w) betalains, (i) 1% (w/w) betalains, (j) 2% (w/w) betalains.

C.1.3 EC-based films

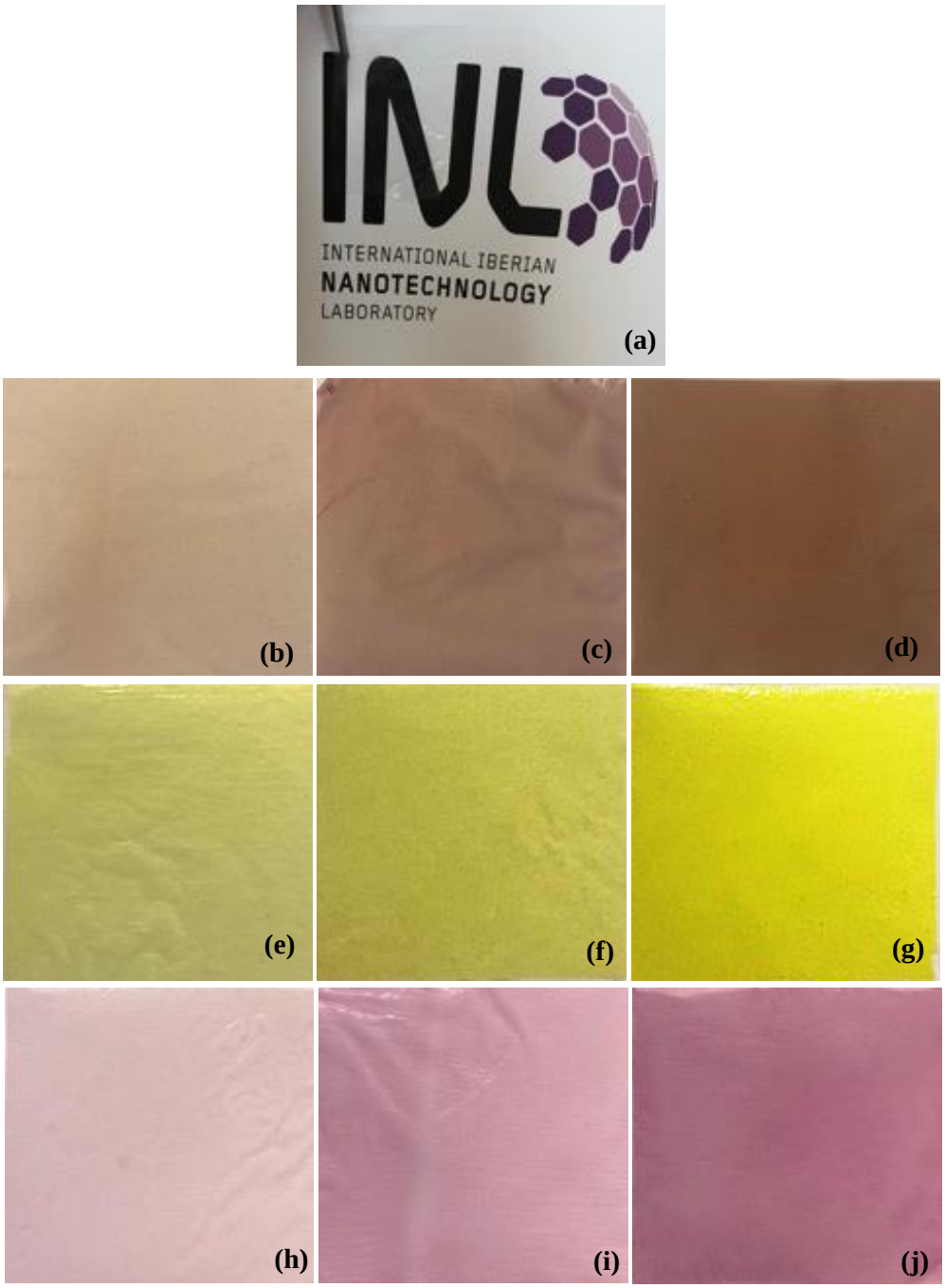

Figure C.1.3.1 – EC-based films with (a) 0% (w/w) natural dye, (b) 0.5% (w/w) anthocyanins, (c) 1% (w/w) anthocyanins, (d) 2% (w/w) anthocyanins, (e) 0.5% (w/w) curcumin, (f) 1% (w/w) curcumin, (g) 2% (w/w) curcumin, (h) 0.5% (w/w) betalains, (i) 1% (w/w) betalains, (j) 2% (w/w) betalains.

C.2 Films pH sensing

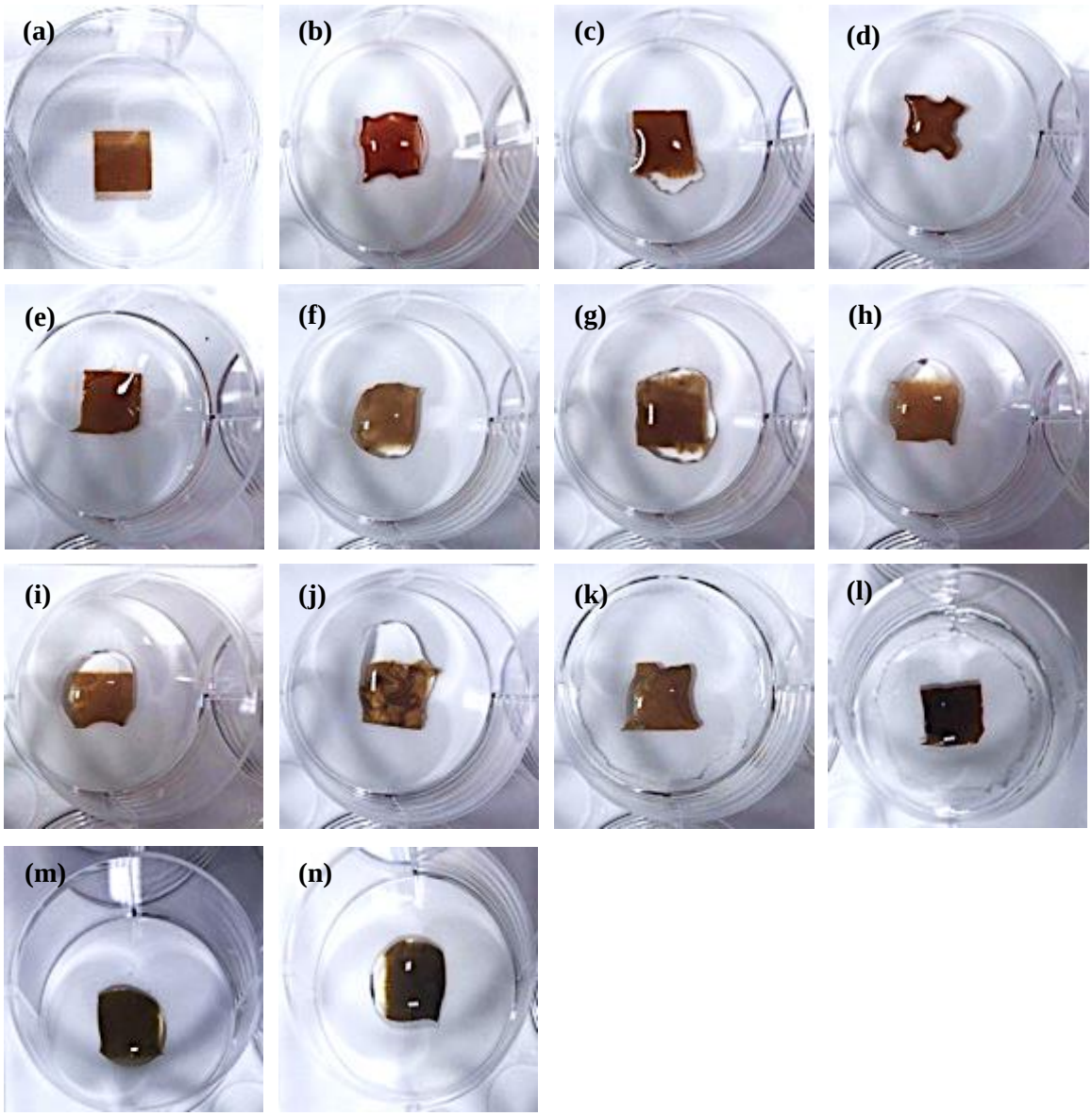

Figure C.2.1 – Carboxymethylcellulose-based films with the incorporation of 0.5% (w/w) of anthocyanins: (a) without the immersion in buffer solutions, (b) to (n) corresponds to the immersion in buffer solutions ranged from pH 1 – 13, respectively.

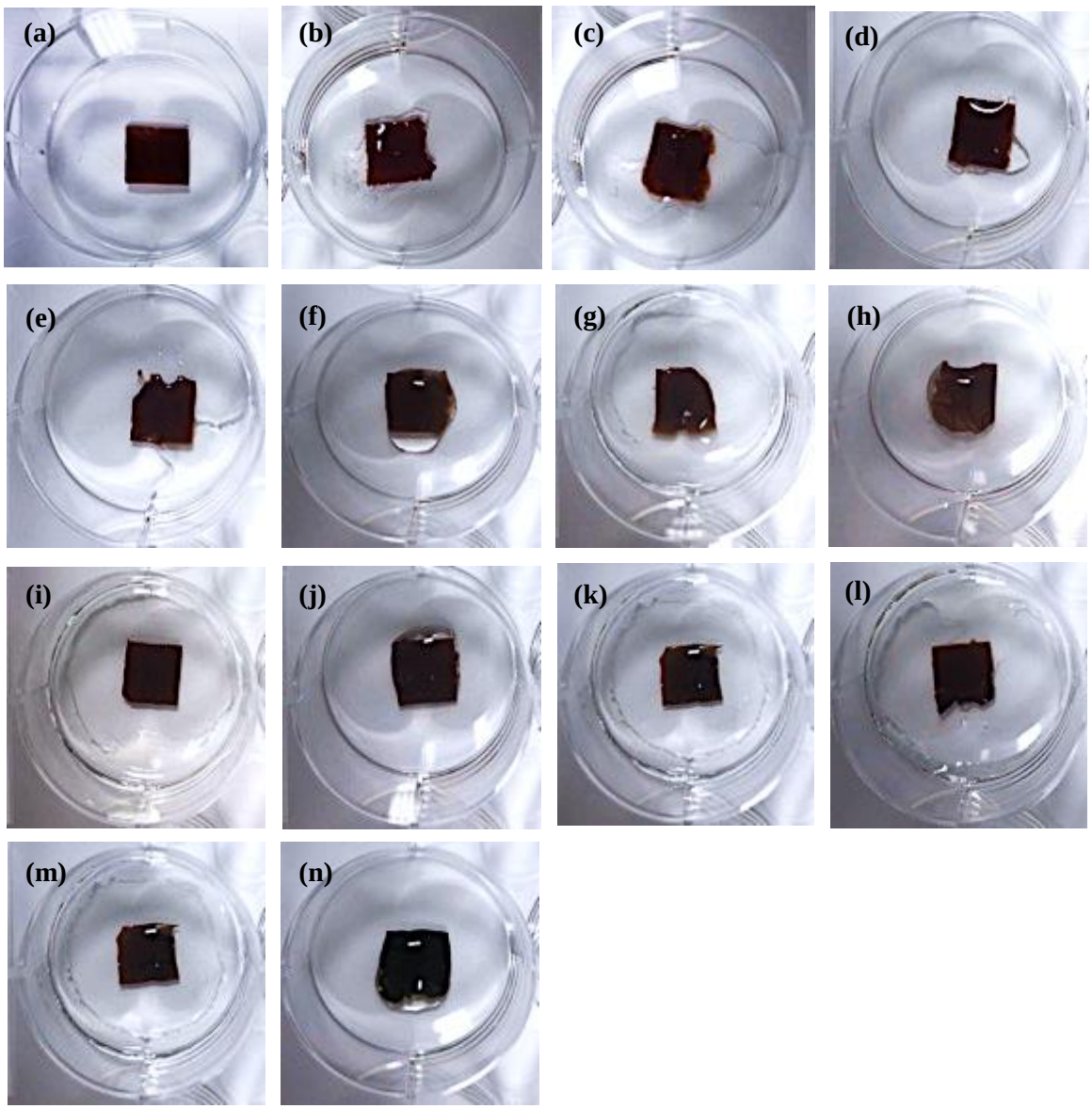

Figure C.2.2 – Carboxymethylcellulose-based films with the incorporation of 1% (w/w) of anthocyanins: (a) without the immersion in buffer solutions, (b) to (n) corresponds to the immersion in buffer solutions ranged from pH 1 – 13, respectively.

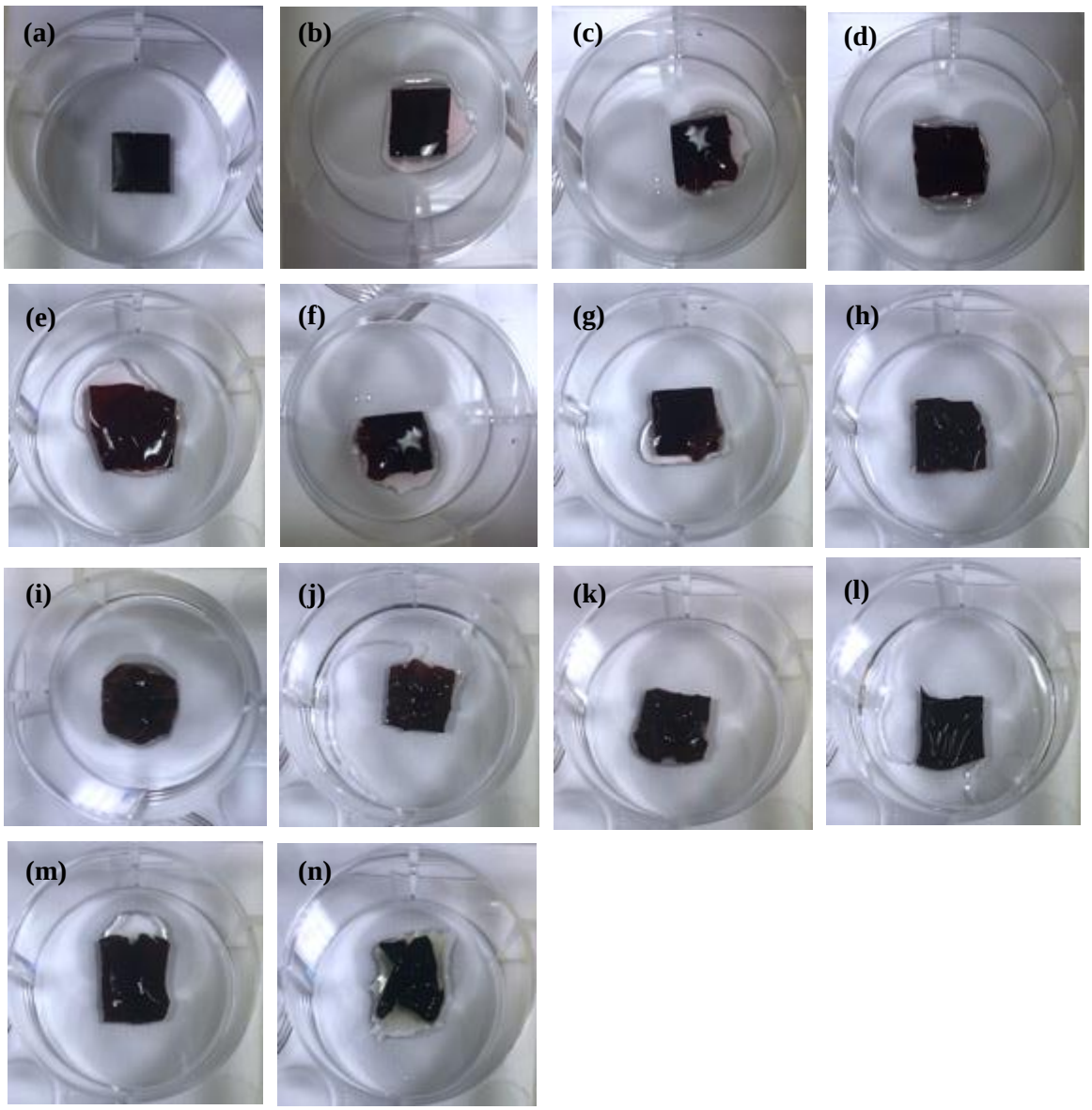

Figure C.2.3 – Carboxymethylcellulose-based films with the incorporation of 2% (w/w) of anthocyanins: (a) without the immersion in buffer solutions, (b) to (n) corresponds to the immersion in buffer solutions ranged from pH 1 – 13, respectively.

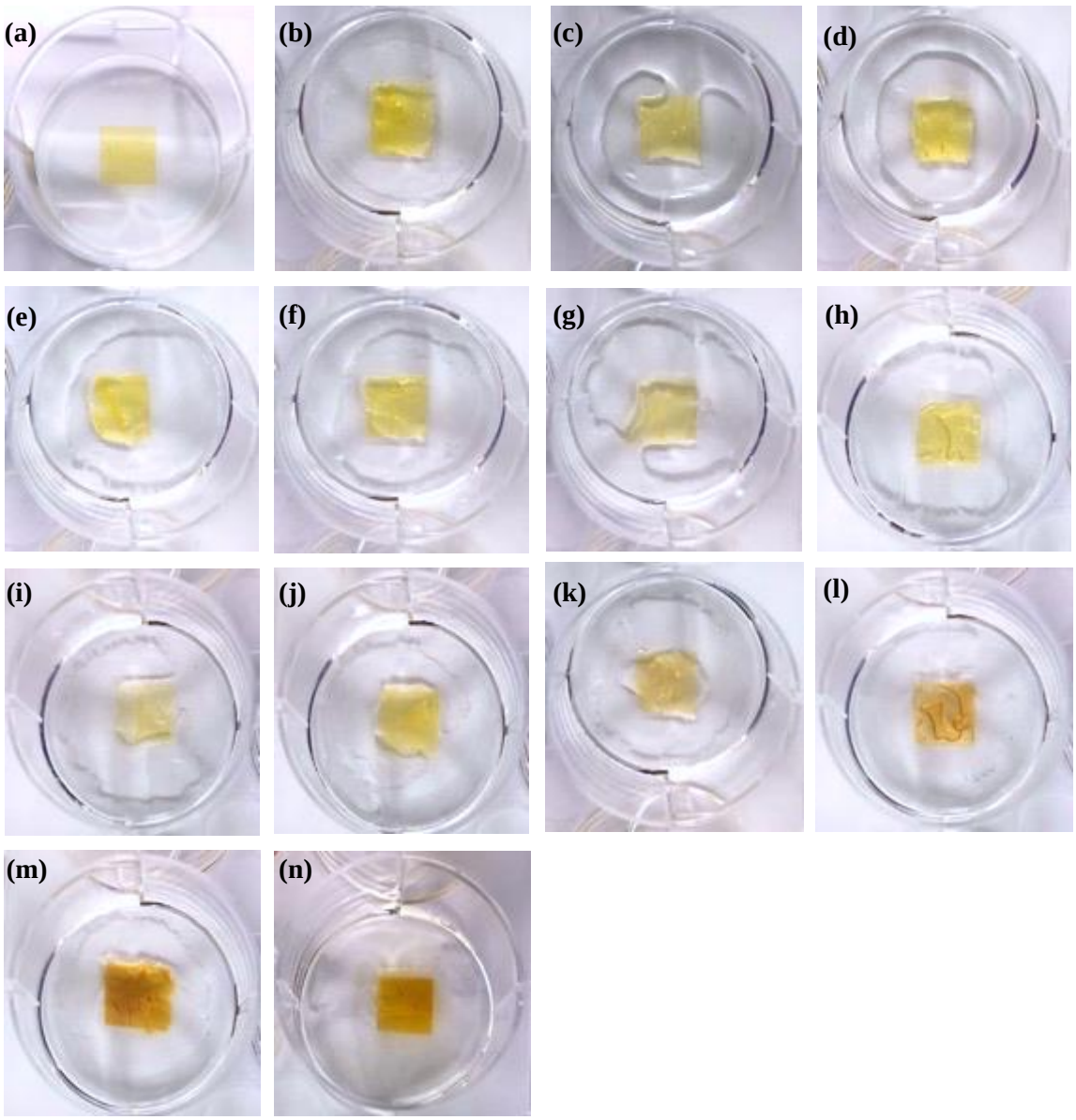

Figure C.2.4 – Carboxymethylcellulose-based films with the incorporation of 0.5% (w/w) of curcumin: (a) without the immersion in buffer solutions, (b) to (n) corresponds to the immersion in buffer solutions ranged from pH 1 – 13, respectively.

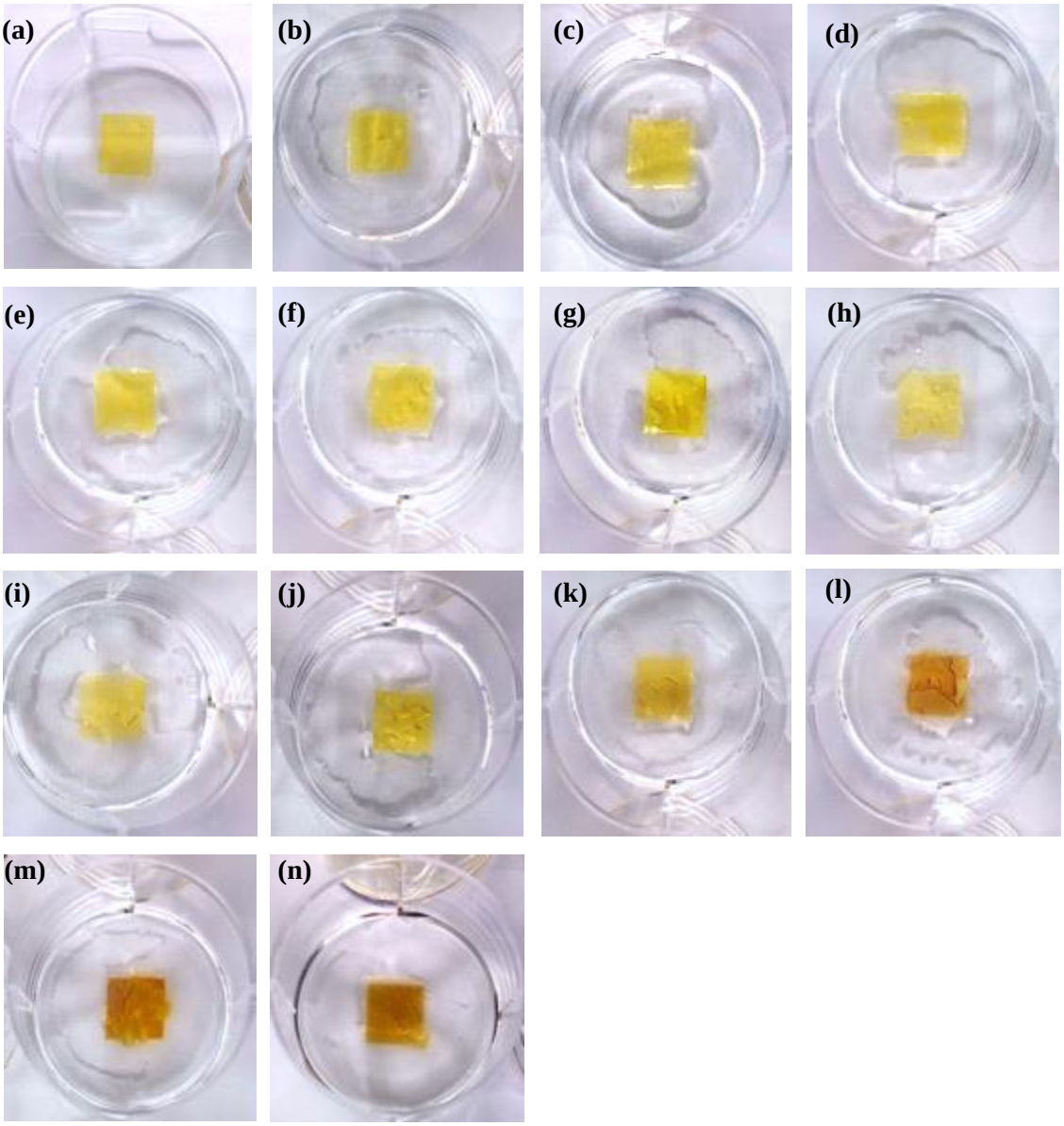

Figure C.2.5 – Carboxymethylcellulose-based films with the incorporation of 1% (w/w) of curcumin: (a) without the immersion in buffer solutions, (b) to (n) corresponds to the immersion in buffer solutions ranged from pH 1 – 13, respectively.

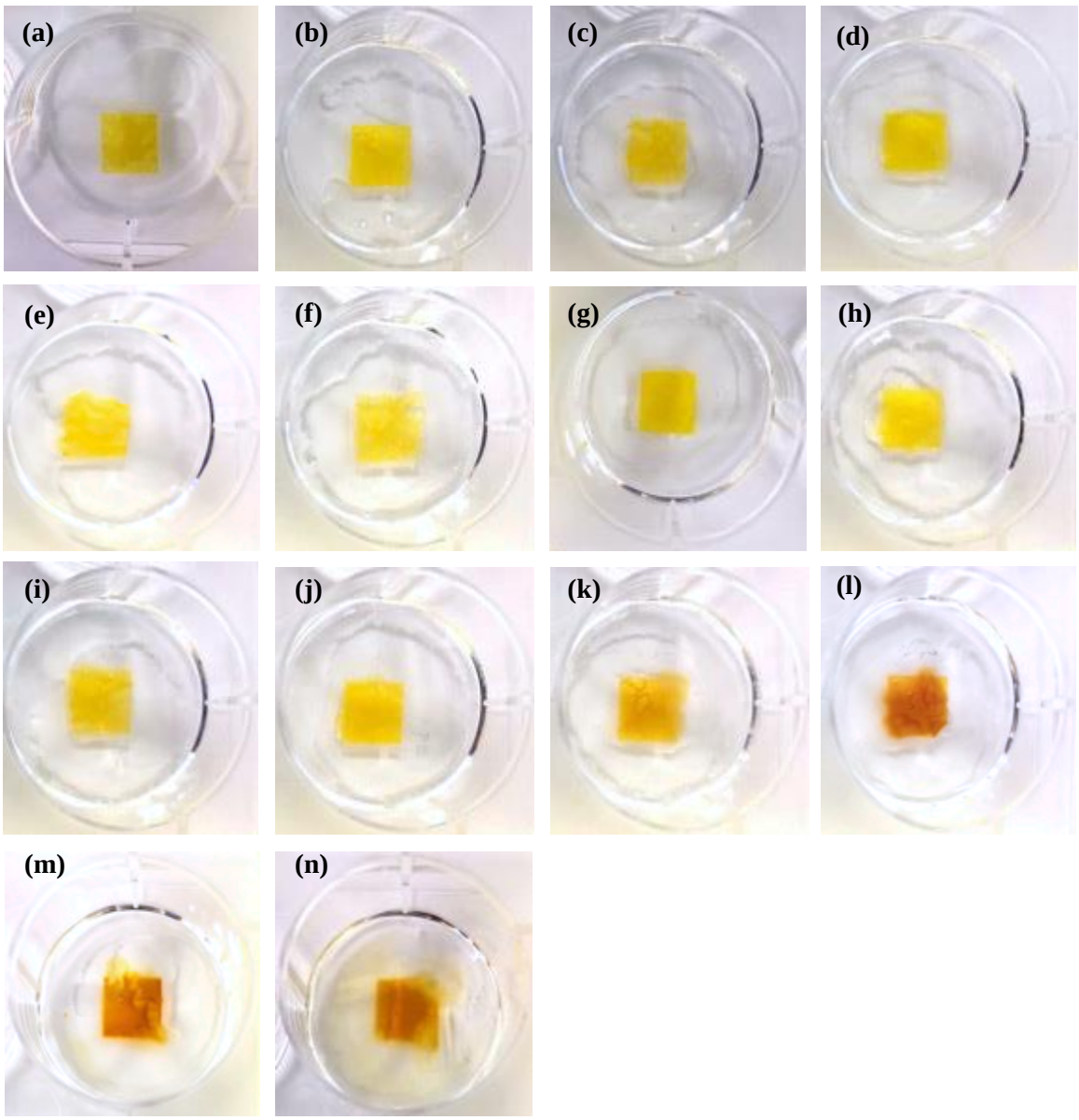

Figure C.2.6 – Carboxymethylcellulose-based films with the incorporation of 2% (w/w) of curcumin: (a) without the immersion in buffer solutions, (b) to (n) corresponds to the immersion in buffer solutions ranged from pH 1 – 13, respectively.

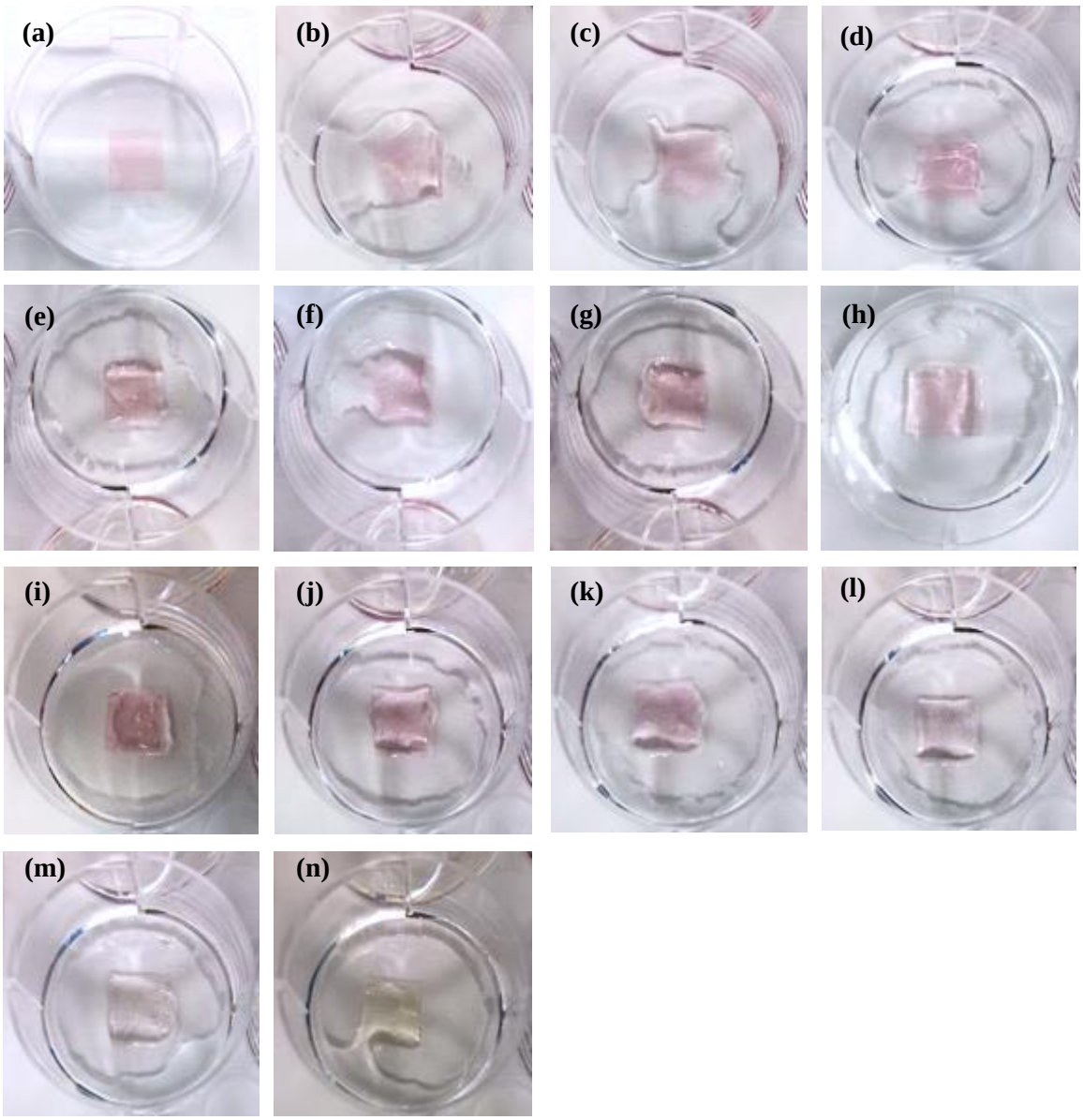

Figure C.2.7 – Carboxymethylcellulose-based films with the incorporation of 0.5% (w/w) of betalains: (a) without the immersion in buffer solutions, (b) to (n) corresponds to the immersion in buffer solutions ranged from pH 1 – 13, respectively.

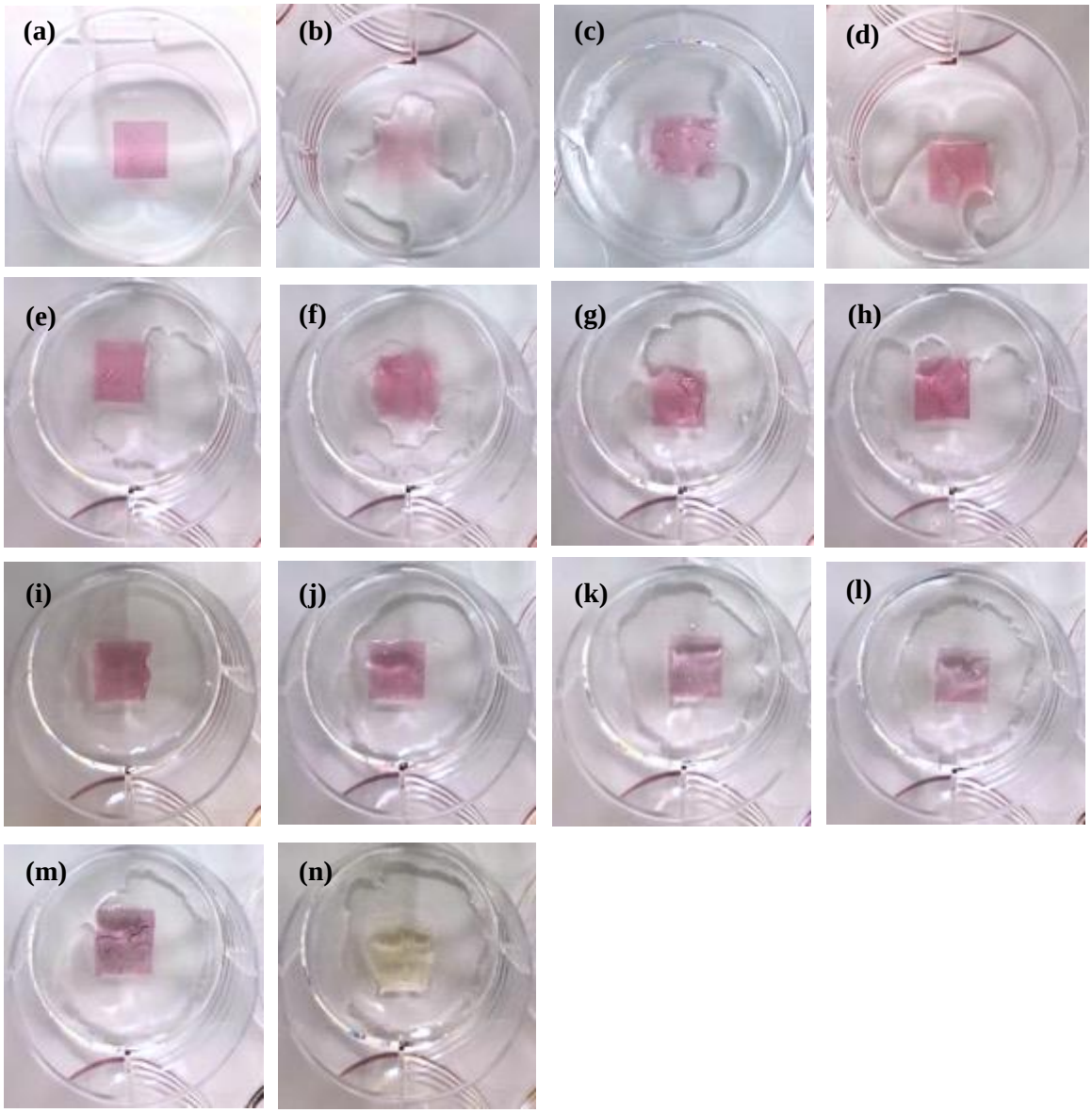

Figure C.2.8 – Carboxymethylcellulose-based films with the incorporation of 1% (w/w) of betalains: (a) without the immersion in buffer solutions, (b) to (n) corresponds to the immersion in buffer solutions ranged from pH 1 – 13, respectively.

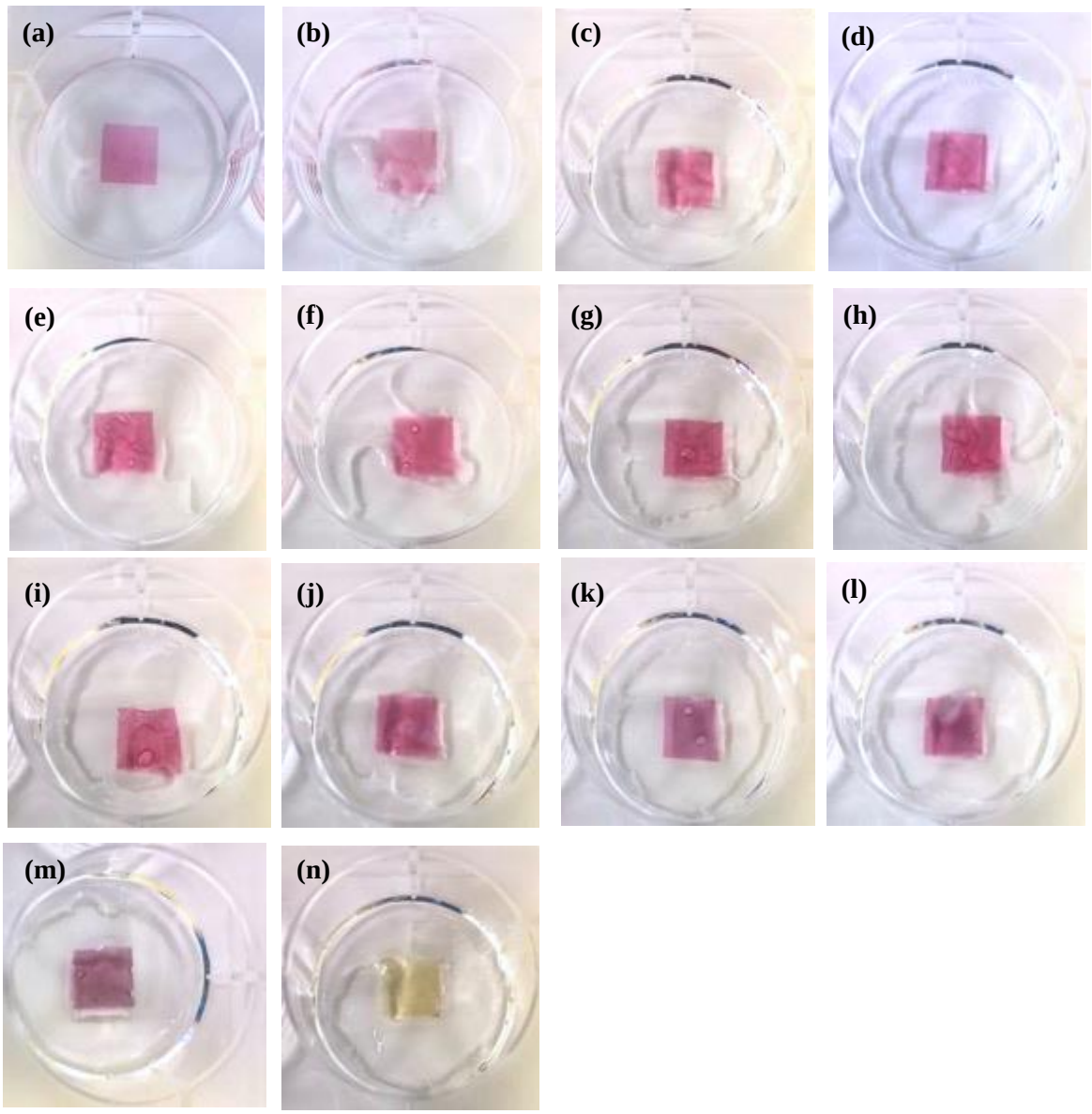

Figure C.2.9 – Carboxymethylcellulose-based films with the incorporation of 2% (w/w) of betalains: (a) without the immersion in buffer solutions, (b) to (n) corresponds to the immersion in buffer solutions ranged from pH 1 – 13, respectively.

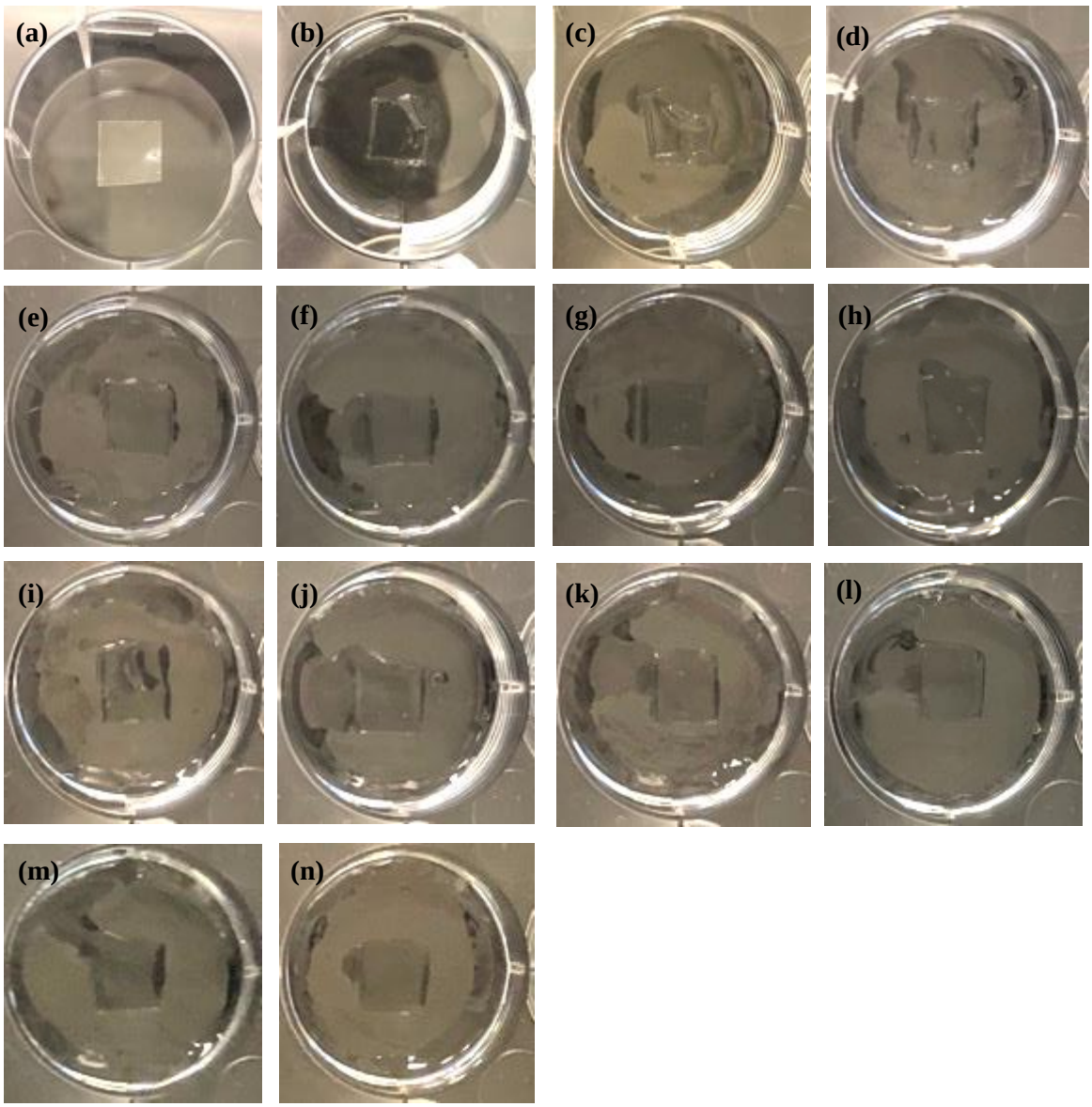

Figure C.2.10 – Carboxymethylcellulose-based films without the incorporation of any natural dye: (a) without the immersion in buffer solutions, (b) to (n) corresponds to the immersion in buffer solutions ranged from pH 1 – 13, respectively.

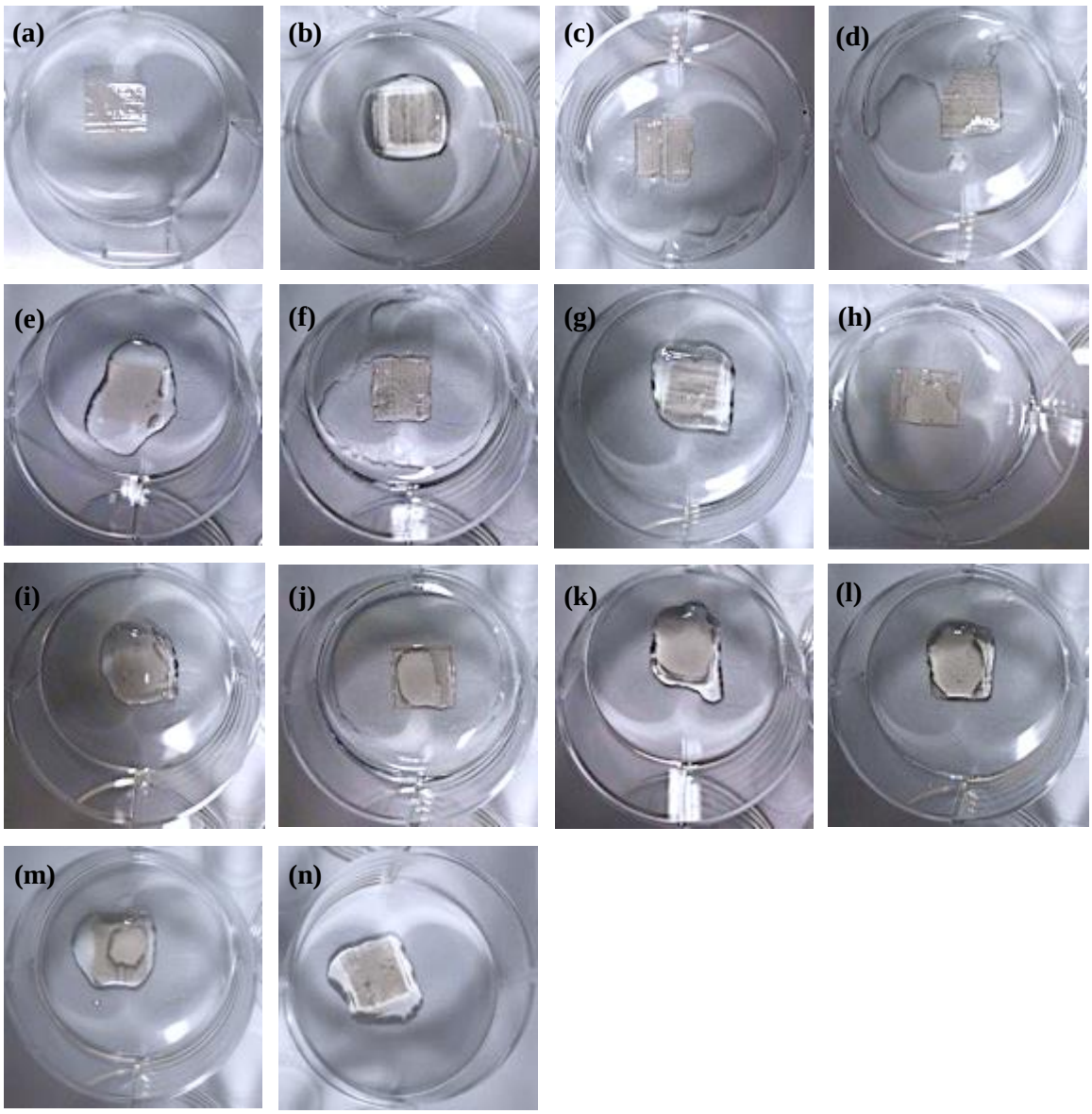

Figure C.2.11 – Cellulose acetate-based films with the incorporation of 0.5% (w/w) of anthocyanins: (a) without the immersion in buffer solutions, (b) to (n) corresponds to the immersion in buffer solutions ranged from pH 1 – 13, respectively.

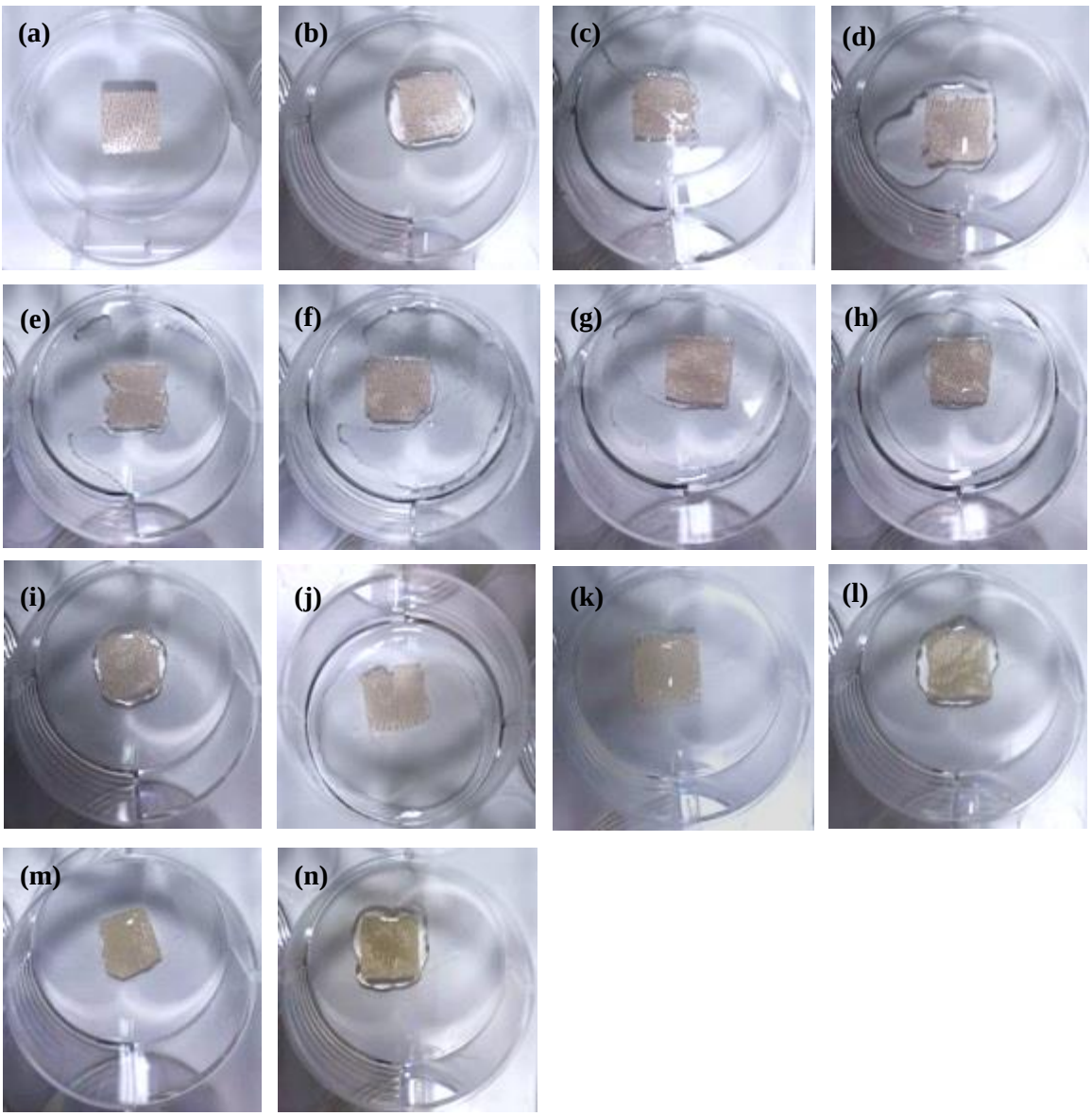

Figure C.2.12 – Cellulose acetate-based films with the incorporation of 1% (w/w) of anthocyanins: (a) without the immersion in buffer solutions, (b) to (n) corresponds to the immersion in buffer solutions ranged from pH 1 – 13, respectively.

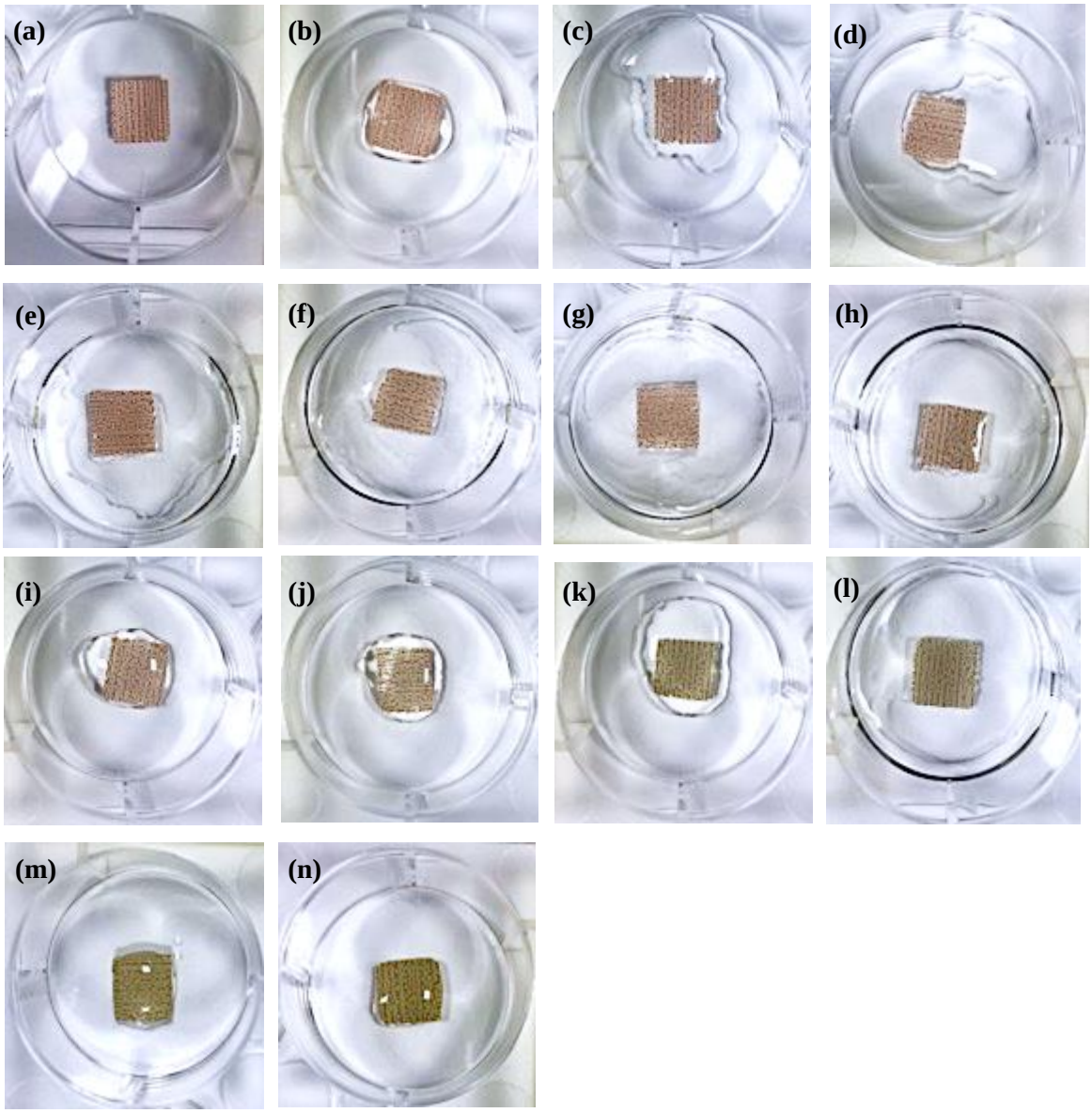

Figure C.2.13 – Cellulose acetate-based films with the incorporation of 2% (w/w) of anthocyanins: (a) without the immersion in buffer solutions, (b) to (n) corresponds to the immersion in buffer solutions ranged from pH 1 – 13, respectively.

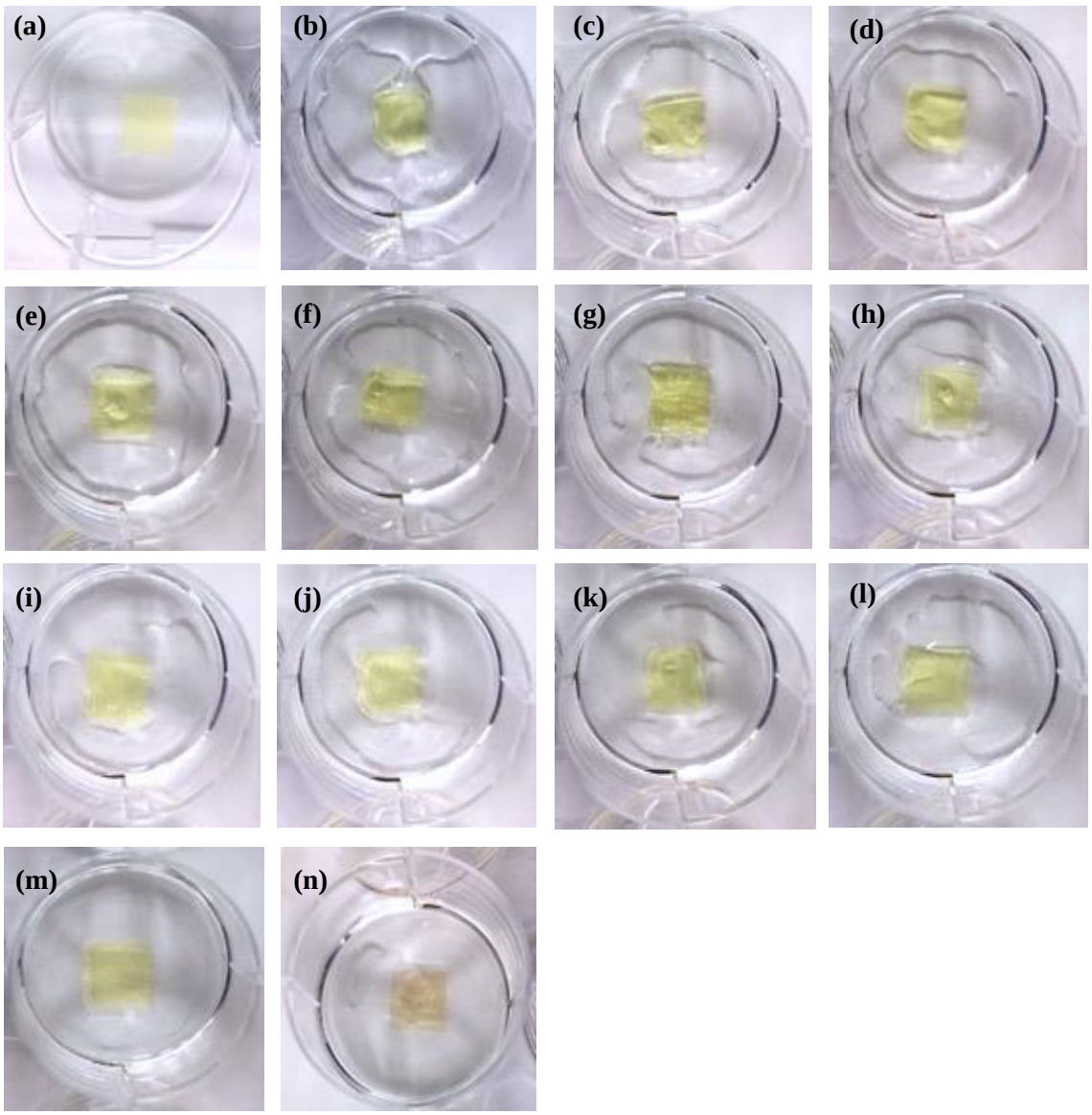

Figure C.2.14 – Cellulose acetate-based films with the incorporation of 0.5% (w/w) of curcumin: (a) without the immersion in buffer solutions, (b) to (n) corresponds to the immersion in buffer solutions ranged from pH 1 – 13, respectively.

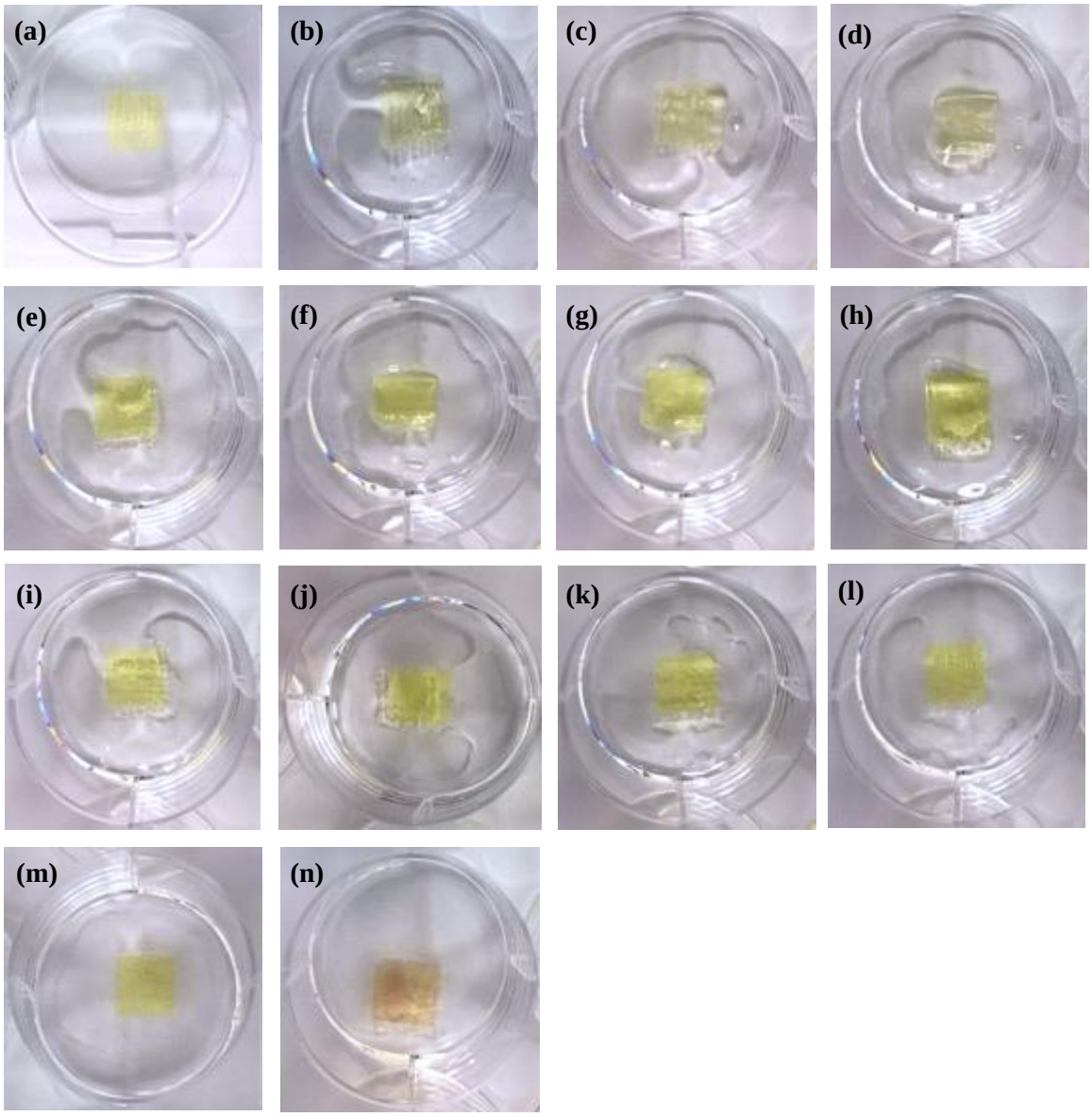

Figure C.2.15 – Cellulose acetate-based films with the incorporation of 1% (w/w) of curcumin: (a) without the immersion in buffer solutions, (b) to (n) corresponds to the immersion in buffer solutions ranged from pH 1 – 13, respectively.

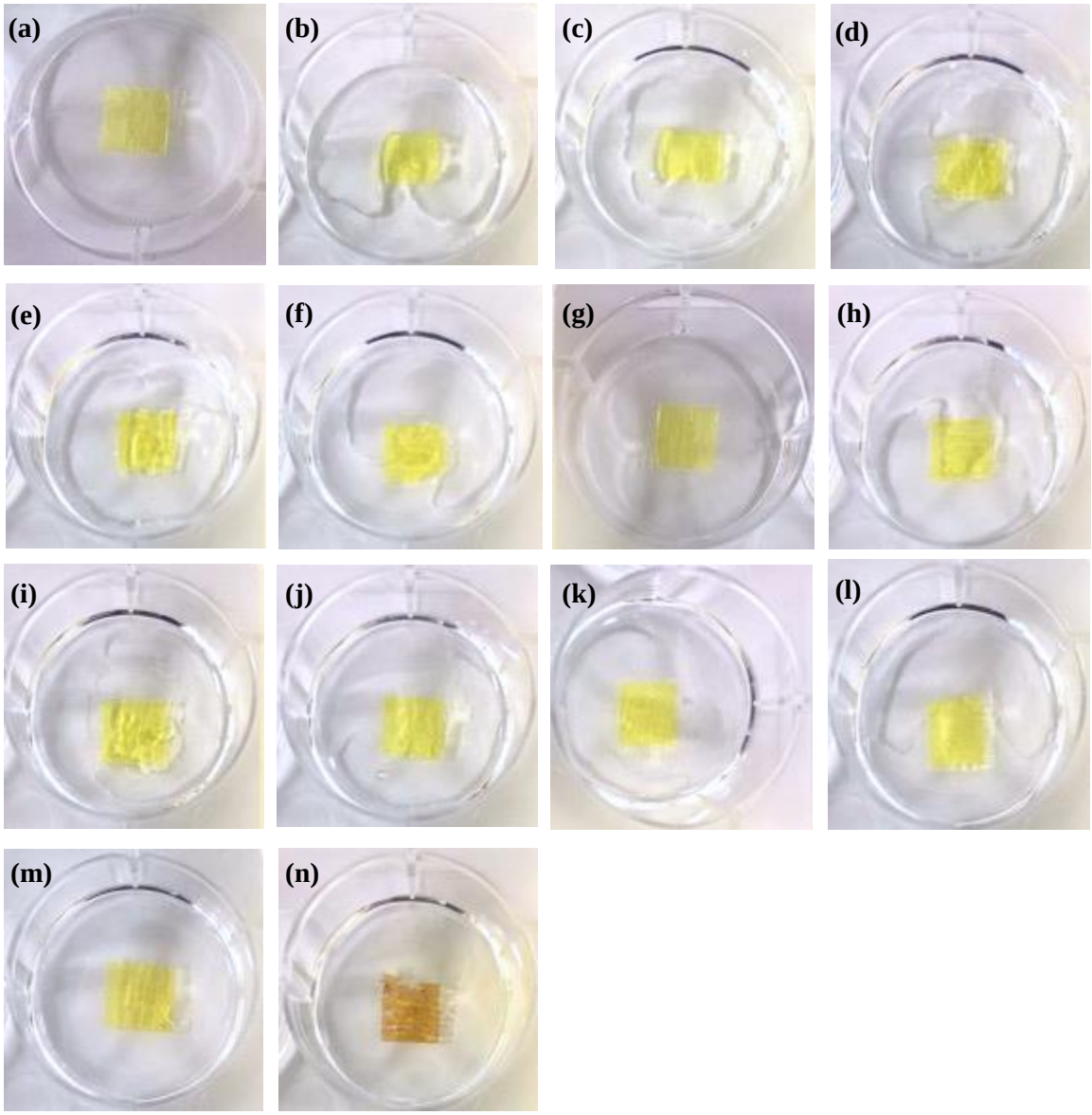

Figure C.2.16 – Cellulose acetate-based films with the incorporation of 2% (w/w) of curcumin: (a) without the immersion in buffer solutions, (b) to (n) corresponds to the immersion in buffer solutions ranged from pH 1 – 13, respectively.

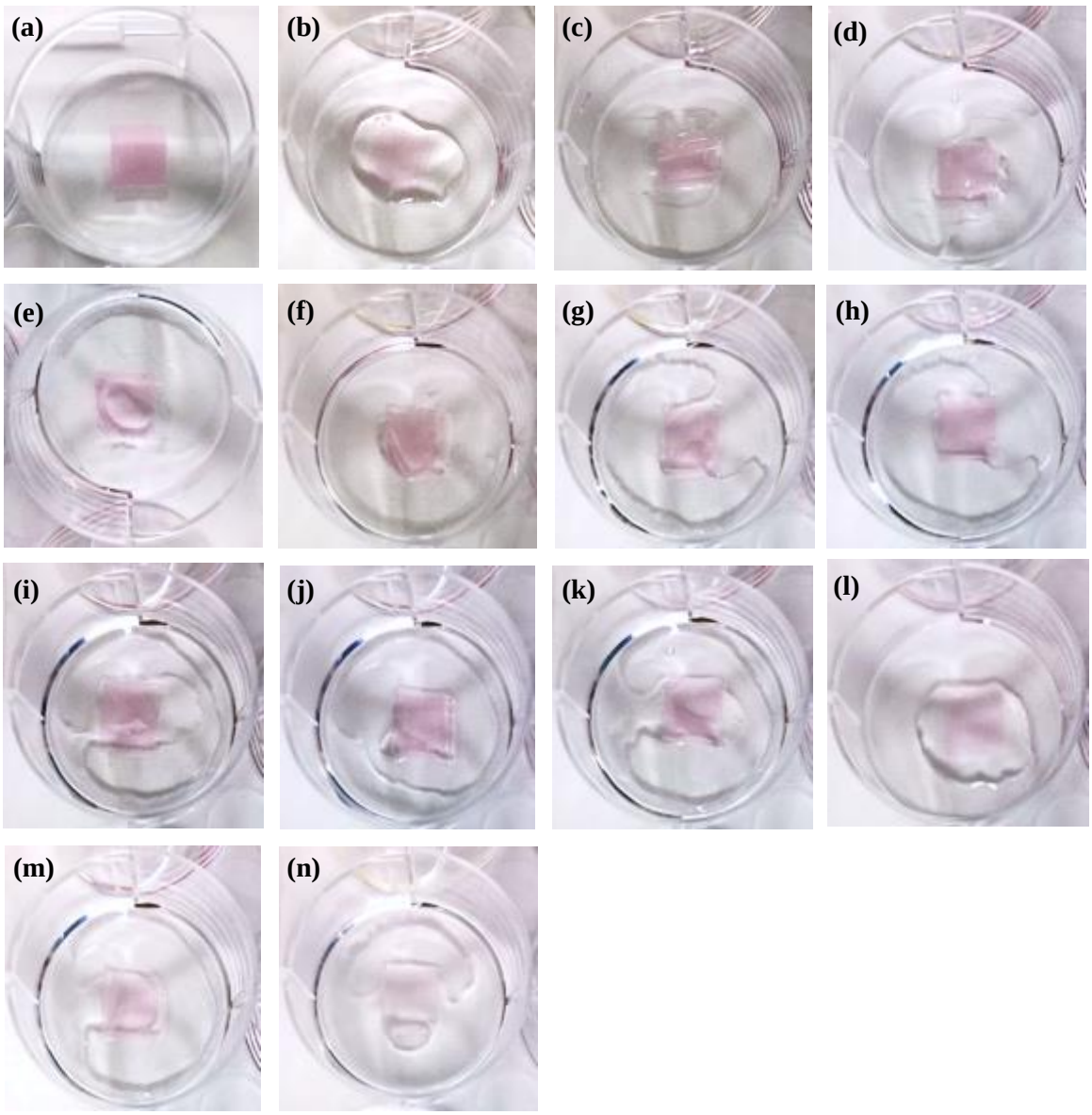

Figure C.2.17 – Cellulose acetate-based films with the incorporation of 0.5% (w/w) of betalains: (a) without the immersion in buffer solutions, (b) to (n) corresponds to the immersion in buffer solutions ranged from pH 1 – 13, respectively.

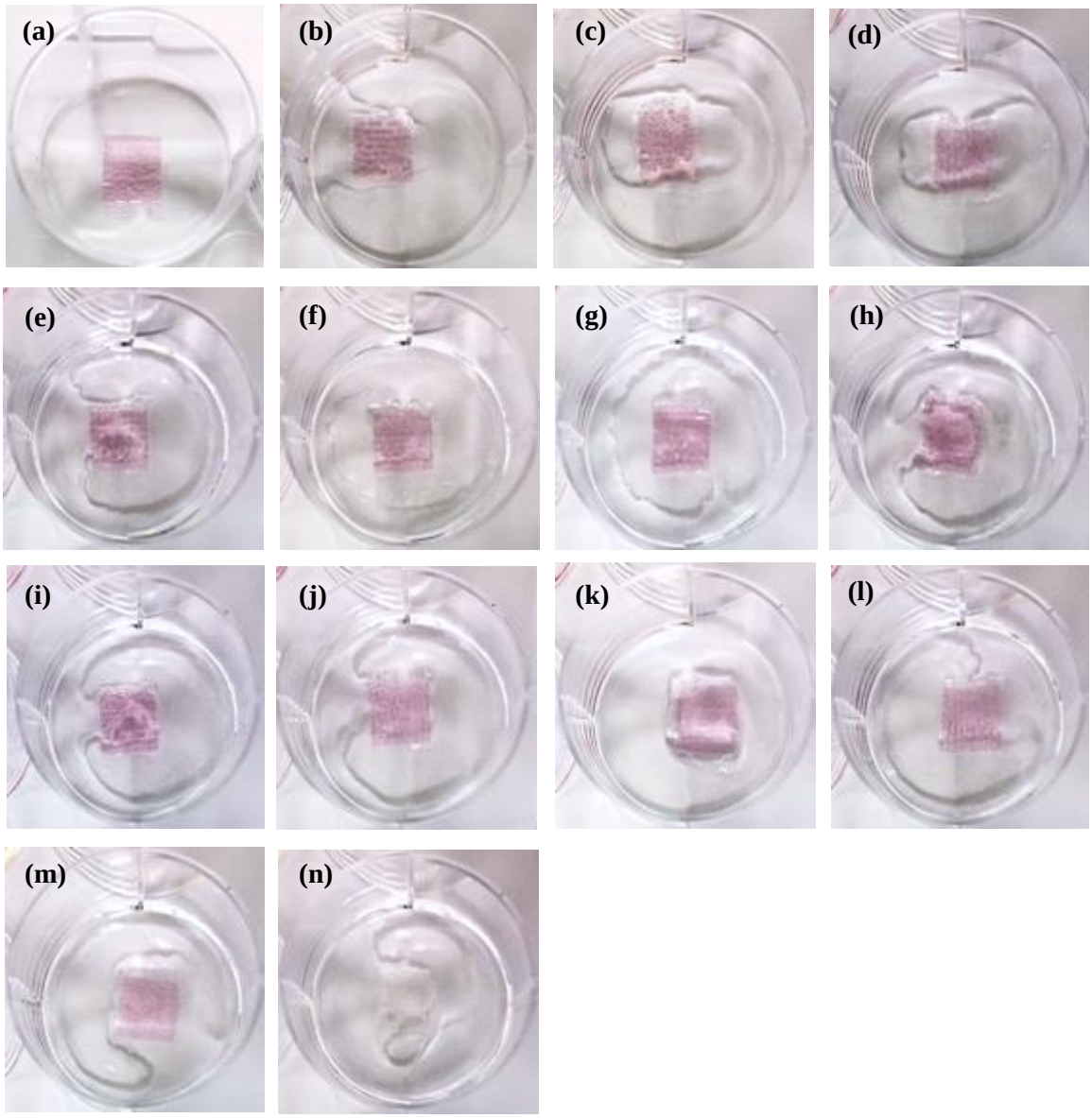

Figure C.2.18 – Cellulose acetate-based films with the incorporation of 1% (w/w) of betalains: (a) without the immersion in buffer solutions, (b) to (n) corresponds to the immersion in buffer solutions ranged from pH 1 – 13, respectively.

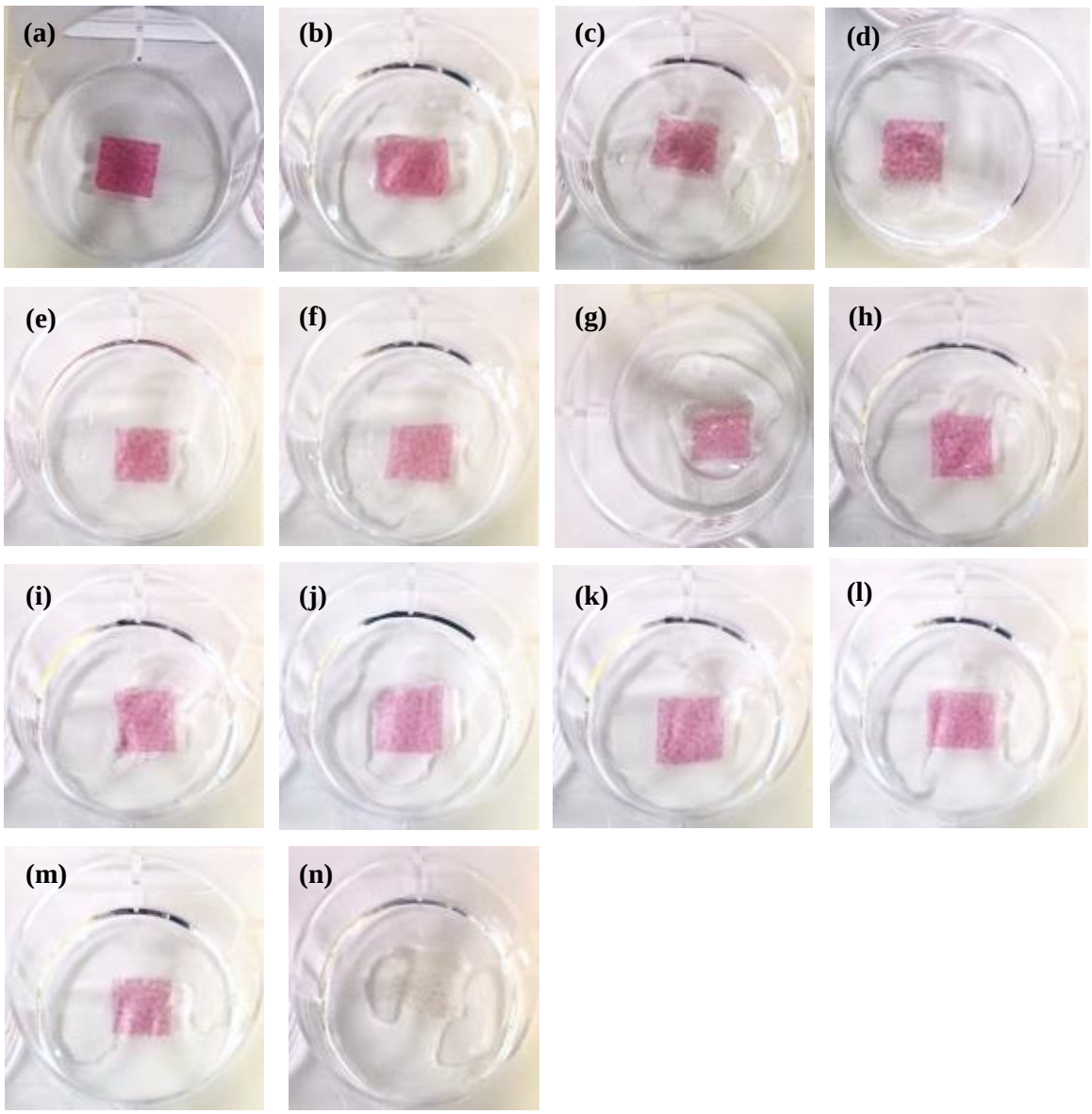

Figure C.2.19 – Cellulose acetate-based films with the incorporation of 2% (w/w) of betalains: (a) without the immersion in buffer solutions, (b) to (n) corresponds to the immersion in buffer solutions ranged from pH 1 – 13, respectively.

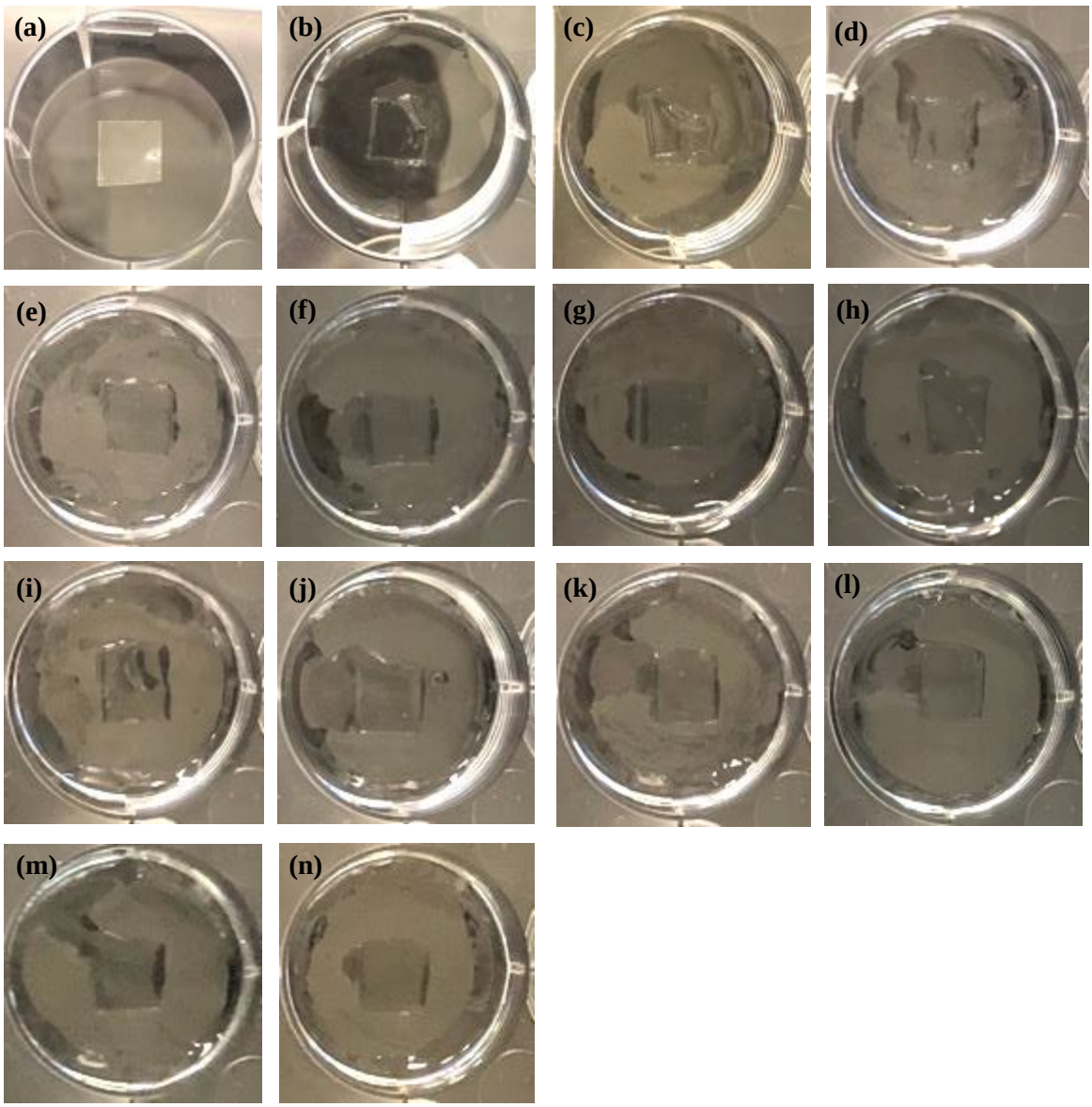

Figure C.2.20 – Cellulose acetate-based films without the incorporation of any natural dye: (a) without the immersion in buffer solutions, (b) to (n) corresponds to the immersion in buffer solutions ranged from pH 1 – 13, respectively.

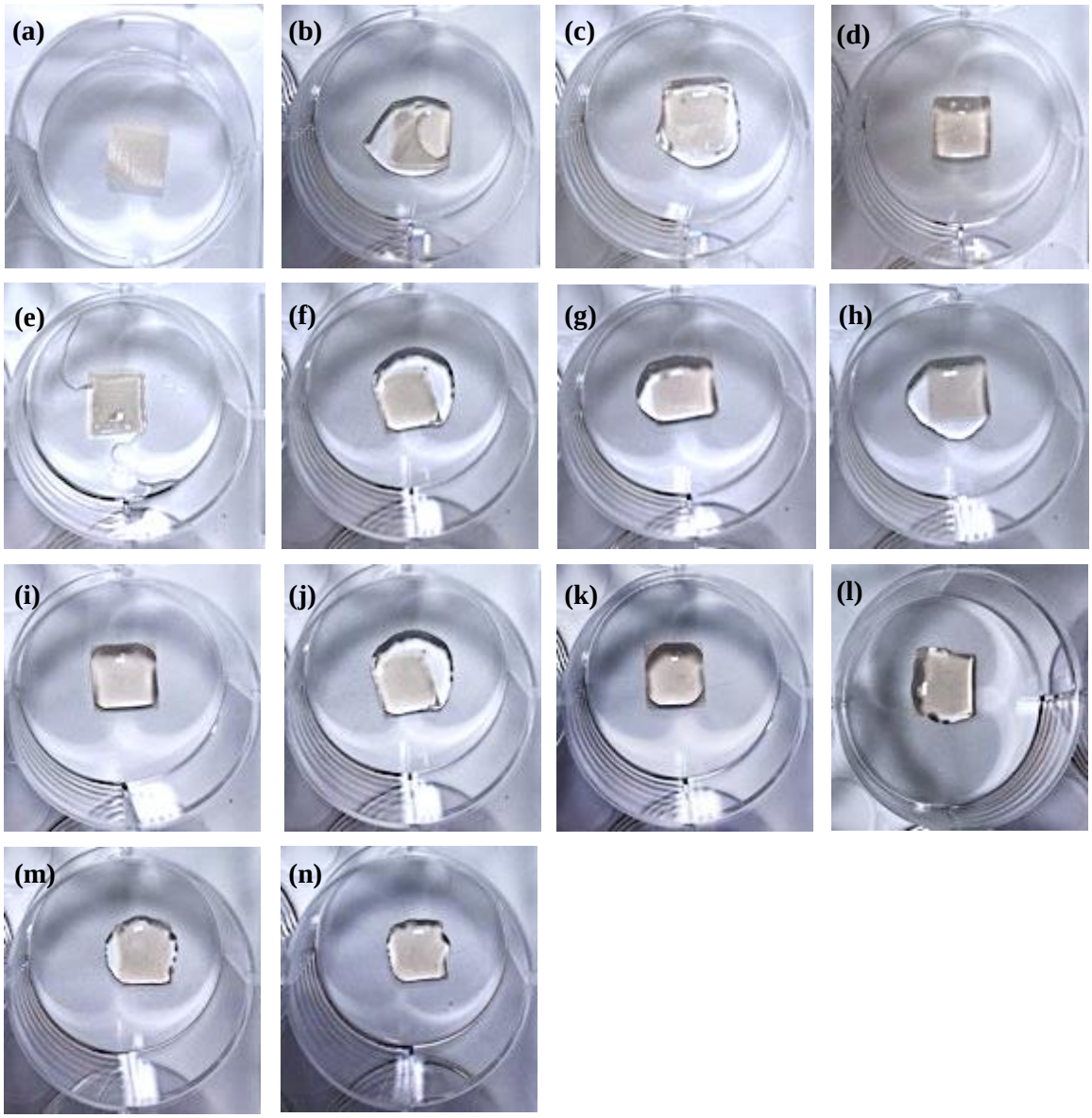

Figure C.2.21 – Ethyl cellulose-based films with the incorporation of 0.5% (w/w) of anthocyanins: (a) without the immersion in buffer solutions, (b) to (n) corresponds to the immersion in buffer solutions ranged from pH 1 – 13, respectively.

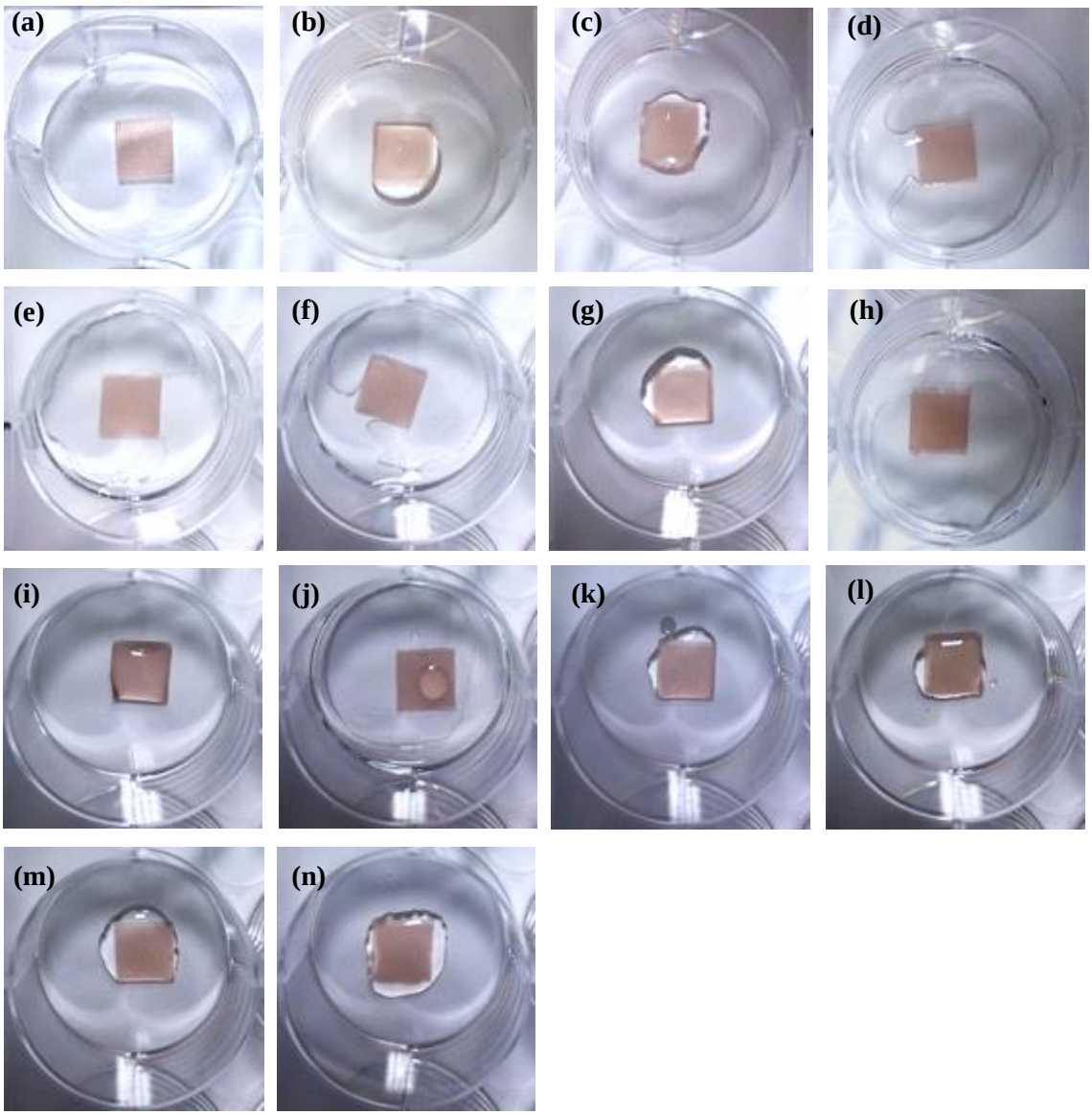

Figure C.2.22 – Ethyl cellulose-based films with the incorporation of 1% (w/w) of anthocyanins: (a) without the immersion in buffer solutions, (b) to (n) corresponds to the immersion in buffer solutions ranged from pH 1 – 13, respectively.

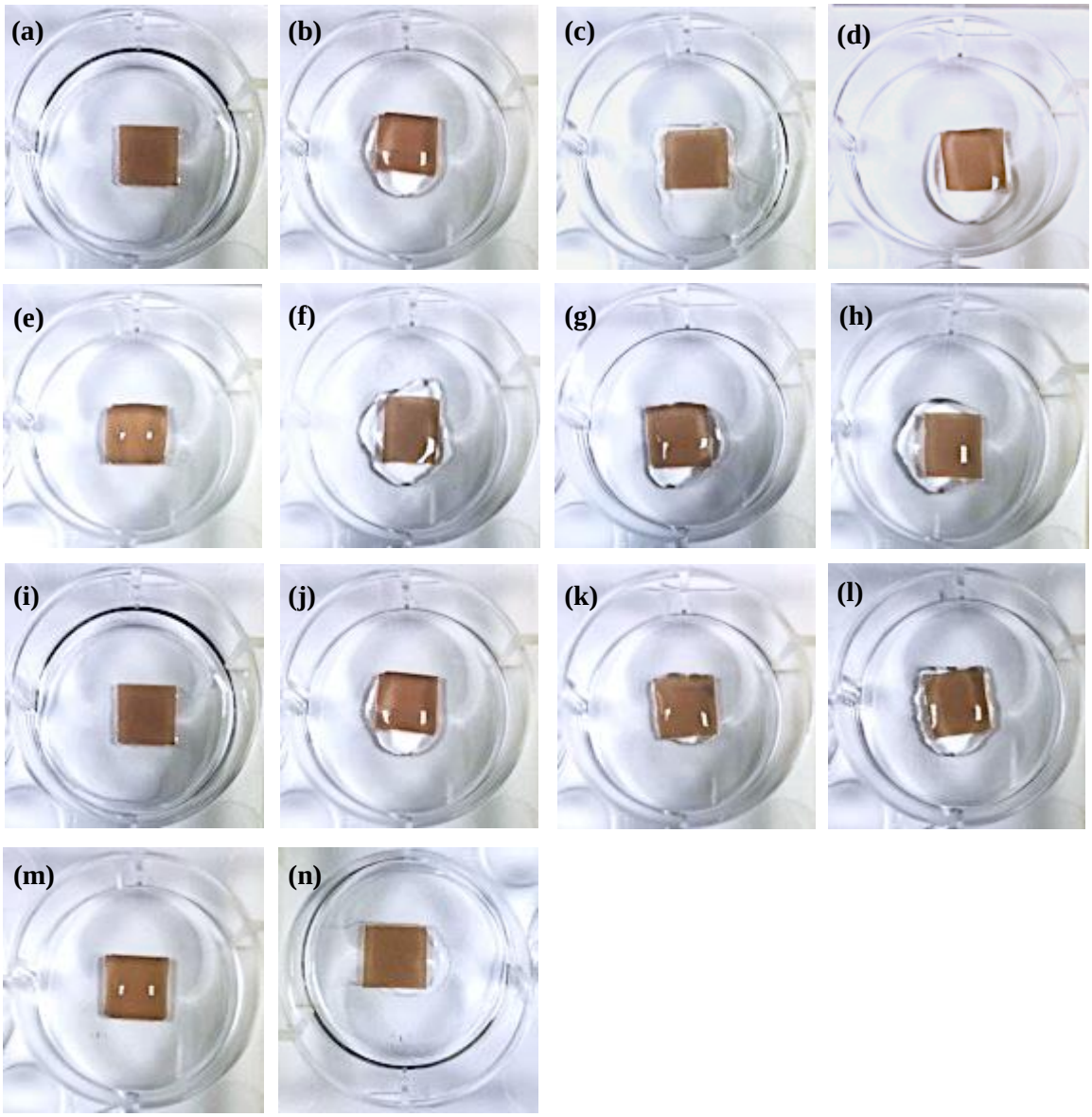

Figure C.2.23 – Ethyl cellulose-based films with the incorporation of 2% (w/w) of anthocyanins: (a) without the immersion in buffer solutions, (b) to (n) corresponds to the immersion in buffer solutions ranged from pH 1 – 13, respectively.

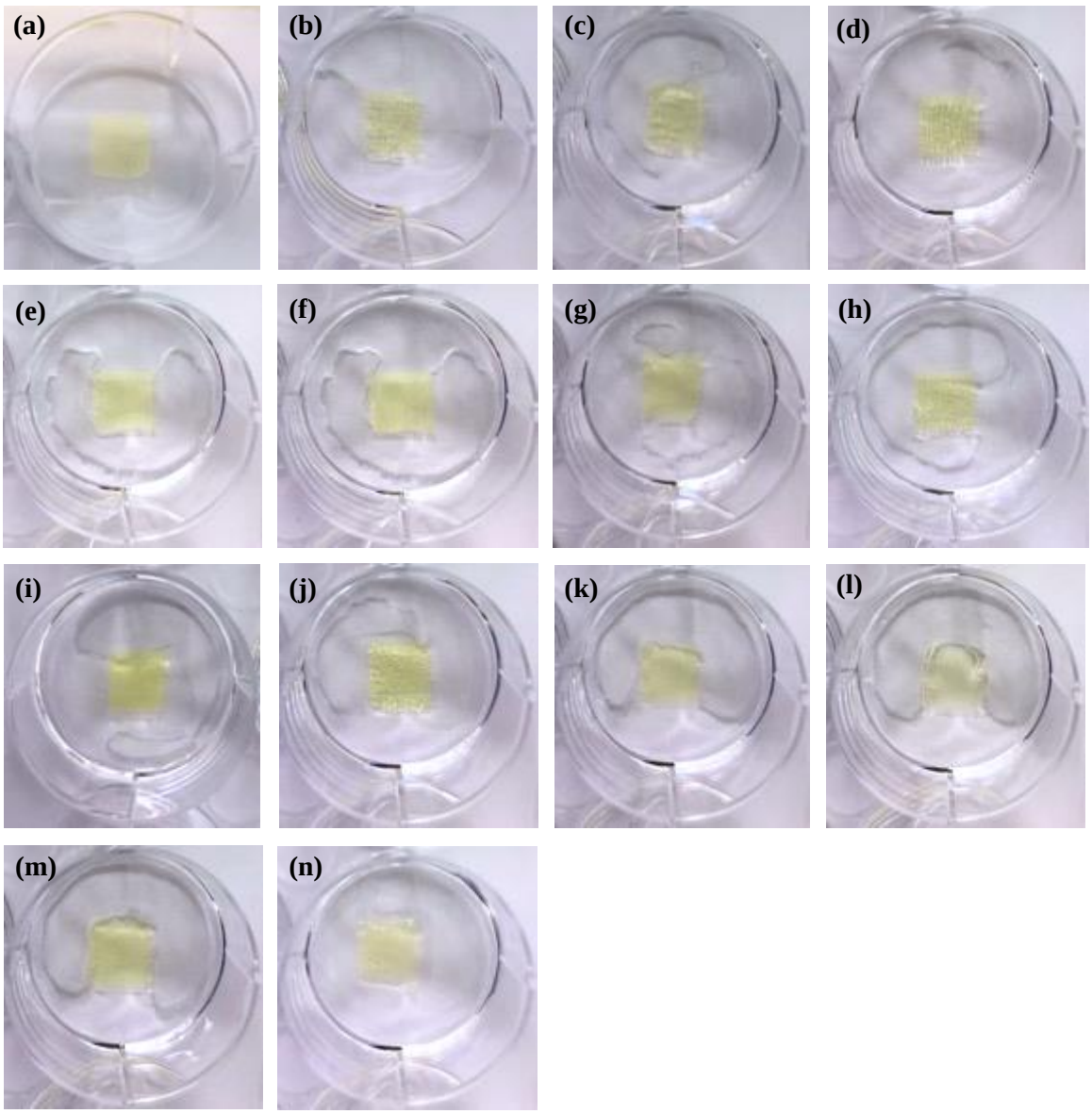

Figure C.2.24 – Ethyl cellulose-based films with the incorporation of 0.5% (w/w) of curcumin: (a) without the immersion in buffer solutions, (b) to (n) corresponds to the immersion in buffer solutions ranged from pH 1 – 13, respectively.

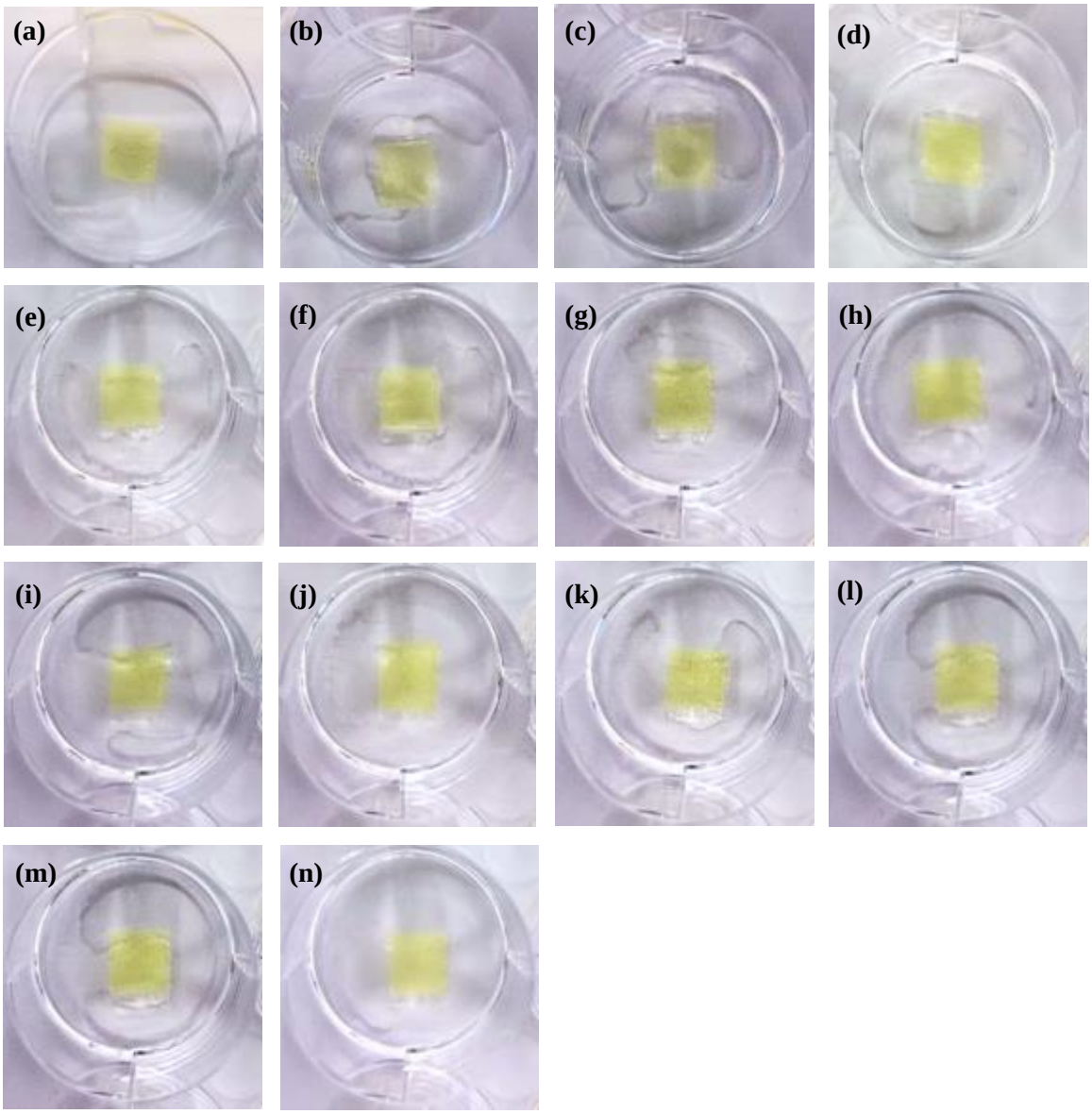

Figure C.2.25 – Ethyl cellulose-based films with the incorporation of 1% (w/w) of curcumin: (a) without the immersion in buffer solutions, (b) to (n) corresponds to the immersion in buffer solutions ranged from pH 1 – 13, respectively.

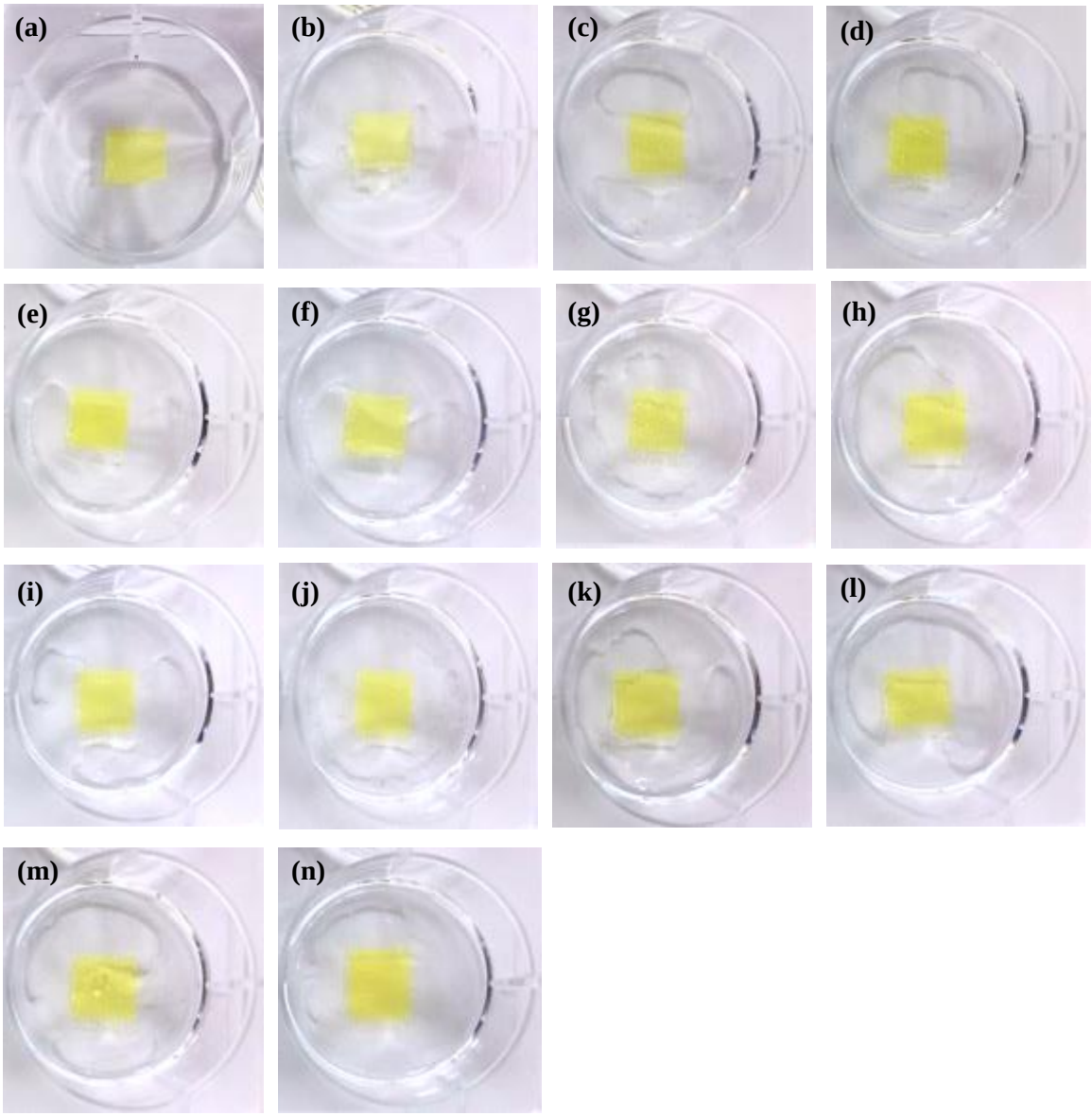

Figure C.2.26 – Ethyl cellulose-based films with the incorporation of 2% (w/w) of curcumin: (a) without the immersion in buffer solutions, (b) to (n) corresponds to the immersion in buffer solutions ranged from pH 1 – 13, respectively.

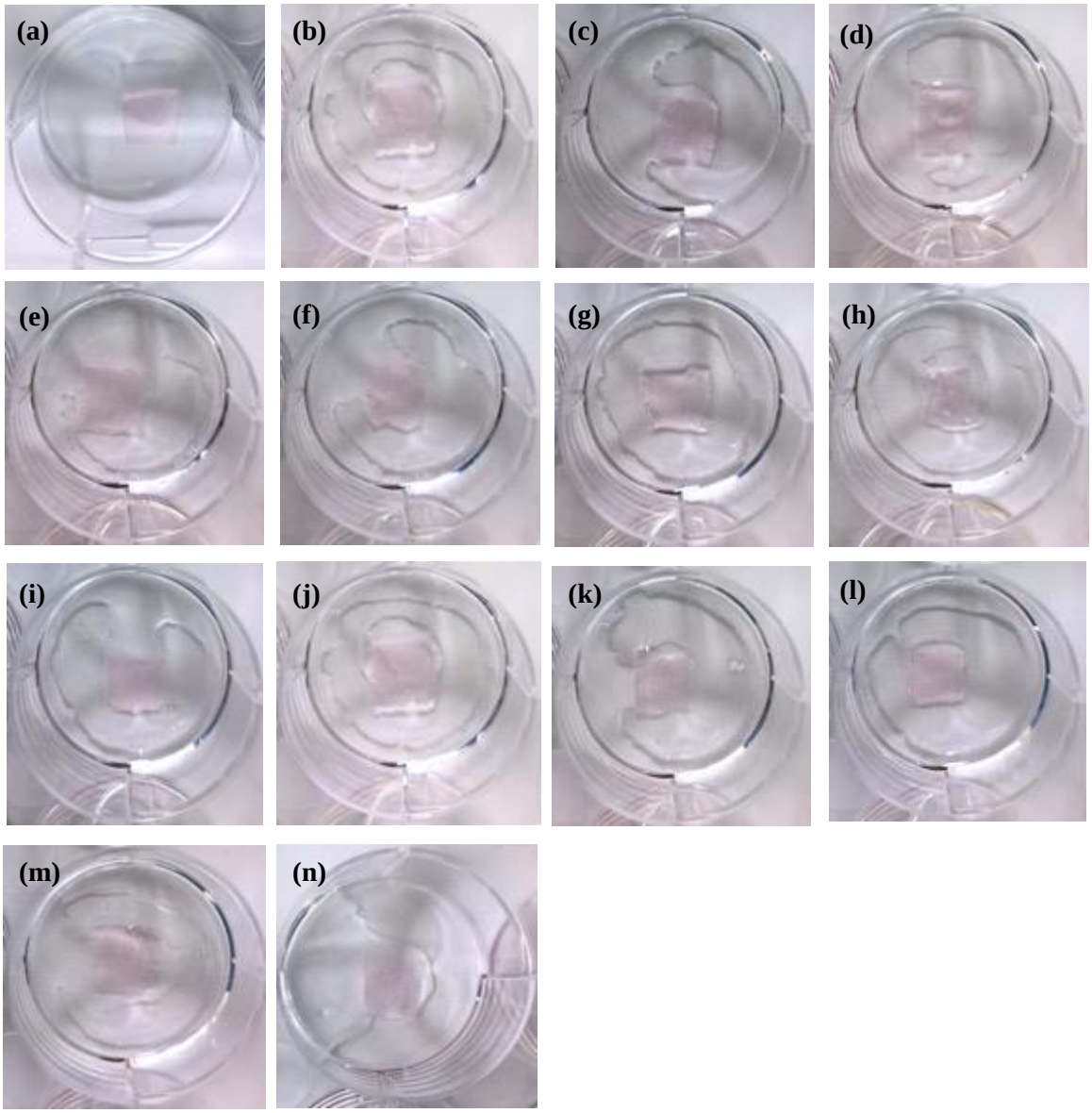

Figure C.2.27 – Ethyl cellulose-based films with the incorporation of 0.5% (w/w) of betalains: (a) without the immersion in buffer solutions, (b) to (n) corresponds to the immersion in buffer solutions ranged from pH 1 – 13, respectively.

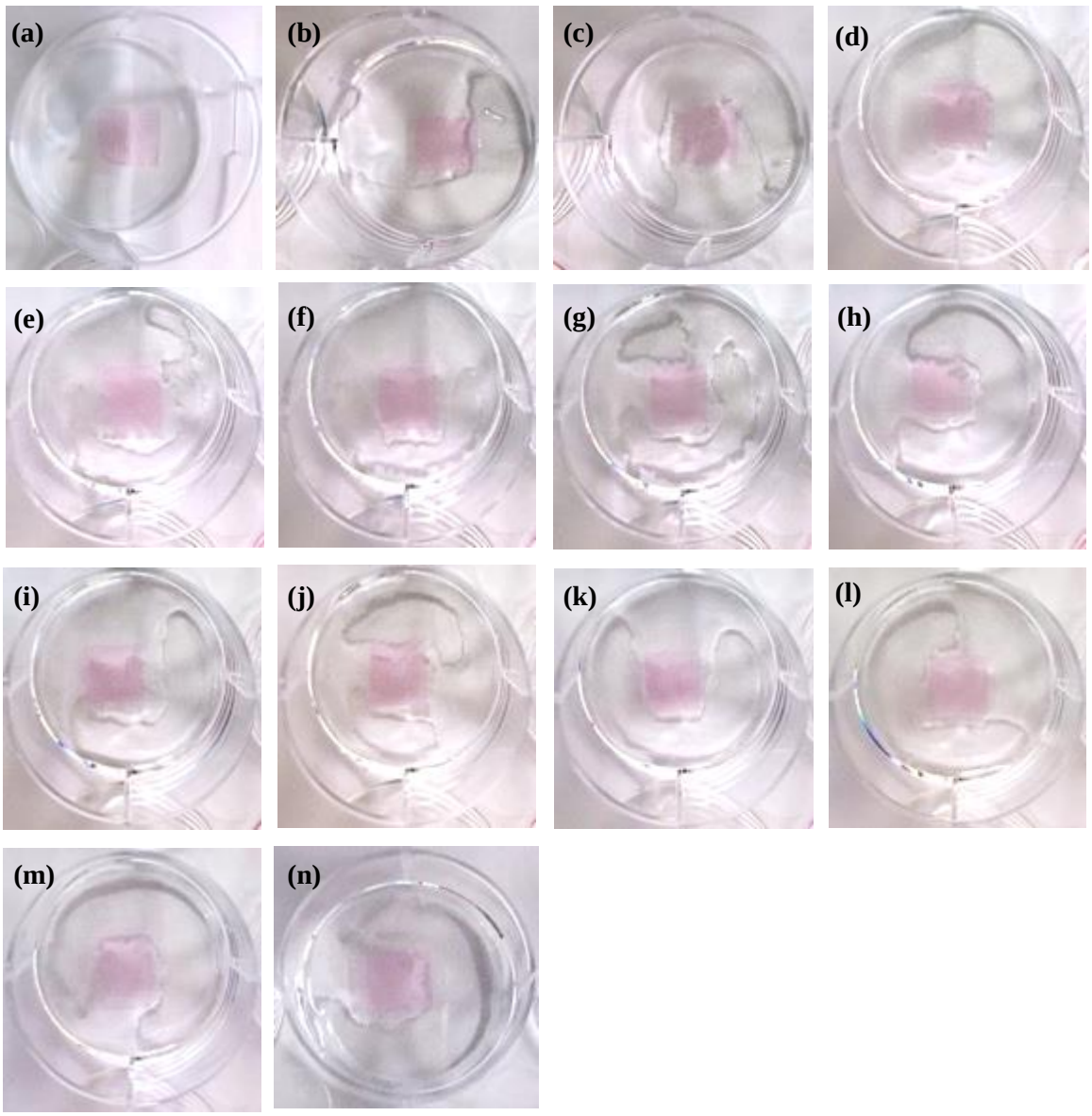

Figure C.2.28 – Ethyl cellulose-based films with the incorporation of 1% (w/w) of betalains: (a) without the immersion in buffer solutions, (b) to (n) corresponds to the immersion in buffer solutions ranged from pH 1 – 13, respectively.

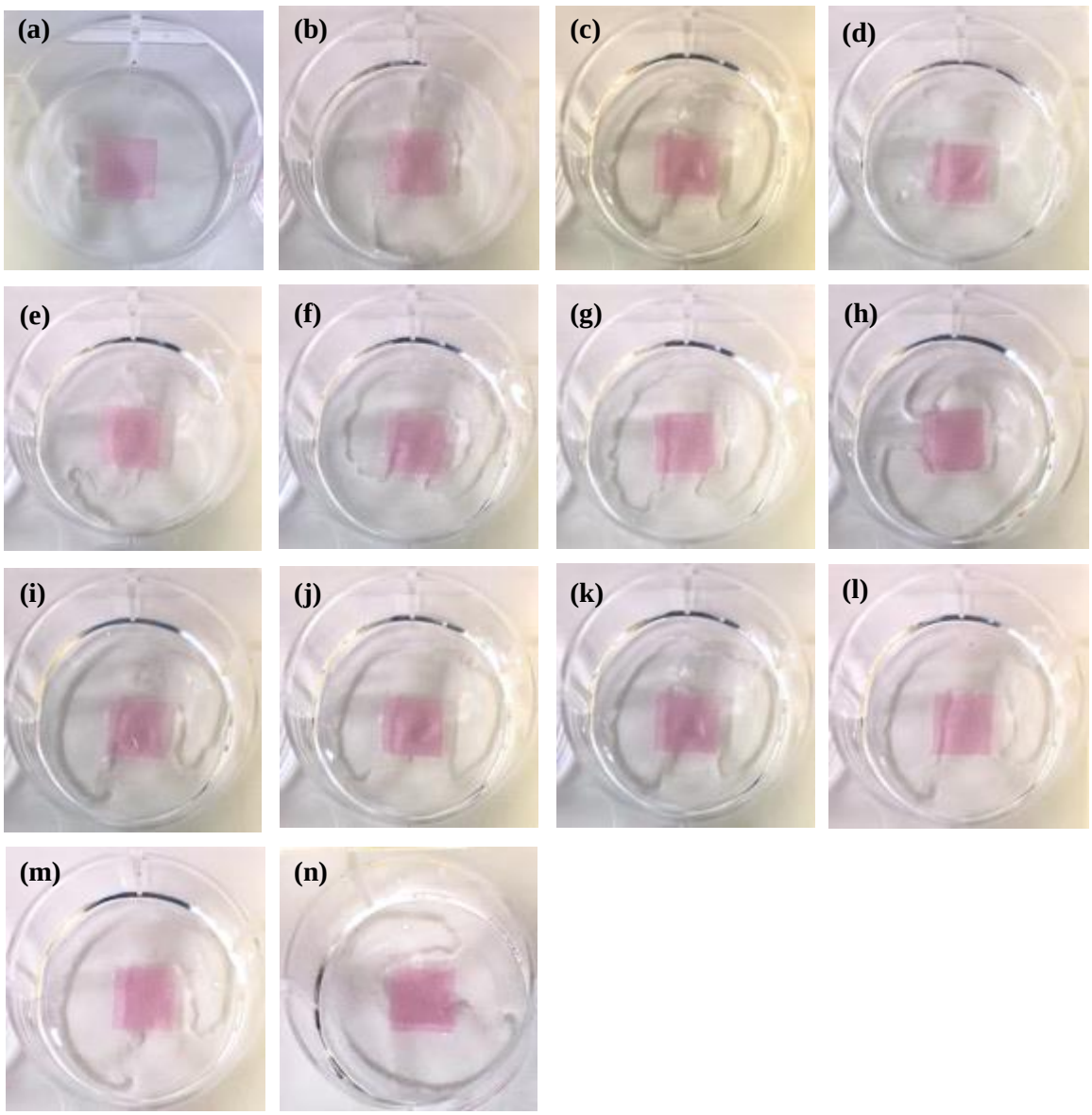

Figure C.2.29 – Ethyl cellulose-based films with the incorporation of 2% (w/w) of betalains: (a) without the immersion in buffer solutions, (b) to (n) corresponds to the immersion in buffer solutions ranged from pH 1 – 13, respectively.

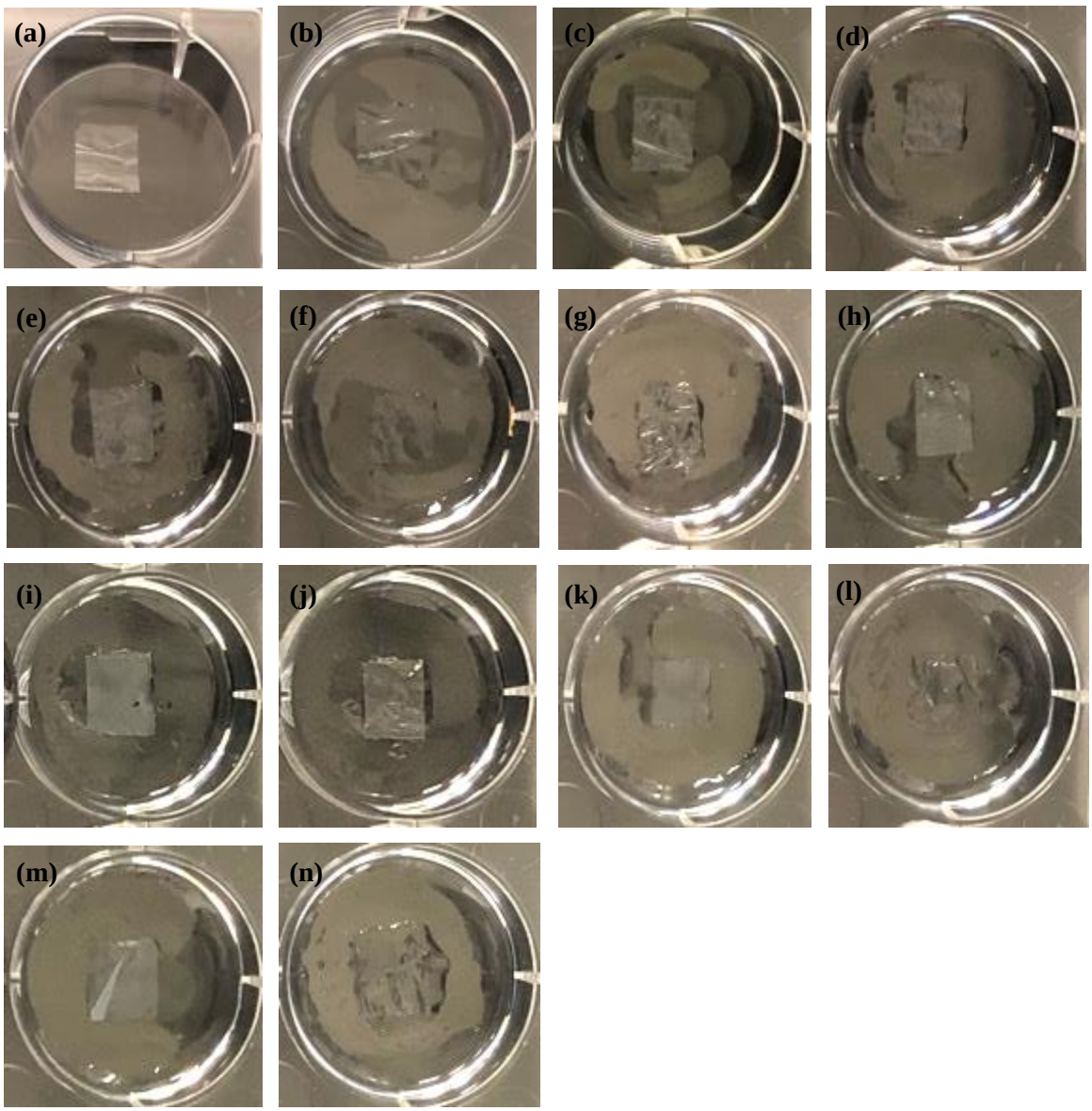

Figure C.2.30 – Ethyl cellulose-based films without the incorporation of any natural dye: (a) without the immersion in buffer solutions, (b) to (n) corresponds to the immersion in buffer solutions ranged from pH 1 – 13, respectively.

C.3 Visual analysis of the films

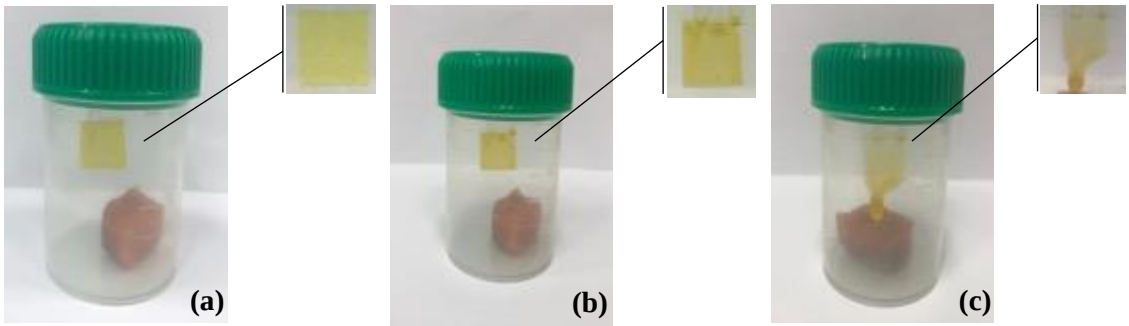

Figure C.3.1 – Visual analysis of carboxymethylcellulose/curcumin films. Figures (a), (b) (c) represent the following three days.

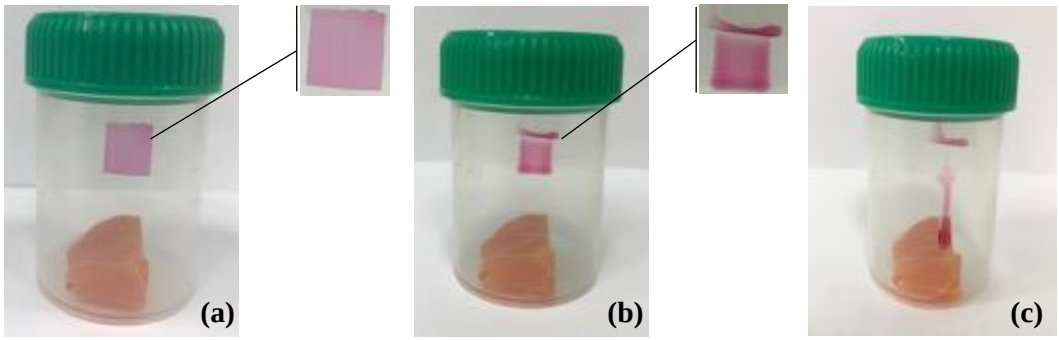

Figure C.3.2 – Visual analysis of carboxymethylcellulose/betalains films. Figures (a), (b) (c) represent the following three days.

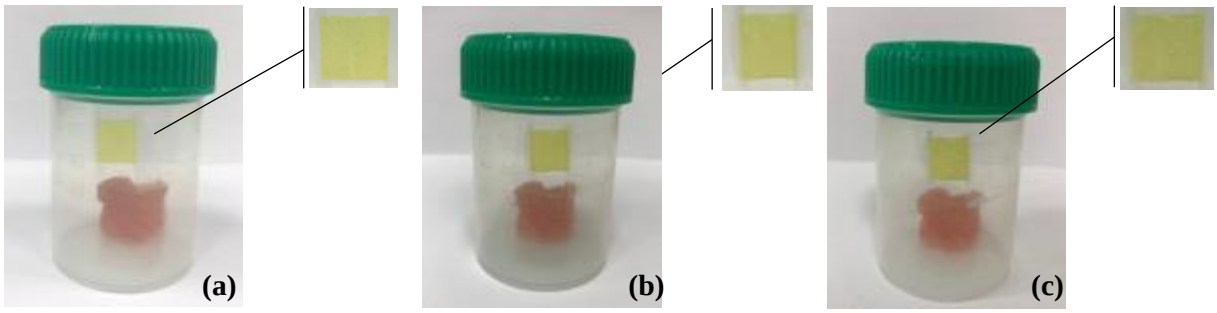

Figure C.3.3 – Visual analysis of cellulose acetate/curcumin films. Figures (a), (b) (c) represent the following three days.

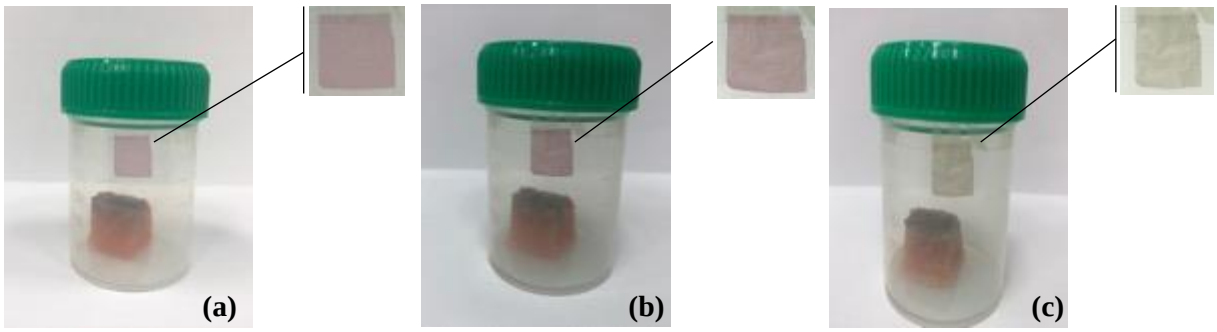

Figure C.3.4 – Visual analysis of cellulose acetate /betalains films. Figures (a), (b) (c) represent the following three days.

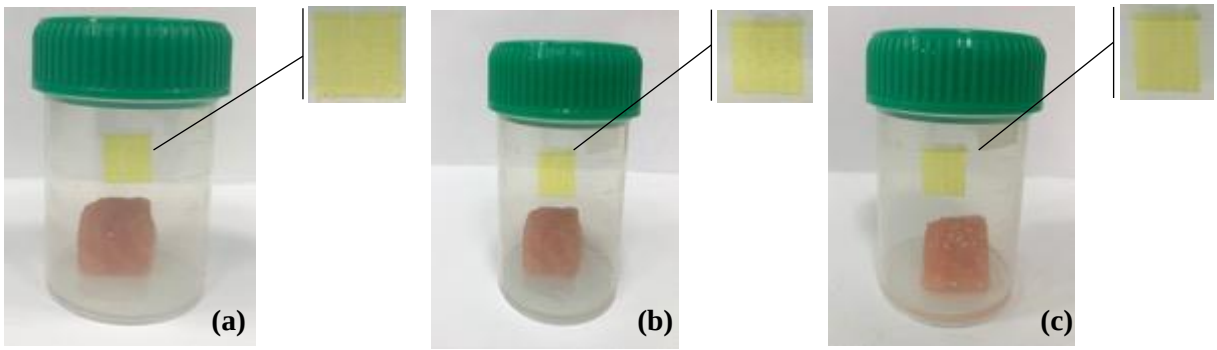

Figure C.3.5 – Visual analysis of ethyl cellulose/curcumin films. Figures (a), (b) (c) represent the following three days.

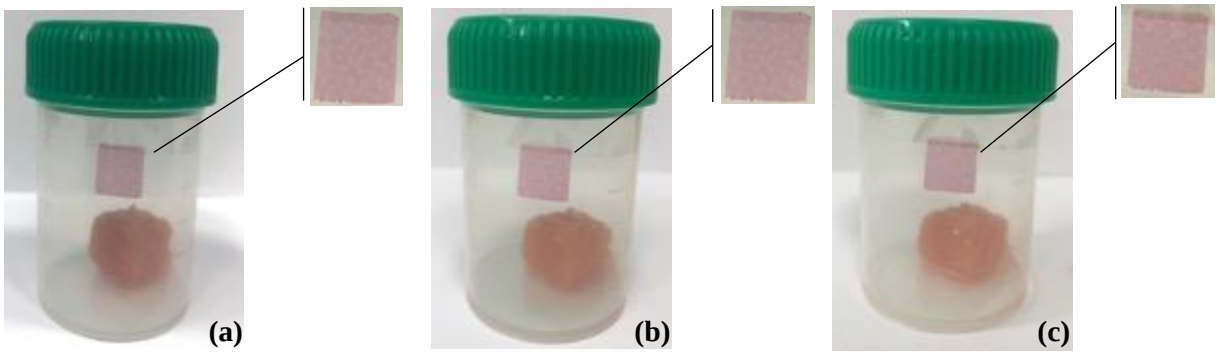

Figure C.3.6 – Visual analysis of ethyl cellulose/betalains films. Figures (a), (b) (c) represent the following three days.